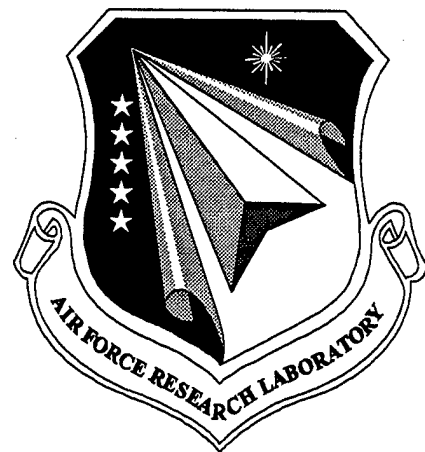


**AFRL-ML-WP-TR-1999-4104**

**MOBILE AUTOMATED SCANNER  
SYSTEM (MAUS)**



Donald D. Palmer, Jr.  
Nancy L. Wood

The Boeing Company  
Military Aircraft and Missile Systems  
P.O. Box 516  
St. Louis, MO 63166

April 1999

Final Report For the Period 01 October 1991 - 15 April 1999

Approved for Public Release; Distribution is Unlimited.

Materials & Manufacturing Directorate  
Air Force Research Laboratory  
Air Force Materiel Command  
Wright-Patterson Air Force Base, Ohio 45433-7734

**QUALITY INSPECTED 4**

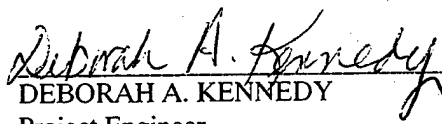
19990820 075

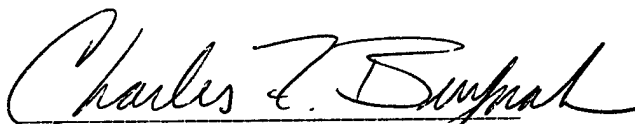
## NOTICE

When Government drawings, specifications, or other data are used for any purpose other than in connection with a definitely related Government procurement operation, the United States Government thereby incurs no responsibility nor any obligation whatsoever; and the fact that the government may have formulated, furnished, or in any way supplied the said drawings, specifications, or other data, is not to be regarded by implication or otherwise as in any manner licensing the holder or any other person or corporation, or conveying any rights or permission to manufacture, use, or sell any patented invention that may in any way be related thereto.

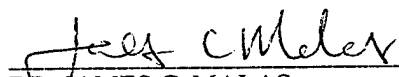
This report has been reviewed by the Office of Public Affairs (ASC/PA) and is releasable to the National Technical Information Service (NTIS). At NTIS, it will be available to the general public, including foreign nations.

This technical report has been reviewed and is approved for publication.

  
DEBORAH A. KENNEDY  
Project Engineer  
Metals Team  
Processing & Fabrication Branch

  
CHARLES F. BUYNAK  
Project Engineer  
Nondestructive Evaluation Branch  
Metals, Ceramics & Nondestructive Evaluation Division

  
BRUCE A. RASMUSSEN  
Chief  
Processing & Fabrication Branch  
Manufacturing Technology Division

  
DR. JAMES C. MALAS  
Acting Chief  
Nondestructive Evaluation Branch  
Metals, Ceramics & Nondestructive Evaluation Division

"If your address has changed, if you wish to be removed from our mailing list, or if the addressee is no longer employed by your organization please notify AFRL/MLMP, Bldg. 653, 2977 P St., Suite 6, W-PAFB, OH 45433-7739 to help us maintain a current mailing list."

Copies of this report should not be returned unless return is required by security considerations, contractual obligations, or notice on a specific document.

# REPORT DOCUMENTATION PAGE

FORM APPROVED  
OMB NO. 0704-0188

Public reporting burden for this collection of information is estimated to average 1 hour per response, including the time for reviewing instructions, searching existing data sources, gathering and maintaining the data needed, and completing and reviewing the collection of information. Send comments regarding this burden estimate or any other aspect of this collection of information, including suggestions for reducing this burden, to Washington Headquarters Services, Directorate for Information Operations and Reports, 1215 Jefferson Davis Highway, Suite 1204, Arlington, VA 22202-4302, and to the Office of Management and Budget, Paperwork Reduction Project (0704-0188), Washington, DC 20503.

1. AGENCY USE ONLY (Leave Blank)		2. REPORT DATE April 1999	3. REPORT TYPE AND DATES COVERED Final 10/01/91 - 04/15/99
4. TITLE AND SUBTITLE Mobile Automated Scanner System (MAUS)			5. FUNDING NUMBERS C F33615-91-C-5664 PE 78011F PR 3153 TA 00 WU 09
6. AUTHOR(S) Donald D. Palmer Jr., Nancy L. Wood			8. PERFORMING ORGANIZATION REPORT NUMBER
7. PERFORMING ORGANIZATION NAME(S) AND ADDRESS(ES) The Boeing Company Military Aircraft and Missile Systems P.O. Box 516 St. Louis, MO 63166			10. SPONSORING/MONITORING AGENCY REP NUMBER AFRL-ML-WP-TR-1999-4104
9. SPONSORING MONITORING AGENCY NAME(S) AND ADDRESS(ES) Materials & Manufacturing Directorate Air Force Research Laboratory Air Force Materiel Command Wright-Patterson AFB, OH 45433-7734 POC: Deborah A. Kennedy, AFRL/MLMP, (937) 255-3612			
11. SUPPLEMENTARY NOTES			
12a. DISTRIBUTION/AVAILABILITY STATEMENT Approved for Public Release; Distribution is Unlimited.			12b. DISTRIBUTION CODE
13. ABSTRACT This report describes the full-scale development of a portable, multi-modal, large area scanning system for nondestructive inspection of airframe structures. The Mobile Automated Scanner (MAUS) incorporated ultrasonic pulse-echo, ultrasonic resonance and eddy current scanning capabilities with scan speeds up to 400 sq. ft./hr. The system generates C-scan formatted data for interpretation and archiving. Prototype systems were deployed at five Air Logistics Centers and two Navy depots for evaluation. The system was subsequently productionized as the MAUS IV.			
14. SUBJECT TERMS Mobile Automated Scanner (MAUS), Ultrasonic, Eddy Current, Resonance, Corrosion Detection, Bond Testing, Multi-Modal, Data Archiving.			15. NUMBER OF PAGES 147
			16. PRICE CODE
17. SECURITY CLASSIFICATION OF REPORT Unclassified	18. SECURITY CLASS OF THIS PAGE. Unclassified	19. SECURITY CLASS OF ABSTRACT Unclassified	20. LIMITATION ABSTRACT SAR

Standard Form 298 (Rev 2-89)  
Prescribed by ANSI Std Z239-18  
298-102

# TABLE OF CONTENTS

## Page

<b>PREFACE .....</b>	<b>xi</b>
<b>1.0 INTRODUCTION .....</b>	<b>1</b>
<b>2.0 SYSTEM FULL SCALE DEVELOPMENT (MAUS III).....</b>	<b>2</b>
2.1 Breadboard Investigation .....	2
2.1.1 Initial Breadboard System.....	2
2.1.2 Assembly of Test Standards.....	9
2.1.3 Performance Studies .....	16
2.1.4 Conclusions.....	19
2.1.5 Prototype Design Concept .....	24
2.2 Prototype Development.....	27
2.2.1 Signal Conditioning Subsystem.....	31
2.2.2 Data Management Subsystem.....	39
2.2.3 Scanner Subsystem .....	43
2.3 Demonstration and Validation .....	50
2.3.1 Delamination and Laminar Flaw Detection.....	51
2.3.2 Adhesive Bondline Flaw Detection .....	56
2.3.3 Repair Verification .....	61
2.3.4 Corrosion Detection.....	64
2.3.5 Crack Detection .....	67
2.3.6 Requested Improvements.....	69
2.4 Field System Development .....	70
2.4.1 General System Operation .....	70
2.4.2 Pulse-Echo Improvements .....	71
2.4.3 Resonance Improvements .....	72
2.4.4 Eddy Current Improvements.....	72
2.4.5 External Equipment Inputs .....	72
2.4.6 Mechanical Scanner Improvements.....	73
2.4.7 Software Improvements .....	74
2.4.8 Portable Soft-Pack Carrying Cases.....	77



	<b>Page</b>
<b>3.0 FIELD SYSTEM DEPLOYMENT (MAUS III)</b> .....	80
3.1 Oklahoma City Air Logistics Center (Tinker AFB, OK).....	80
3.2 Ogden Air Logistics Center (Hill AFB, UT).....	81
3.3 Sacramento Air Logistics Center (McClellan AFB, CA).....	81
3.4 Air Force Research Laboratory (Wright-Patterson AFB, OH).....	82
3.5 Naval Aircraft Applications .....	83
3.6 Warner-Robins Air Logistics Center (Robins AFB, GA) .....	84
3.7 San Antonio Air Logistics Center (Kelly AFB, TX).....	84
<b>4.0 PRODUCTION PROTOTYPE DEMONSTRATION/VALIDATION (MAUS IV)</b> .....	85
4.1 Bondline Inspection Sensor Evaluation .....	86
4.1.1 Pitch/Catch Resonance .....	86
4.1.2 Mechanical Impedance Analysis (MIA) .....	86
4.1.3 MIA – Bondcheck.....	87
4.1.4 Tap Test .....	87
4.1.5 Eddy Sonics .....	88
4.1.6 Microwave .....	88
4.1.7 Summary of Signal Conditioning Improvements .....	88
4.2 Circuit Board Enhancements.....	89
4.2.1 CPU board .....	89
4.2.2 Front Panel.....	90
4.2.3 Timing/Digitizer Board.....	90
4.2.4 Continuous Wave Circuit Boards .....	91
4.2.5 Motion Control Processor.....	91
4.3 Ergonomic Enhancements.....	91
4.3.1 Flexible Track Concept.....	92
4.3.2 Flexible Track Production .....	92
4.3.3 Track Carriage Design .....	95
4.3.4 Variable Stroke Scanner Design .....	97
4.3.5 Hand Scanner Design Review .....	98
4.4 Operator Interface Improvements .....	99
4.4.1 Standard Windows NT/95 Features .....	99
4.4.2 Program Layout.....	99
4.4.3 Variable Adjustments .....	100
4.4.4 System Startup .....	101
4.4.5 Control Page .....	102

	<b>Page</b>
4.4.6 Overview Page.....	103
4.4.7 Data System Setup – General Format.....	104
4.4.8 Pulse-Echo Data System Setup.....	105
4.4.9 Resonance Data System Setup.....	109
4.4.10 Pitch/Catch Resonance and MIA Data System Setup.....	111
4.4.11 Eddy Current Data System Setup.....	112
4.4.12 C-scan Data Display .....	113
4.5 Production Readiness Review.....	119
4.6 System Performance Evaluation .....	122
4.6.1 Software Issues .....	124
4.6.2 Hardware Issues .....	124
4.6.3 Suggested Improvements.....	124
4.6.4 Inspection Application Evaluations .....	125
4.7 Implementation Plan .....	127
4.7.1 Training.....	128
4.7.2 Safety Issues.....	128
4.7.3 Maintenance Plans .....	128
4.7.4 Software Support .....	129
4.7.5 Spare Part Provisioning .....	130
<b>5.0 CONCLUSIONS .....</b>	<b>133</b>
<b>6.0 RECOMMENDATIONS.....</b>	<b>134</b>
<b>7.0 REFERENCES.....</b>	<b>135</b>

## LIST OF FIGURES

	Title	Page
Figure 2.1.1-1.	MAUS Development Station .....	4
Figure 2.1.1-2.	MAUS Development Station Block Diagram.....	5
Figure 2.1.1-3.	Initial Continuous Wave Breadboard System.....	5
Figure 2.1.1-4.	Continuous Wave Breadboard System Block Diagram.....	6
Figure 2.1.1-5.	Scanner Modified for Inspection of Curved Surfaces.....	8
Figure 2.1.1-6.	Scanner Modified with Loop Spring Sensor Mount .....	8
Figure 2.1.2-1.	Description of Test Articles.....	10
Figure 2.1.2-2.	Carbon/Epoxy Skins- Aluminum Core/Tapered (Standard #1).....	12
Figure 2.1.2-3.	Carbon/Epoxy Skins-Aluminum Core/Constant (Standard #2).....	12
Figure 2.1.2-4.	Aluminum Skins-Aluminum Core/Tapered (Standard #3).....	12
Figure 2.1.2-5.	Aluminum Skins-Aluminum Core/Constant (Standard #4) .....	13
Figure 2.1.2-6.	Quartz/Epoxy Laminate-Contoured (Standard #6).....	13
Figure 2.1.2-7.	Kevlar/Epoxy Laminate (Standard #7) .....	14
Figure 2.1.2-8.	Carbon/Epoxy Hat-Stiffened (Standard #8).....	14
Figure 2.1.2-9.	Stitched Carbon/Epoxy-T-stiffened (Standard #10).....	14
Figure 2.1.2-10.	Quartz-Carbon/Epoxy Hybrid Skins-Fiberglass/Phenolic Core (Standard #12).....	15
Figure 2.1.2-11.	Aluminum-Aluminum Adhesive Bond (Standard #13).....	15
Figure 2.1.2-12.	Kevlar/Epoxy Skins-Fiberglass/Phenolic Core (Standard #17).....	15
Figure 2.1.2-13.	Carbon/Epoxy Laminate/Variable Thickness (Standard #23) .....	16
Figure 2.1.3-1.	Mobile Automated Scanner "House of Quality" .....	17
Figure 2.1.3-2.	Performance Evaluation Record .....	18
Figure 2.1.4-1.	Baseline Scan of Carbon/Epoxy Step Wedge (Standard #23) .....	19
Figure 2.1.4-2.	Scan Speed vs. Defect Detection Capability (Pulse-Echo).....	20
Figure 2.1.4-3.	Scan Speed vs. Defect Detection Capability (Resonance).....	21
Figure 2.1.4-4.	Multi-Modal C-scan Image (Ultrasonic Resonance/Eddy Current).....	22
Figure 2.1.4-5.	Correlation Study Summary.....	23
Figure 2.1.4-6.	Ultrasonic Resonance Scan of Multi-Layered Adhesive Bonded Aluminum Structure .....	24
Figure 2.1.5-1.	Target Goals for LACIS/MAUS Signal Conditioning Package .....	25

	<b>Title</b>	<b>Page</b>
Figure 2.2-1.	Prototype MAUS III System .....	27
Figure 2.2-2.	Additional Scanners for MAUS III .....	28
Figure 2.2-3.	MAUS III Physical Parameters vs. Design Goals .....	28
Figure 2.2-4.	MAUS III Signal Conditioning Specifications .....	29
Figure 2.2-5.	MAUS III Data System Specifications .....	30
Figure 2.2.1-1.	Schematic of MAUS III Signal Conditioning Enclosure .....	31
Figure 2.2.1-2.	Summary of Signal Conditioning Subsystem Components and Their Functions.....	32
Figure 2.2.1-3.	Timing Function Specifications .....	34
Figure 2.2.1-4.	Pulser/Receiver Board Specification .....	34
Figure 2.2.1-5.	Specifications for the Video and Amplitude Detection Board .....	35
Figure 2.2.1-6.	Specifications for the Pulse-Echo Data Conversion Board .....	36
Figure 2.2.1-7.	Specifications for the Signal Digitizer Board .....	37
Figure 2.2.1-8.	Specifications for RES/EC Frequency Generation Board .....	37
Figure 2.2.1-9.	Specifications for the RES/EC Signal Conditioning Board.....	38
Figure 2.2.1-10.	Specifications for the Motion Control Processor Board .....	39
Figure 2.2.2-1.	Data Management System Features .....	40
Figure 2.2.2-2.	Prototype MAUS III System with Laptop Computer.....	41
Figure 2.2.2-3.	MAUS III Computer Workspace - Complete Menus .....	42
Figure 2.2.3-1.	MAUS III Scanner Subsystem .....	43
Figure 2.2.3-2.	Common Scanner Subsystem Features .....	44
Figure 2.2.3-3.	Unique Scanner Subsystem Features .....	44
Figure 2.2.3-4.	Tight-Access Scanner .....	45
Figure 2.2.3-5.	Curve Following Scanner .....	46
Figure 2.2.3-6.	Large Area Scanner.....	46
Figure 2.2.3-7.	Small Scanner (Disassembled) .....	47
Figure 2.2.3-8.	Curve Following Scanner (Disassembled).....	47
Figure 2.2.3-9.	Sensor Mount Clamps for Small and Curve Following Scanners .....	48
Figure 2.2.3-10.	Available Sensor Gimbals .....	49
Figure 2.2.3-11.	Sensor Adapters with Sensors Installed.....	50
Figure 2.3.1-1.	MAUS III Pulse-Echo depth C-scan of Carbon/Epoxy Test Standard .....	52

	Title	Page
Figure 2.3.1-2.	Impact Damage in a Carbon/Epoxy Laminate Structure .....	53
Figure 2.3.1-3.	MAUS III Pulse-Echo Amplitude C-scan of Milstar Radome.....	53
Figure 2.3.1-4.	Resonance Phase C-scan of Milstar Radome.....	54
Figure 2.3.1-5.	MAUS III Evaluation of A-10 at SC-ALC .....	55
Figure 2.3.1-6.	MAUS III Scanner Positioned on A-10 Leading Edge .....	55
Figure 2.3.1-7.	Ultrasonic Resonance C-scan of an A-10 Leading Edge .....	56
Figure 2.3.2-1.	MAUS III Resonance Phase C-scan of Bondline Defects in E-3 Radome Standard .....	57
Figure 2.3.2-2.	MAUS III Resonance Phase C-scan of Edge Delamination at the Closure Rib on a B-1 Trailing Edge .....	58
Figure 2.3.2-3.	MAUS III Resonance Phase C-scan of Bondline Void on B-1 Trailing Edge .....	58
Figure 2.3.2-4.	MAUS III Resonance Phase C-scan of B-1 Outer Wing Fairing (Composite Skin/Non-Metallic Honeycomb Core) .....	58
Figure 2.3.2-5.	MAUS III Resonance C-scan of Bondline Flaws in T-38 Wing Tip Standard .....	59
Figure 2.3.2-6.	MAUS III Resonance Phase C-scan of Boeing 727 Rudder Tab (Aluminum Skin/Aluminum Core).....	60
Figure 2.3.2-7.	Bondline Voids in a Bonded Composite Spoiler Standard (Composite Skins/Non-Metallic Core).....	61
Figure 2.3.3-1.	MAUS III Inspection of Boron/Epoxy Patch on F-16 Lower Wing Skin...	62
Figure 2.3.3-2.	MAUS III Pulse-Echo Amplitude C-scan of Boron/Epoxy Patch Standard .....	62
Figure 2.3.3-3.	MAUS III Resonance Phase C-scan of Boron/Epoxy Multiple Patch Standard .....	63
Figure 2.3.3-4.	MAUS III Resonance C-scan of Boron/Epoxy Patch on Fuselage Panel ...	63
Figure 2.3.4-1.	KC-135 Pilot Drain Hole .....	64
Figure 2.3.4-2.	MAUS III Inspection of KC-135 Pilot Drain Hole .....	65
Figure 2.3.4-3.	MAUS III Eddy Current C-Scan of KC-135 Pilot Drain Hole .....	65
Figure 2.3.4-4.	MAUS III Eddy Current Phase C-scan of KC-135 Fuselage Lap Joint.....	66
Figure 2.3.4-5.	MAUS III Pulse-Echo Amplitude C-scan of Boeing 707 Fuselage Skin With Suspected Exfoliation Around Fasteners .....	66
Figure 2.3.4-6.	MAUS III Eddy Current Phase C-scan of DC-10 Fuselage Skin.....	67

	Title	Page
Figure 2.3.5-1.	MAUS III Eddy Current C-scan of Fatigue Cracks in F-4 Horizontal Stabilizer .....	68
Figure 2.4.6-1.	Original Gimbal Design.....	73
Figure 2.4.6-2.	Modified Gimbal Design .....	73
Figure 2.4.6-3.	Pen Marking Concept .....	74
Figure 2.4.7-1.	DAC Curve Menu.....	75
Figure 2.4.7-2.	MAUS III Impedance Plane Display.....	76
Figure 2.4.7-3.	Original Inspection Data Collected in Strips .....	76
Figure 2.4.7-4.	Data Strips Selected from Original Data File .....	76
Figure 2.4.7-5.	Data Strips Repositioned to Create Full Image Data File.....	77
Figure 2.4.8-1.	Soft-Pack Case for MAUS III.....	77
Figure 2.4.8-2.	Soft-Pack Case Showing Storage Capability for MAUS III Components .....	78
Figure 2.4.8-3.	MAUS III Soft-Pack Carrying Case Showing Anti-Reflection Screen Shield .....	78
Figure 3.1-1.	MAUS III Evaluation of KC-135 Lap Joints at OC-ALC .....	80
Figure 3.2-1.	MAUS III Evaluation of F-16 Vertical Stabilizer Leading Edge and Inlet Duct at OO-ALC.....	81
Figure 3.4-1.	Evaluation of MAUS III at the Indianapolis Motor Speedway.....	82
Figure 3.4-2.	MAUS III Evaluation of DC-10 Fuselage Structure at Northwest Airlines.....	83
Figure 3.5-1.	MAUS III Evaluation of F/A-18E/F at Patuxent River, MD .....	84
Figure 4.2-1.	Summary of Circuit Card Changes Implemented in MAUS IV .....	89
Figure 4.3.2-1.	Flexible Track Design.....	94
Figure 4.3.2-2.	Flexible Track Attached to KC-135 Fuselage .....	94
Figure 4.3.3-1.	MAUS IV Carriage Motor/Resolver.....	96
Figure 4.3.4-1.	MAUS IV Variable Stroke Scanner.....	97
Figure 4.4.2-1.	MAUS IV System Set-Up Window .....	100
Figure 4.4.3-1.	Set-Up Window Showing Numerical and List Variable Settings.....	101
Figure 4.4.5-1.	MAUS IV Control Page Window .....	102
Figure 4.4.6-1.	MAUS IV Overview Page Window .....	104
Figure 4.4.8-1.	MAUS IV Pulse-Echo Sensor Window.....	105

	<b>Title</b>	<b>Page</b>
Figure 4.4.8-2.	MAUS IV Pulse-Echo Distance-Amplitude Curve Window.....	106
Figure 4.4.8-3.	MAUS IV Pulse-Echo Gate Window .....	107
Figure 4.4.8-4.	MAUS IV Pulse-Echo Options Pages.....	108
Figure 4.4.9-1.	MAUS IV Resonance Sensors Window .....	109
Figure 4.4.9-2.	MAUS IV Resonance Options Window.....	110
Figure 4.4.10-1.	MAUS IV Pitch/Catch-MIA Sensor Window .....	111
Figure 4.4.11-1.	MAUS IV Eddy Current Sensor Window.....	112
Figure 4.4.12-1.	MAUS IV C-Scan Window (Single Scan).....	114
Figure 4.4.12-2.	MAUS IV C-Scan Window (Double Scan).....	115
Figure 4.4.12-3.	MAUS IV Scanner Control Toolbar .....	116
Figure 4.4.12-4.	Effects of Changing High/Low Color Ranges .....	116
Figure 4.4.12-5.	Effects of Masking Feature.....	117
Figure 4.4.12-6.	Window Showing Far Move Function.....	117
Figure 4.4.12-7.	Window Illustrating the Data Combine Function.....	118
Figure 4.4.12-8.	Window Illustrating Data Merge Function .....	119
Figure 4.5-1.	Protoype MAUS IV System.....	120
Figure 4.5-2.	Summary of MAUS IV Software Functions.....	120
Figure 4.5-3.	Summary of MAUS IV Signal Conditioning Functions.....	121
Figure 4.5-4.	Outline of ACCESS Database .....	121
Figure 4.6-1.	Summary of MAUS IV Evaluation Process at OC-ALC.....	123
Figure 4.6-2.	Summary of MAUS IV Evaluation Log Items Documented at OC-ALC.....	123
Figure 4.6.4-1.	MAUS IV Eddy Current C-Scan of Corroded KC-135 Lap Joint .....	126
Figure 4.6.4-2.	MAUS IV MIA C-Scan of Unbonds in E-3 Rotodome Test Standard.....	127
Figure 4.7.5-1.	Consumable Items.....	130
Figure 4.7.5-2.	Recommended Spare Parts Inventory .....	130
Figure 4.7.5-3.	Complete Listing of Spare Parts for MAUS IV .....	131

## **PREFACE**

This report describes the work performed under U.S. Air Force contract F33615-91-C-5664, "Large Area Composite Inspection System", from 01 October 1991 to 15 April 1999. This report is submitted in compliance with the subject contract, CDRL Item A006. The program was managed by The Boeing Company, P.O. Box 516, St. Louis, MO 63166, under the technical direction of Mr. Charles Buynak, and Ms. Deborah Kennedy at the Air Force Research Laboratory.

The program was conducted by the Nondestructive Evaluation Group within the Boeing Phantom Works under the direction of Donald D. Palmer, Jr., Program Manager and Nancy L. Wood, Principal Investigator. During the course of the project, program management responsibilities also resided with Mark Reighard, Catherine Sabinash and Dr. Dianne Chong. Major contributors of the multi-disciplinary team included David Fortner (System Integration), Gene Myers (Mechanical Design), Mike Vandernoot and Steve Strouse (Software Development), John Vreuls and Doug Trimble (Network Configuration).



## 1.0 INTRODUCTION

With forecasted reductions in defense spending, reducing the cost of maintaining aircraft currently in the U.S. Air Force inventory becomes paramount. A significant portion of the cost of maintaining aircraft lies in nondestructive inspection (NDI), such as those performed during the Programmed Depot Maintenance (PDM) process. NDI methods are used to detect cracks caused by fatigue, corrosion, bondline flaws, defects and geometric anomalies in metal and composite structures. Given this, elimination of NDI from the PDM process is impossible; however, automation of various NDI processes would significantly reduce the cycle times involved during inspection. Significant reductions in inspection cycle time would significantly reduce maintenance costs.

With this in mind, the Air Force has undertaken an effort to develop portable, automated NDI technology to accomplish these cycle time reduction goals. The approach selected was to build on technology incorporated in the Mobile Automated Ultrasonic Scanner (MAUS) sponsored by the Materials Directorate at the Air Force Research Laboratory (AFRL) and developed by McDonnell Douglas Corporation in the late 1980's. The first MAUS, or MAUS I, was a portable system capable of performing ultrasonic pulse-echo inspection. The MAUS II took advantage of new technologies to dramatically reduce the size and weight of the system. The objectives of the "Large Area Composite Inspection System" program, also funded by the Materials Directorate, were to build on the MAUS technology by incorporating additional inspection modes such as ultrasonic resonance and eddy current, improve system portability through miniaturization and establish data archiving capabilities. The successful development of the MAUS III system, which met all of the goals prescribed in the program, prompted the Manufacturing Directorate at AFRL to productionize the system and lay the foundation for implementation into the PDM process. The productionized system, known as the MAUS IV, improved on the MAUS III by incorporating additional sensor modes for bond testing, PC-based software and a flexible scanning track for remote scanning. This report details the development efforts surrounding the MAUS III and MAUS IV systems, discusses the respective evaluations at the various Air Logistics Centers and identifies the steps taken towards implementation.

## **2.0 SYSTEM FULL SCALE DEVELOPMENT (MAUS III)**

### **2.1 Breadboard Investigation**

The initial inspection approach proposed for this program was developed from extensive experience accumulated using the first two generations of the Mobile Automated Ultrasonic Scanner. Development work performed under internal funding prior to the LACIS program demonstrated the feasibility of adding multiple inspection modes to the MAUS. Ultrasonic pulse-echo and resonance methods provided valuable information relative to composites and bonded structures, respectively. Eddy current methods showed promise for evaluating metallic structures for crack and corrosion detection. The primary objective of the Breadboard Investigation task was to establish a database of information on each of these inspection methods, to identify representative materials and structures, to define the appropriate technique for each type of aircraft structure and to optimize the performance characteristics for each inspection.

#### **2.1.1 Initial Breadboard System**

The initial breadboard system development was limited to the modification of existing equipment to address the multiple inspection method issues [1]. Two existing MAUS systems were made available for development activities. The first was the MAUS Development Station, a non-portable version of the MAUS affixed in the Automated Systems Laboratory. This system was linked to the software development facility so that rapid software changes could be made and evaluated. The second was a production-based MAUS utilized by the Quality Assurance organization at McDonnell Aircraft Company. This was a portable, stand-alone system that incorporated only pulse-echo time-of-flight capability.

The inspection methods investigated can be easily separated into two categories. The ultrasonic depth and amplitude inspection methods utilize pulsed wave signals to determine changes in material characteristics. Ultrasonic resonance and eddy current methods use changes in a continuous wave signal to ascertain changes in material properties. Since each category requires distinctly different signal conditioning approaches, two breadboard systems were assembled to enable discrete investigation of the pulsed-wave and continuous wave methods.

### ***Pulsed-Wave Breadboard System***

The MAUS Development station was modified to evaluate the pulsed-wave inspection methods. Both hardware and software changes were required to include the pulse-echo amplitude inspection mode in this system. The analog hardware in the MAUS system was separated into distinct modules. The design enabled easy integration of new hardware functions into the existing system. The ultrasonic analog hardware required to sense pulse-echo amplitude signals was added to the existing modular hardware. This consisted of two hardware modules, an Amplitude Detection Module and a High Resolution Gate Module.

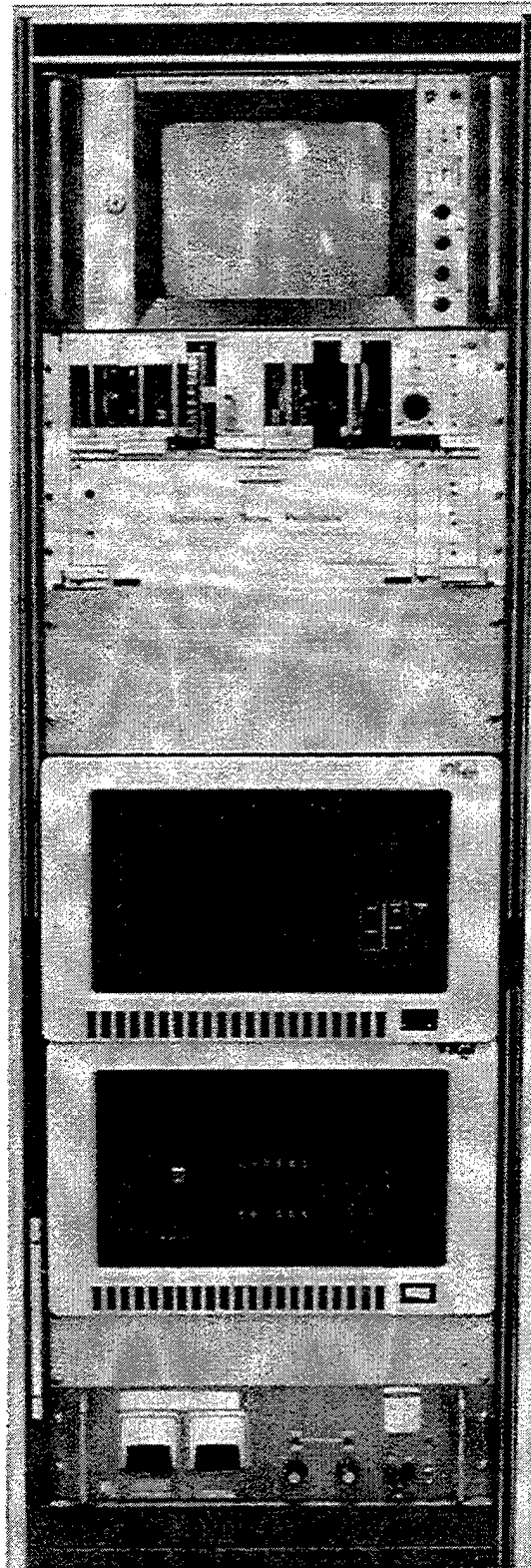
The Amplitude Detection circuitry identified changes in the amplitude of the reflected ultrasonic signal that occurred within an operator-selected gate. These changes in amplitude, or attenuation of the signal were related to changes in the material properties of the structure. In laminate materials, attenuation changes can indicate delaminations, foreign object inclusions, or porosity. In bonded structures, these changes can indicate variations in bondline properties, such as adhesive voids or separations. An Amplitude Detection Module was assembled and installed in the MAUS Development Station.

The High Resolution Gate Module was assembled and installed in the MAUS Development Station to replace the existing gate circuitry. This new module generates an amplitude gate with very fine resolution. This is required for thin-skinned bonded structures so that the amplitude gate can be set for bondline evaluations.

Several software modifications were required to fully integrate the Amplitude Detection module and the High Resolution Gate module into the Development Station. These software changes included drivers for each module and system set-up software to set the parameters for the acquisition and display of the amplitude data. Figure 2.1.1-1 illustrates the MAUS Development Station as configured for the pulsed wave breadboard system. A block diagram of the system is shown in Figure 2.1.1-2.

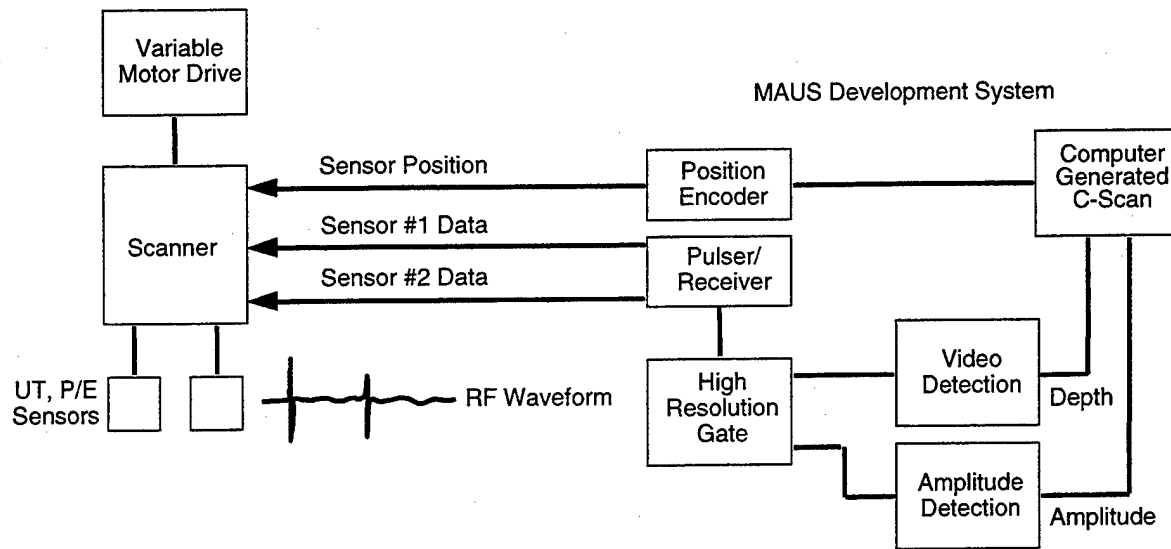
### ***Continuous Wave Breadboard System***

During the early stages of the program, the production MAUS system was modified to evaluate the continuous wave inspection methods. The primary MAUS modification was the addition of an A/D signal converter module to the MAUS analog hardware. Signal conditioning



GP94051001.cvs

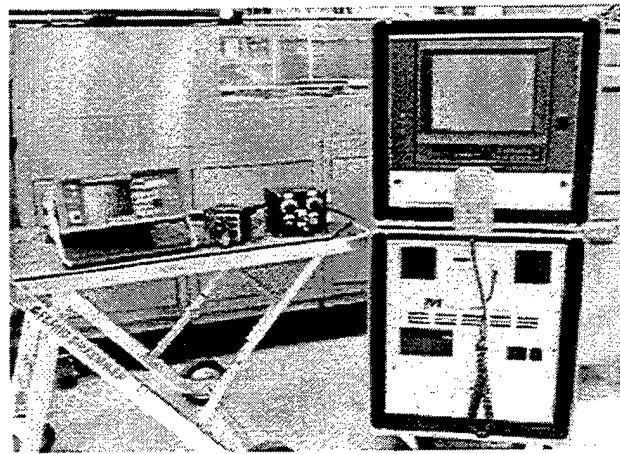
**Figure 2.1.1-1. MAUS Development Station**



GP94031002.cvs

**Figure 2.1.1-2. MAUS Development Station Block Diagram**

hardware was assembled to excite and measure the continuous wave responses from the resonance and eddy current transducers. This hardware was connected to the MAUS through the A/D signal converter module. Figures 2.1.1-3 and 2.1.1-4 show the equipment and a functional block diagram of the system, respectively.



GP94031003.cvs

**Figure 2.1.1-3. Initial Continuous Wave Breadboard System**

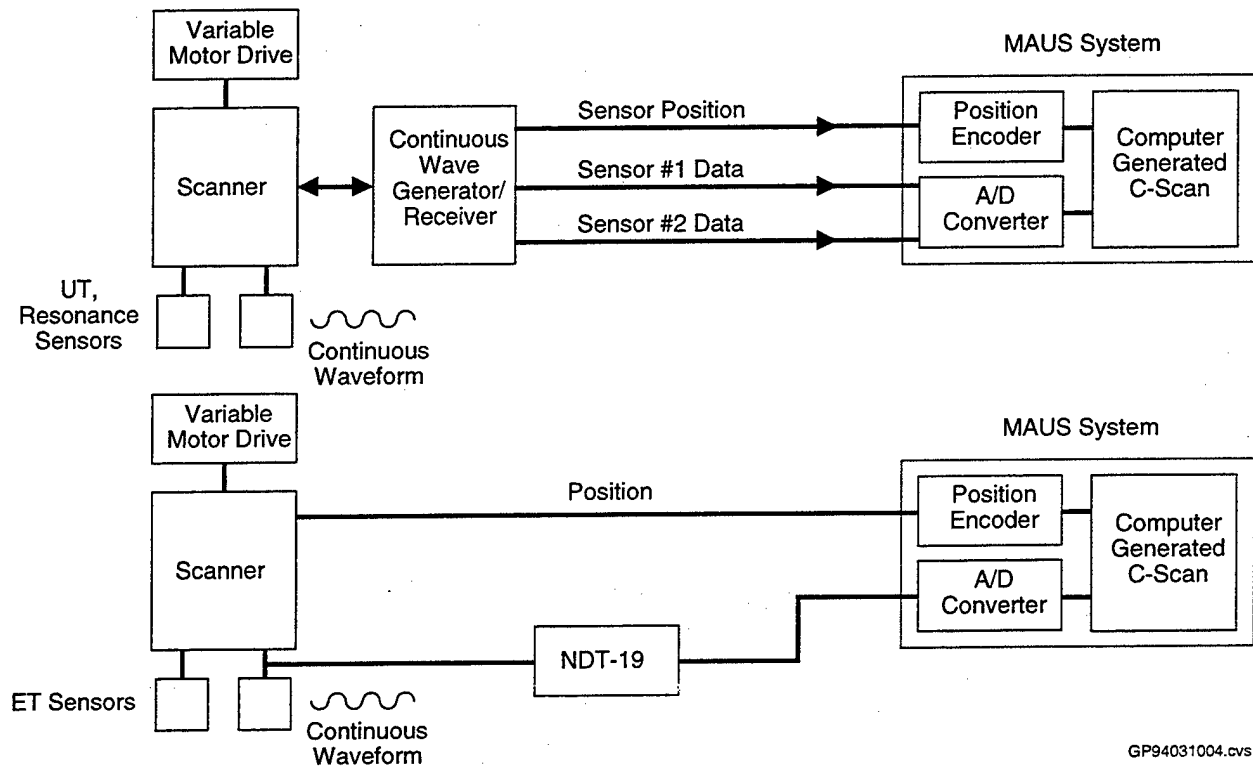


**Figure 2.1.1-4. Continuous Wave Breadboard System Block Diagram**

A “black box” resonance specifically developed for the MAUS was used in the original breadboard assembly. This circuit generated continuous wave signals for resonance transducers and detected changes in the magnitude of the continuous wave signal. These changes in signal magnitude correspond with changes in stiffness within a structure.

The eddy current inspection method was introduced by interfacing a Nortec NDT-19 eddy current flaw detector with the MAUS system. The NDT-19 generates continuous wave signals to drive eddy current sensors. It detects electrical changes in a balanced bridge circuit that are associated with changes in the eddy current field induced in the material. Changes in material properties caused by cracks and/or corrosion can be related to changes in the eddy current field. Amplitude changes in the impedance plane display of the NDT-19 were measured using the MAUS.

### ***Breadboard System Modifications***

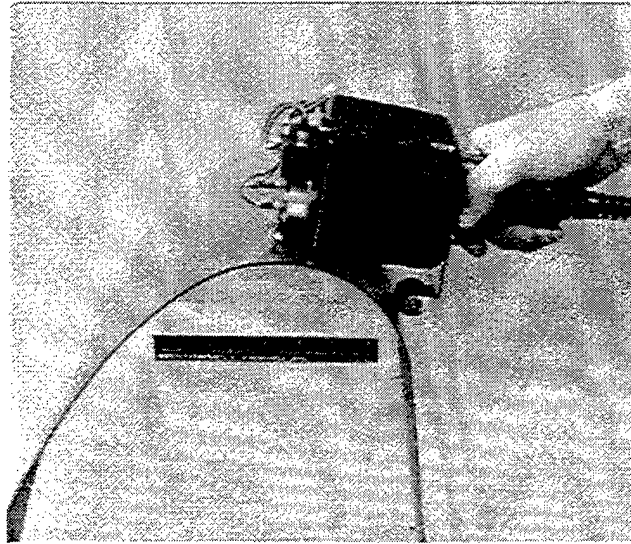
The initial breadboard approach was adequate in verifying the potential benefits of multi-modal inspection system. However, it was not possible to evaluate the inspection parameters such as speed, resolution and sensitivity of the continuous wave modes with this original

breadboard set-up. As a result, the MAUS Development Station was re-configured to include a continuous wave phase detection circuit module.

The prototype continuous wave signal generation and detection circuit was designed to allow full evaluation of the acquisition rates, resolution and sensitivity that could be obtained with the resonance and eddy current inspection modes. The continuous wave phase detection module was used to excite and translate signals from a variety of sensors. The frequency synthesis portion of the circuit generated frequencies ranging from 500 Hz to 2 MHz. The phase detection portion of the circuit measured changes in the continuous wave signal that were induced by changes in structural properties. Phase shifts between the drive and receive signals ranging from 0 to 360 degrees were measured. This module also included circuitry to detect amplitude changes in the continuous wave signal. However, this portion of the module was not implemented during the breadboard phase.

### ***MAUS Scanner Modifications***

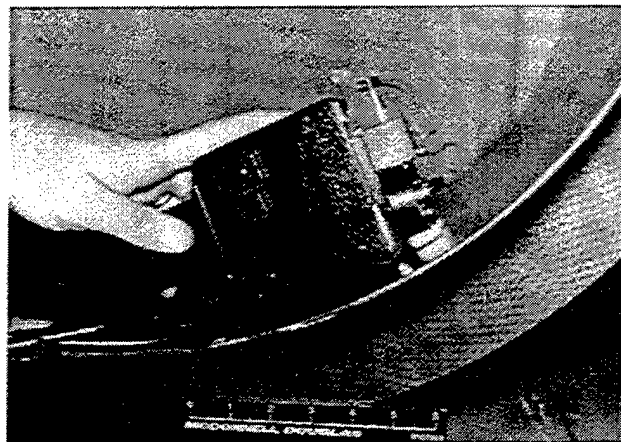
Several modifications to the MAUS scanner were needed to fulfill the requirements of the performance study. Changes were required to allow variable speed adjustments, as well as improvements in the curve-following capabilities of the scanner. A variable power supply was used to drive the DC motor in the scanner. Small changes in the scanner cable were made to connect the supply directly to the scanner motor. The variable power supply allowed precise adjustment of the scan speed for 10, 20 and 30 in/sec. Adjust brackets were also added to the front and back of the scanner to position the scanner on surfaces with convex and concave curvatures. It was important in pulse-echo and resonance testing to orient the sensors such that they are perpendicular to the inspection surface. Constant contact with the surface was required to maintain good signal response. Two adjust brackets were used to hold the scanner sensors perpendicular to the part surface and were quite effective on surfaces with constant curvature. However, when changes in curvature were encountered, the brackets required adjustment to maintain the correct sensor alignment. The rear bracket is shown in Figure 2.1.1-5.



GP94031005.cvs

**Figure 2.1.1-5. Scanner Modified for Inspection of Curved Surfaces**

The resonance inspection mode was very sensitive to changes in contact between the sensor and the surface of the structure. A loop spring was added to the front of the scanner to hold the sensors tightly against the part. This approach proved to be useful for holding the pulse-echo amplitude probes perpendicular to a curved surface as well. The loop spring scanner modification is shown in Figure 2.1.1-6.



GP94031006.cvs

**Figure 2.1.1-6. Scanner Modified with Loop Spring Sensor Mount**



## **2.1.2 Assembly of Test Standards**

### ***Test Article Acquisition***

To provide a substantial cost savings to the program, existing test articles were acquired. This set of test articles included components from previous engineering test programs, scrapped production parts and ongoing developmental efforts. The goal of this subtask was to obtain a broad range of standards to cover the majority of material/structure configurations that may be encountered during a MAUS inspection. These standards also included a range of defect types and geometries that may be encountered during a field inspection. A comprehensive list of the test articles, along with their attributes, is shown in Figure 2.1.2-1.

### ***Test Article Modification***

Selected test articles that did not already contain representative defects were modified to incorporate them. The reference defects added were designed to demonstrate specific inspection capabilities. In most cases, flat bottom holes were machined on the back-side of the standard to generate a reference reflector of a given size at a desired depth. In the solid laminate standards, very small near surface reference reflectors were used to define and demonstrate the detectability limits of the breadboard system. For both metallic and composite bonded assemblies, the flat bottom holes were machined from the back-side of the panel to the bondline interface. The adhesive at the bondline was generally machined away, but in some instances the adhesive was left to simulate the variations that could occur relative to disbonding. Photographs of a representative set of the standards used are shown in Figures 2.1.2-2 through 2.1.2-13.

### ***Baseline Investigations***

Each standard was inspected prior to being used in the performance studies in order to accurately determine its baseline condition. Ultrasonic through-transmission, ultrasonic time-of-flight and radiographic techniques were used to characterize the standards. The ultrasonic data were collected using the production-based automated ultrasonic scanning system (AUSS). The radiographic data were acquired using a static, film-based process.

No.	Material	Construction	Dimensions (in.)	Defect	
				Type	Size (in.)
1	Carbon/Epoxy Skins Aluminum Honeycomb Core	Honeycomb Bonded Assembly Taper Section	6.0 x 6.0 x (1 to 0.4) Skin 0.045 Thick	Cell Repair (1 Total)	1.0 dia
2	Carbon/Epoxy Skins Aluminum Honeycomb	Honeycomb Bonded Assembly Reference Standard	12.0 x 12.0 x 1.06 Skin 0.040 Thick	Crushed Core (4 Total) Unbonds (4 Total) Delaminations (6 Total) Blown Core (2 Total)	0.25 x 0.25 (Delam Only) 0.5 x 0.5 1.0 x 1.0 1 Cell x 1.5 (Standard 2-2)
3	Aluminum Skin Aluminum Honeycomb Core	F/A-18 Leading Edge (Doubler to Core Section)	6.75 x 18.0 x 5.0 Skin 0.0540 - 0.230 Thick	Simulated Unbonds in Doubler and Core (5 Total)	2-0.75 dia Inserts in Doubler 2-0.75 dia Inserts in Skin 1-0.75x2.0 dia Inserts in Skin
4	Aluminum Skin Aluminum Honeycomb Core	F/A-18 Leading Edge (Doubler to Core Section)	Skin 4.5 x 10.6 x 1.1 Thick 0.040 - 0.25	Simulated Unbonds In Doubler (2 Total)	0.75 x 4.5 0.25 x 4.5
5	Carbon/Epoxy Skins Aluminum Honeycomb Titanium Closure	F/A-18 Horizontal Stabilizer Tip	32.0 x 13.0 x 1.3 C/E Skin: 0.085 Thick Ti Closure: 0.035 Thick	Flat Bottom Holes to Simulate C/E to Ti Unbond in Closure (3 Total)	<b>Diameter</b> <b>Depth</b> 0.125 0.085 0.250 0.085 0.50 0.085
6	Polymer Matrix Composite	Leading Edge Radius Section	12.0 Wide x 4.0 Radius Skin 0.090 Thick	Flat Bottom Holes (7 Total)  Slots (4 Total)	<b>Diameter</b> <b>Depth</b> 0.25 0.20 & 0.080 0.125 0.20 & 0.080 0.25 x 1.0 x 0.02 Deep 0.125 x 1.0 x 0.080 Deep
7	Kevlar/Epoxy	Laminate	9.25 x 10.0 x 0.220	Flat Bottom Holes (9 Total)	<b>Diameter</b> <b>Depth</b> 0.125 0.007 0.25 0.015 1.0 0.025
8	Carbon/Epoxy	Cocured Structure With Hat Stiffeners	30.0 x 24.0 x 0.080 Skin Flange: 0.10 Thick	Flat Bottom Holes (6 Total)	<b>Diameter</b> <b>Depth</b> 0.125 0.040 0.25 0.040 0.50 0.040
9	Glass/Epoxy	Laminate Large Radius	17 x 12 x 0.21 Approx 24.0 Radius	High Degree of Porosity Flat Bottom Holes (9 Total)	<b>Diameter</b> <b>Depth</b> 0.125 0.030 0.50 0.125 1.00 0.165
10	Carbon/Epoxy	Laminate With T-Stiffener Cocured and Kevlar Stitched	12.0 x 8.0 x 0.10 0.05 - 0.10 @ Stiffener	Flat Bottom Holes (5 Total)	0.125, 0.25 dia and 0.375 dia at 0.050 and 0.080 Depth
11	Kevlar/Epoxy and Carbon/ Epoxy Spliced Skins, Fiberglass/Phenolic Core	Honeycomb Assembly With Tapering Spliced Skins	7.0 x 5.25 x 0.275 C/E: 0.05 - 0.230 Thick K/E: 0.05 Thick	Shims Between Skin and Core (8 Total)	0.125 Wide 1.25 and 6.75 Long
12	Kevlar/Epoxy and Carbon/ Epoxy Spliced Skins, Fiberglass/Phenolic Core	Honeycomb Assembly With Tapering Spliced Skins	8.0 x 5.0 x 1.275 C/E: 0.085-0.150 Thick K/E: 0.05-0.085 Thick	Shims Between Skin and Core (6 Total)	0.125 Wide 1.25 and 7.87 Long
13	Aluminum	Adhesively Bonded Assembly With Multiple Substructures (T & J-Stiffeners, Doublers)	12.0 x 8.0 Thicknesses: 0.08, 0.05, 0.04, and 0.160	Unbonds (18 Total) 8 - 1st Layer 3 - 3rd Layer 6 - 2nd Layer 1 - 4th Layer	0.5 Squares
14	Aluminum	Adhesively Bonded Skins	18.0 x 6.0 Thicknesses of Each Skin: 0.012 and 0.016	Unbonds (3 Total)	0.5 Square 1.0 Square 1.0 x 2.0

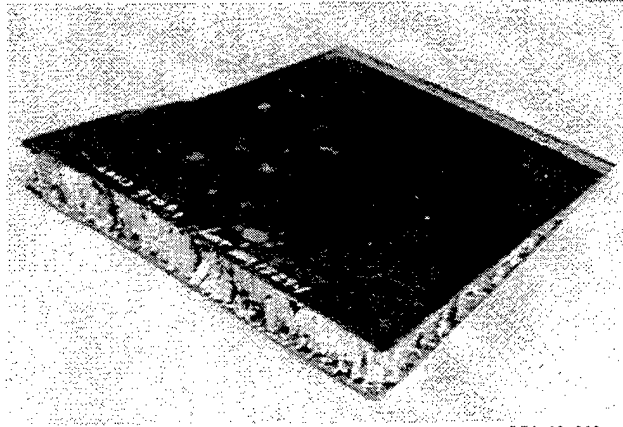
GP94031007.cvs

Figure 2.1.2-1. Description of Test Articles

No.	Material	Construction	Dimensions (in.)	Defect	
				Type	Size (in.)
15	Aluminum	Adhesively Bonded Skins	18.0 x 6.0 Thicknesses of Each Skin: 0.020 and 0.032	Unbonds (3 Total)	0.5 Square 1.0 Square 1.0 x 2.0
16	Aluminum	Adhesively Bonded Skins	18.0 x 6.0 Thicknesses of Each Skin: 0.016 and 0.025	Unbonds (3 Total) Slots (6 Total)	0.5 Square; 1.0 Square; 1.0 x 2.0 0.01 x 0.25 x 0.02 0.015 x 0.45 x 0.02 0.012 x 0.34 x 0.02 0.010 x 0.25 x 0.02 0.020 x 0.54 x 0.02
17	Kevlar/Epoxy Skins Fiberglass/Phenolic Core	Honeycomb Assembly	12.0 x 9.0 x 5.0 Skins: 0.06 Thick	High Attenuation Skin Simulated Unbonds at Core (3 Total)	<b>Diameter</b> <b>Depth</b> 0.25 0.06 0.50 0.06 1.00 0.06
18	Aluminum	2 in. Wide Doubler to Skin Section	12.0 x 8.0 x 0.062 Doubler: 0.150 Thick	Flat Bottom Holes (2 Total)	0.75 dia Each (1 - 0.062 Depth, 2 - 0.064 + 18 mils Adhesive Depth)
19	Aluminum	Riveted Skin	12.0 x 6.0 1st Layer: 0.04 Thick 2nd Layer: 0.063 Thick	Slots at Fasteners Represent Cracks (8 Total)	<b>Lengths in First Layer:</b> 0.05, 0.14, 0.25, 0.4 <b>Lengths in Second Layer:</b> 0.20, 0.35, 0.50, 0.75
20	Aluminum	Riveted Skin	12.0 x 6.0 1st Layer: 0.04 Thick 2nd Layer: 0.063 Thick	Corrosion at Fasteners (8 Total)	0.50 x 0.25 Area and 0.5 x 1.0 Area on Each Layer
21	Aluminum	Skin	12.0 x 6.0 x 0.063	Flat Bottom Holes (5 Total) Around Fastener Holes	<b>Percent Material Removed:</b> 3, 6, 9, 12, 15 (All With 0.5 dia)
22	Carbon/Epoxy	Laminate	8.0 x 5.0 x 0.5	Flat Bottom Holes (17 Total)	(14) 0.50 dia and (3) 0.75 dia Depth Ranges From 0.009 to 0.440
23	Carbon/Epoxy	Stepwedge Laminate	18.0 x 12.0 Thickness From 0.02 to 1.0 (10 Steps)	Flat Bottom Holes (28 Total) Inserts (21 Total)	0.25 and 0.50 dia 0.5 Square (at 10 mils From Front Surface and 10 mils From Back Surface)
24	Quartz/Epoxy Skins Rohacell Core	Bonded Assembly, Resin Transfer Molded	32.0 x 15.0 x 0.75 Skins: 0.03 Thick	Flat Bottom Holes (6 Total)	0.25, 0.5, 1.0 dia 0.050 and 0.25 Depth
25	Quartz/Epoxy	Unidirectional Laminate	13.0 x 13.0 x 0.20	Flat Bottom Holes (9 Total)	0.125, 0.25, 1.0 dia, Depth Range from 0.007, 0.012, & 0.025
26	Thermoplastic	Laminate	8.5 x 8.5 x 0.50 0.06 to 0.50 (6 Steps)	Flat Bottom Holes (24 Total) Inserts (12 Total)	0.25, 0.312, 0.375, 0.50 dia 0.25, 0.312, 0.375, 0.50
27	Aluminum	Plate (Fatigue Specimens)	12.0 x 4.0 x 0.5	Fatigue Cracks (23 Total)	Ranging From 0.009 x 0.05 to (L/D) 0.053 x 0.121
28	Aluminum	Plate (EDM Notch Specimens)	12.0 x 4.0 x 0.5	EDM Notches (29 Total)	Ranging From 0.005 x 0.017 (L/D) to 0.054 x 0.152
29	Carbon/Epoxy	Laminate	3.0 x 12.0 x 0.25	Carbon Epoxy Patch	Voids With Various Sizes to be Compared With X-Ray
30	Carbon/Epoxy	Laminate F-18 Wing Skin	24.0 x 30.0 x 0.90	Flat Bottom Hole (12 Total) 3 - 3rd Layer 1 - 4th Layer	<b>Diameter</b> <b>Depth</b> 0.125 0.010 0.25 0.015 1.0 0.025

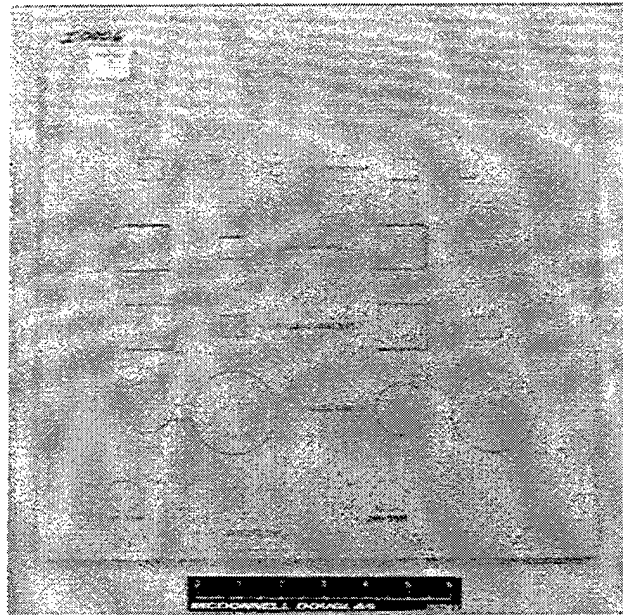
GP94031008.cvs

Figure 2.1.2-1. Description of Test Articles (Cont.)



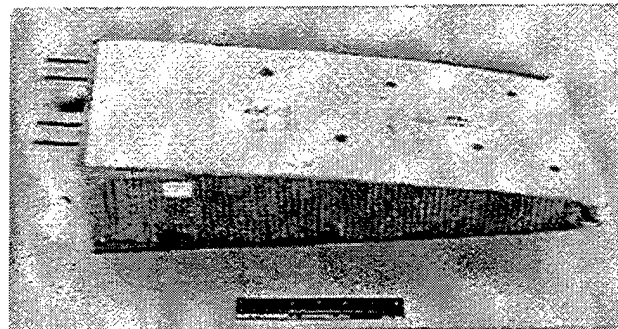
GP94031009.cvs

**Figure 2.1.2-2. Carbon/Epoxy Skins- Aluminum Core/Tapered (Standard #1)**



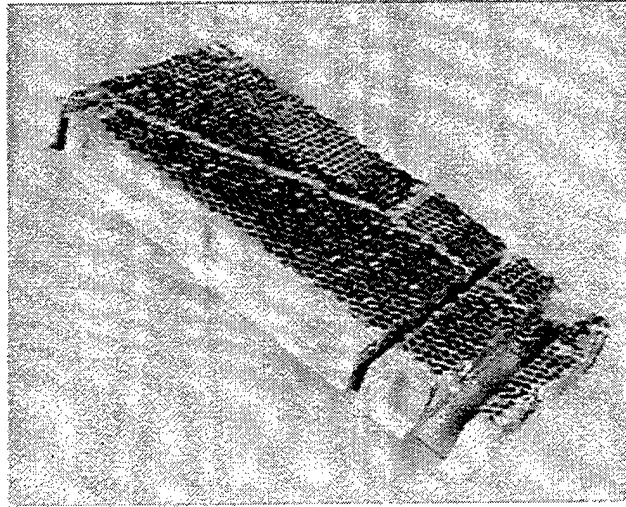
GP94031010.cvs

**Figure 2.1.2-3. Carbon/Epoxy Skins-Aluminum Core/Constant (Standard #2)**



GP94031011.cvs

**Figure 2.1.2-4. Aluminum Skins-Aluminum Core/Tapered (Standard #3)**



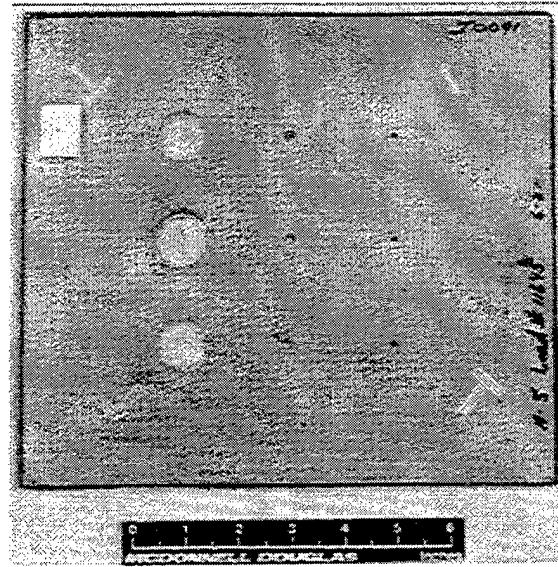
GP94031012.cvs

**Figure 2.1.2-5. Aluminum Skins-Aluminum Core/Constant (Standard #4)**



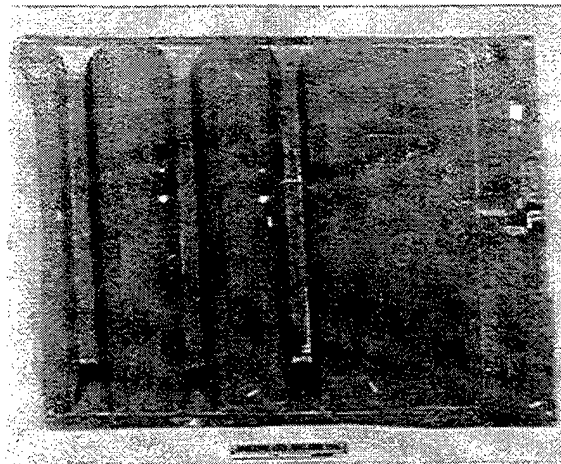
GP94031013.cvs

**Figure 2.1.2-6. Quartz/Epoxy Laminate-Contoured (Standard #6)**



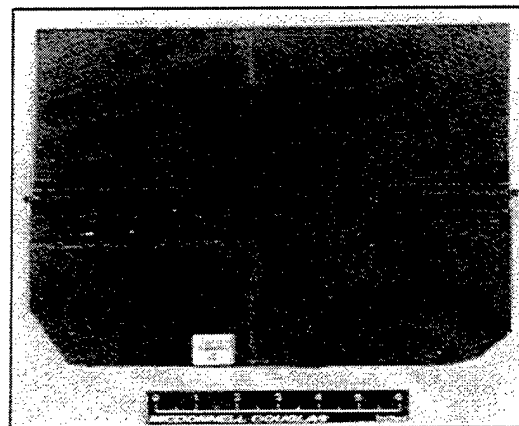
GP94031014.cvs

Figure 2.1.2-7. Kevlar/Epoxy Laminate (Standard #7)



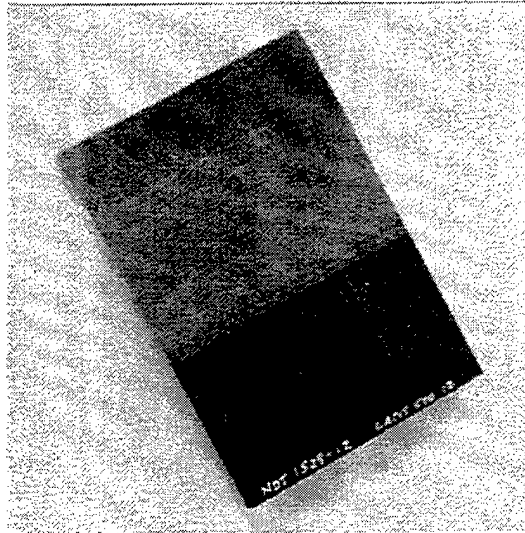
GP94031015.cvs

Figure 2.1.2-8. Carbon/Epoxy Hat-Stiffened (Standard #8)



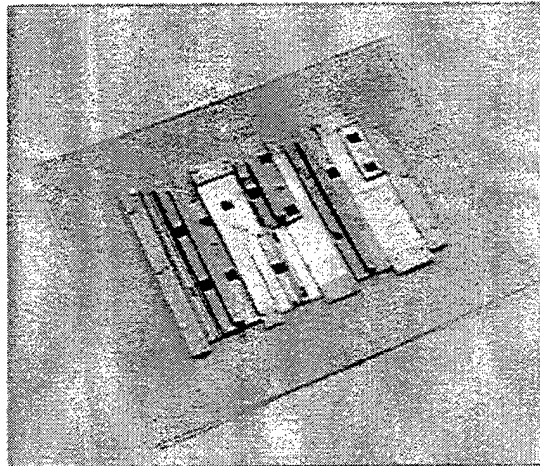
GP94031016.cvs

Figure 2.1.2-9. Stitched Carbon/Epoxy-T-stiffened (Standard #10)



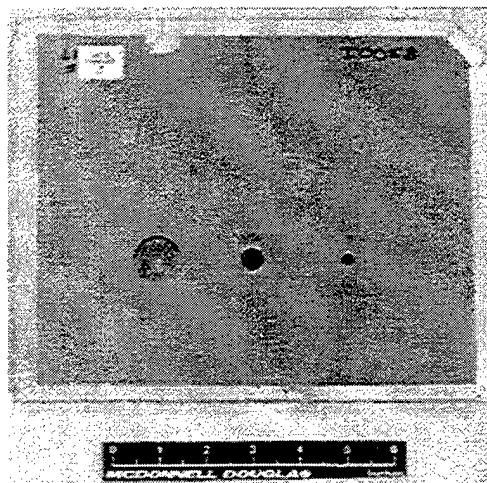
GP94031017.cvs

**Figure 2.1.2-10. Quartz-Carbon/Epoxy Hybrid Skins-Fiberglass/Phenolic Core (Standard #12)**



GP94031018.cvs

**Figure 2.1.2-11. Aluminum-Aluminum Adhesive Bond (Standard #13)**



GP94031019.cvs

**Figure 2.1.2-12. Kevlar/Epoxy Skins-Fiberglass/Phenolic Core (Standard #17)**

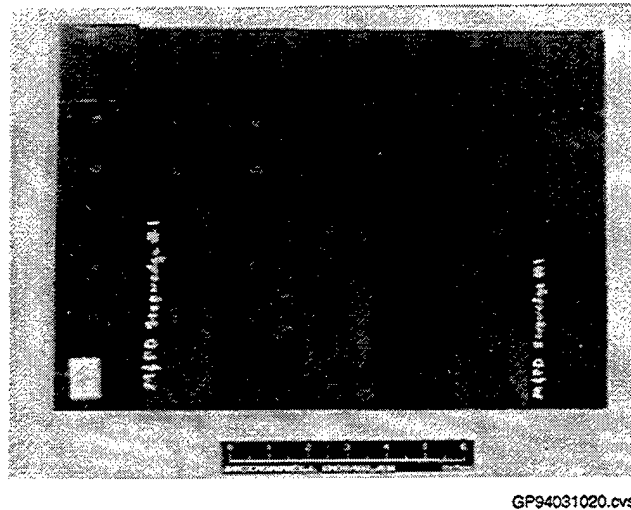


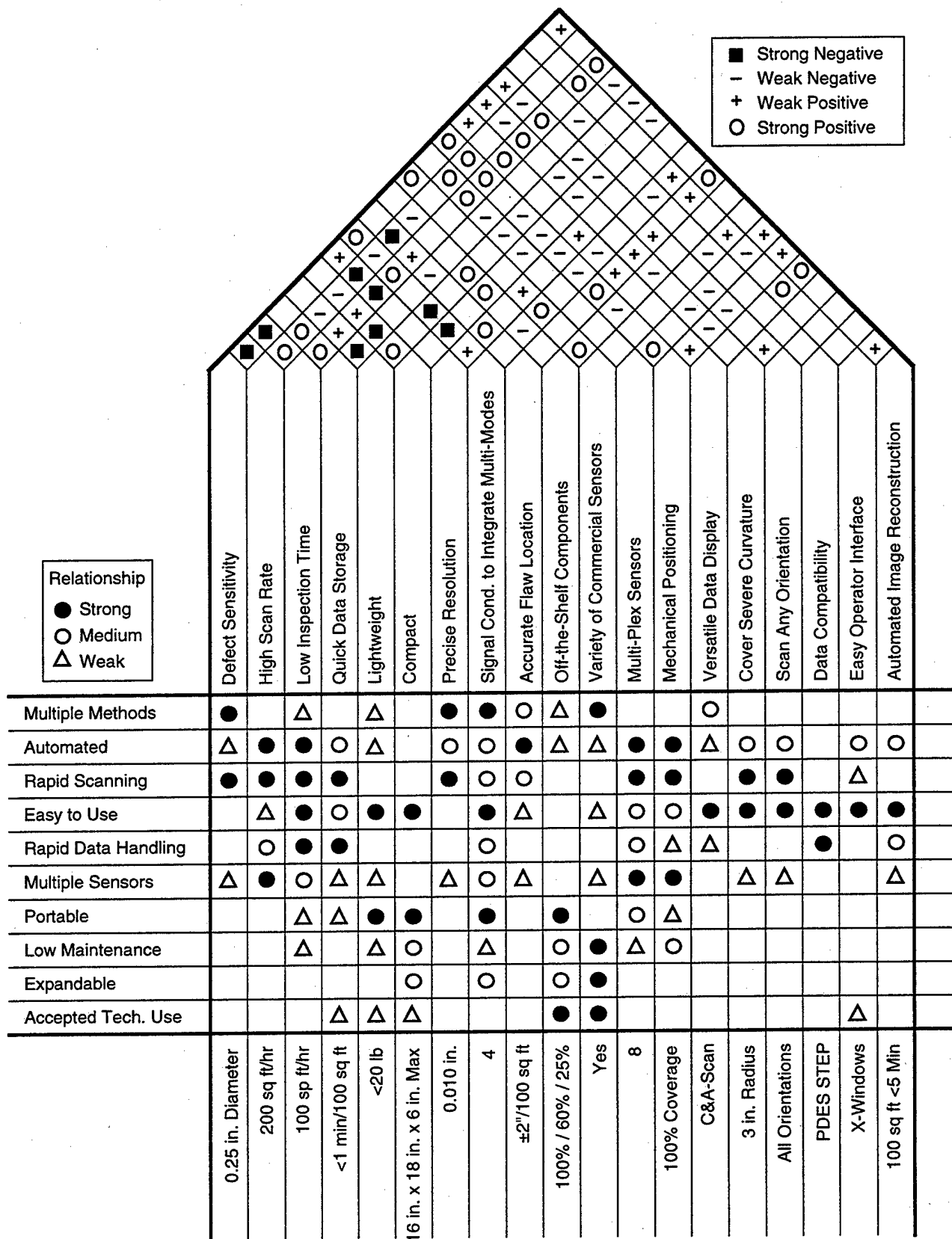
**Figure 2.1.2-13. Carbon/Epoxy Laminate/Variable Thickness (Standard #23)**

### **2.1.3 Performance Studies**

#### ***Quality Function Deployment (QFD)***

During the early stages of the program, QFD was used to assist in determining the areas that would benefit from further breadboard investigations. QFD is a structured planning tool that deploys customer requirements or expectations throughout the product development process. QFD is a multi-step process that compares the customer requirements for the product against the methods for achieving those requirements. The methods for achieving the customers “wants” (or “hows”) are also correlated to determine their interactions. The correlation identifies “hows” that either conflict or have a positive or synergistic effect when both actions are taken simultaneously. The identified conflicts help to highlight areas that require further investigation or the performance of trade studies. All of the information pertaining to the QFD process was displayed in a matrix called a “House of Quality”. The House of Quality developed during the initial stages of the program is shown in Figure 2.1.3-1. This evaluation not only assisted in identifying important design considerations, but also served as an effective communication tool that conveyed the rationale for design decisions to the customer. The primary result from this analysis was that there is a trade-off expected between obtaining high defect sensitivity while maintaining rapid inspection rates. It was also determined that the incorporation of multiple inspection modes would have a significant effect on the ability to minimize its size and weight. As a result, the performance studies focused on these major concerns.





GP94031021.cvs

Figure 2.1.3-1. Mobile Automated Scanner "House of Quality"

## Multi-Modal Evaluation of Test Articles

Each test article was interrogated using each of the inspection modes. For recording and comparison purposes, a matrix correlating each mode to the applicable performance parameters was generated. Results of the evaluation were determined subjectively and subsequently recorded. An example of the recording form and description of the evaluation criteria used is shown in Figure 2.1.3-2.

LACIS-1 Specimen #2 C/E Skins / Aluminum H/C Assembly		PERFORMANCE PARAMETER			
METHOD / DEFECT TYPE	Freq.	Defect Sensitivity 15 / 20 / 30	Precise Resolution 15 / 20 / 30	Image Repeatability 15 / 20 / 30	Ease of Use
Eddy Current					
Crushed Core					
Unbonds		N/A	N/A	N/A	
Delaminations		N/A	N/A	N/A	
Blown Core					
Resonance	161 KHz				○
Crushed Core		● ○ △	○ △ △	○ ○ ○	
Unbonds		● ● ●	● ● ●	● ● ●	
Delaminations		● ● ●	● ● ●	● ● ●	
Blown Core		X X X	X X X	X X X	
UT/P-E Time-of-flight	2.25 MHz				△
Crushed Core		X X X	X X X	X X X	
Unbonds		X X X	X X X	X X X	
Delaminations		● ● ●	● ● ●	● ● ●	
Blown Core		X X X	X X X	X X X	
UT/P-E Amplitude	2.25 MHz				△
Crushed Core		● ● ●	● ● ●	● ● ●	
Unbonds		● ● ●	● ● ●	● ● ●	
Delaminations		● ● ●	● ● ●	● ● ●	
Blown Core		△ X X	△ X X	△ X X	
<b>CRITERIA</b> <b>Defect Sensitivity</b> ● - Readily detects smallest defect ○ - Smallest defect barely detectable △ - Detects large defect only X - Cannot detect defect <b>Resolution / Edge Definition</b> ● - Clearly displays edges of all defects ○ - Slight hysteresis around edges of defects; .040" hysteresis △ - Moderate hysteresis; blurred image of defect edges .080" hysteresis X - Unacceptable hysteresis; greater than .120" hysteresis <b>Repeatability</b> ● - Defects detected and image sized within 10% each scan ○ - Defects detected and image sized within 25% each scan △ - Defects detected and image sized within 50% each scan X - Cannot detect defect <b>Ease of Use</b> ● - Simple to set up ○ - Requires minimal training to first set up △ - Equivalent to standard manual flaw detector X - More difficult than standard manual flaw detector					
<b>Notes:</b> (1)- This std. contains defects in two different cell sizes (2)- Blown core defects consist of 1 cell width only and are considered an extremely minor condition (3)- Higher scan speed appear to result in a slight increase in image repeatability					

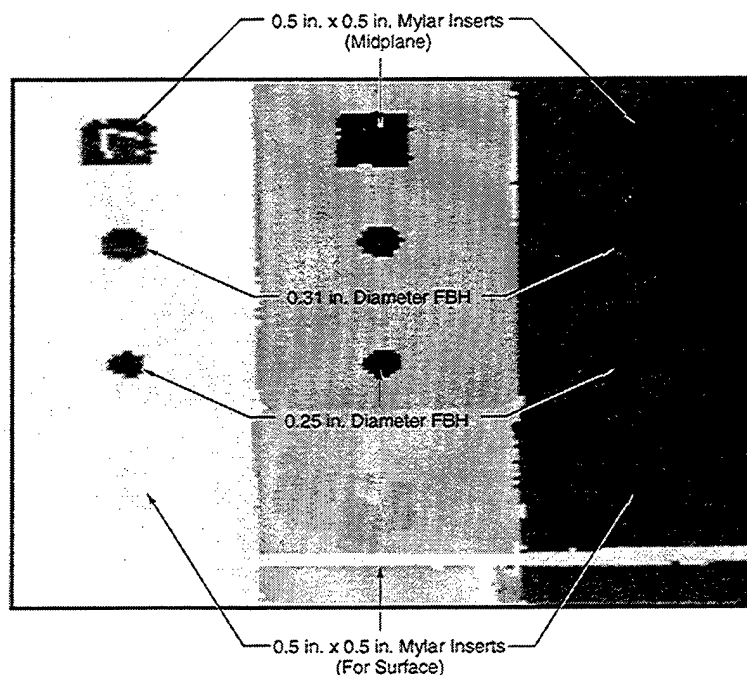
GP94031022.cvs

Figure 2.1.3-2. Performance Evaluation Record

## 2.1.4 Conclusions

### Scanning Speed

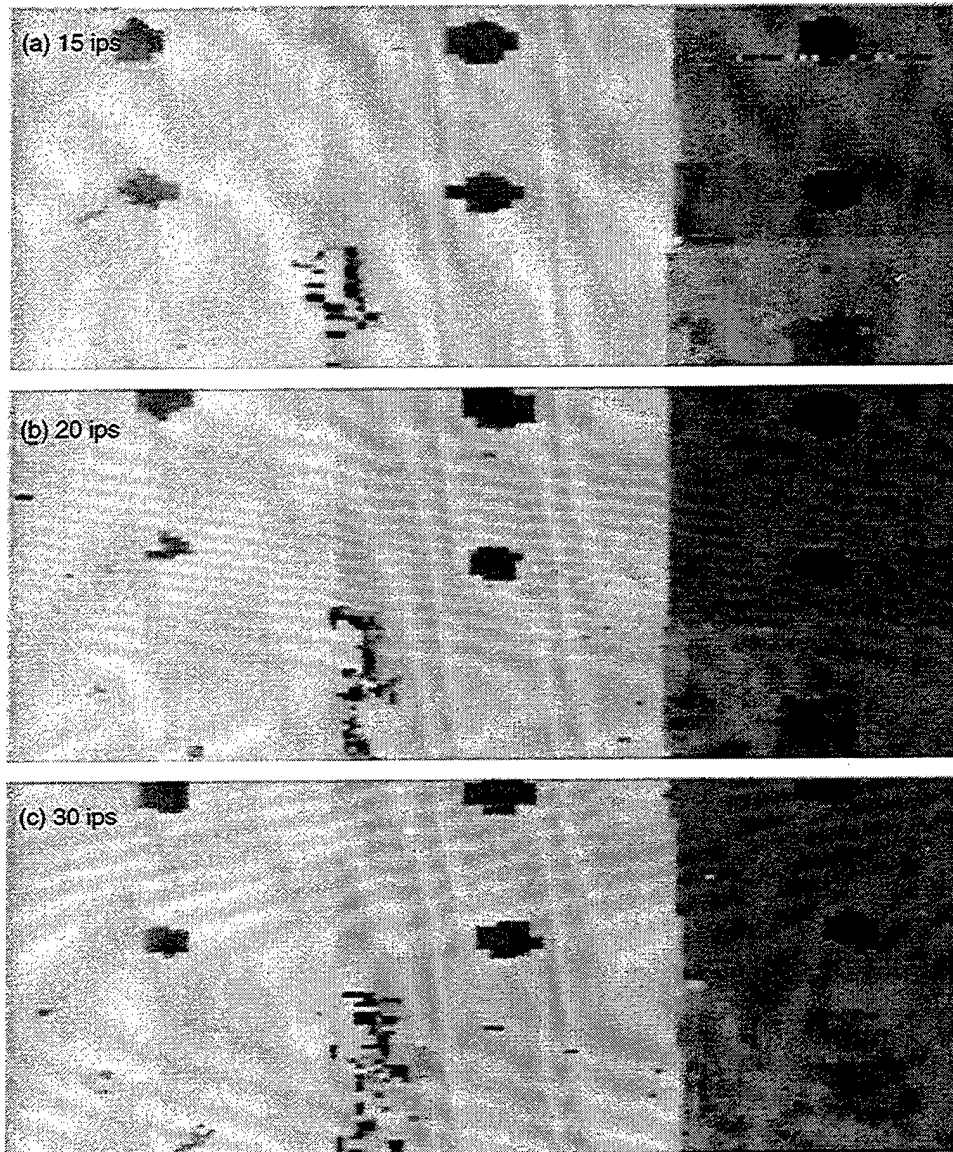
The effect of scanning speed on the ability of each mode to detect small flaws was investigated. Also evaluated was the effect of scanning speed on defect sizing using each inspection mode. Figure 2.1.4-1 shows presents the baseline ultrasonic C-scan of a section of Standard #23 (Carbon/Epoxy step wedge). The defect sizes, types and locations are identified in the figure. Figure 2.1.4-2 shows scans of the same test standard taken at three different scan speeds. The scans were generated using a pulse-echo time-of-flight technique driven by the breadboard system. Set-up parameters and scan speeds are also shown in Figure 2.1.4-2. The images shown indicate that increasing the scan speed in pulse-echo mode resulted in no apparent degradation in defect detection or sizing. Some slight variations exist between the images from the laboratory ultrasonic scanning system used for baseline scanning and the breadboard MAUS.



System	Eng Lab ADIS
Transducer:	7.5 MHz, 0.5 in. Diameter, Immersion
Thickness:	3
Filter:	2
Threshold:	40
CGA:	E5
Gate Start:	113
Gate Width:	107
Near Index:	0.040 in.

GP94031023.cvs

Figure 2.1.4-1. Baseline Scan of Carbon/Epoxy Step Wedge (Standard #23)



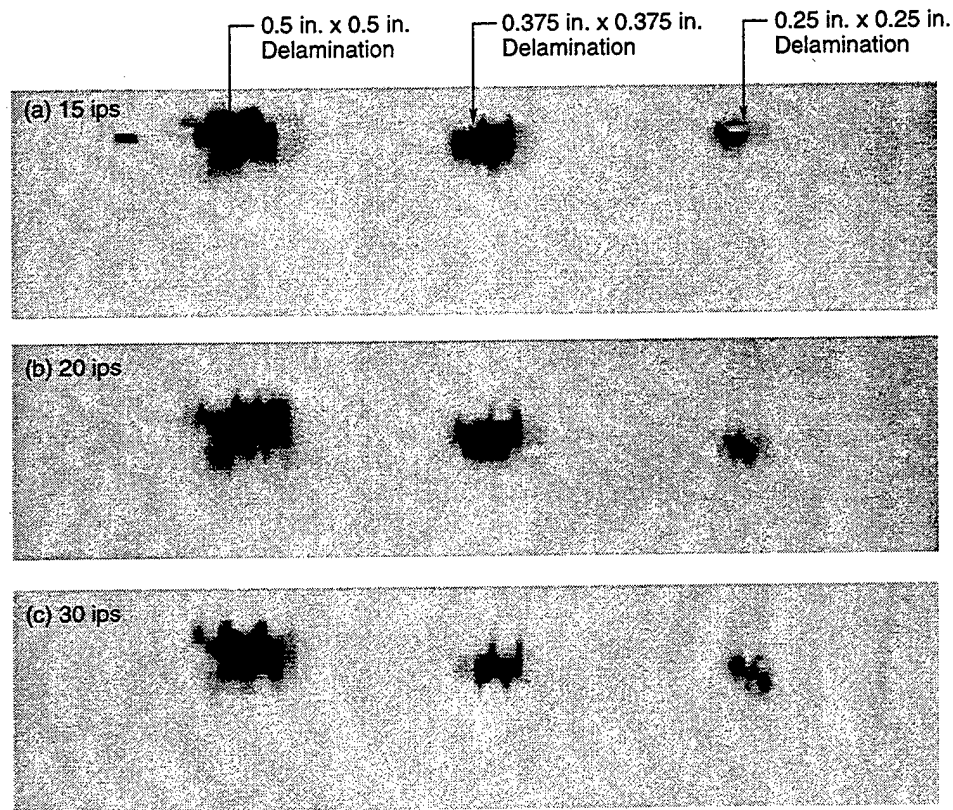
System	MAUS Development Station
Transducer:	5 MHz, 0.25 in. Diameter, Contact Delay
Thickness:	3
Filter:	2
Threshold:	40
TCG Slope:	L1
Gate Start:	14
Gate Width:	15
Near Isolation:	1.49

GP94031024.cvs

**Figure 2.1.4-2. Scan Speed vs. Defect Detection Capability (Pulse-Echo)**

The variations were expected and were due primarily to system differences (transducer diameter, sampling rates, etc.).

Figure 2.1.4-3 shows ultrasonic resonance C-scans generated at three different scanning speeds. Standard #2 (carbon/epoxy skins/aluminum core) was used for this investigation. The variation in scan speed relative to resonance inspection also shows no significant degradation in the ability to consistently image the flaws.



System:	Continuous Wave Breadboard System
Transducer:	150 KHz, 0.6 in. Diameter, Resonance
Channel:	1
Black Box:	519
Voltage:	15V

GP94031025.cvs

**Figure 2.1.4-3. Scan Speed vs. Defect Detection Capability (Resonance)**

From the scanning speed studies, it was determined that image quality and defect sensitivity were not significantly affected by increasing the scan speed. However, increasing the scan speed

did have an adverse effect on the operator's ability to guide and control the scanner. This effect was a major item addressed during the scanner design in the prototype development phase.

### ***Multi-Modal Eddy Current/Ultrasonic Capability***

One concern was the feasibility of scanning simultaneously using eddy current and ultrasonic scanning modes and the effect the ultrasonic couplant would have on the eddy current inspection. A combined inspection was performed on Standard #16 (Aluminum/Aluminum Bond) using ultrasonic resonance and eddy current. Figure 2.1.4-4 shows the images generated during the inspection. No detrimental effects were observed in the eddy current scan due to the presence of couplant.

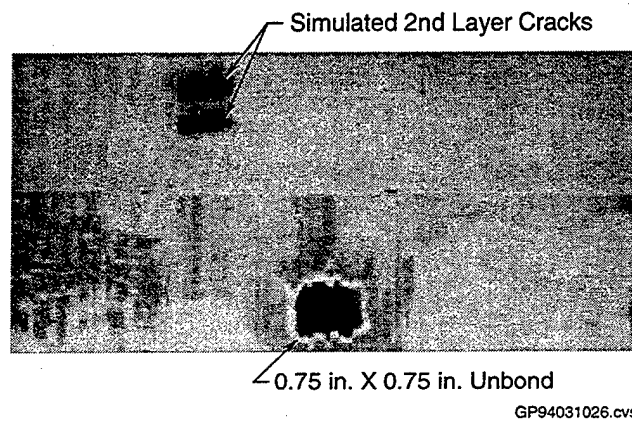


**Figure 2.1.4-4. Multi-Modal C-scan Image (Ultrasonic Resonance/Eddy Current)**

### ***Defect Detection/Inspection Mode Correlation***

As part of the breadboard development task, the applicability of all inspection modes relative to material/structure was determined. A table is presented in Figure 2.1.4-5 that correlates the inspection modes with the test standards and associated defects. The following conclusions were derived from this investigation:

- All defects in each test article were detected using at least one method
- Pulse-echo ultrasonics had superior flaw image definition capabilities
- Continuous wave ultrasonic resonance mode was required in order to detect defects in thin-skin bonded assemblies or multi-layer structures (see Figure 2.1.4-6).
- Eddy current was required only for detection of cracks and corrosion in metallic structures.

No.	Material	Construction	Defect		Eddy Current	Resonance	Amplitude	Time-of-Flight
			Type	Size (in.)				
1	Carbon/Epoxy Skins Aluminum Honeycomb Core	Honeycomb Bonded Assembly Taper Section	Cell Repair (1 Total)	1.0 dia	X	X		
2	Carbon/Epoxy Skins Aluminum Honeycomb	Honeycomb Bonded Assembly Reference Standard	Crushed Core (4 Total) Unbonds (4 Total) Delaminations (6 Total) Blown Core (2 Total)	0.25 x 0.25 (Delamination Only) 0.5 x 0.5 1.0 x 1.0 1 Cell x 1.5 (Standard 2-2)	X X X X	X X X X	X X X X	
3	Aluminum Skin Aluminum Honeycomb Core	F/A-18 Leading Edge (Doubler to Core Section)	Simulated Unbonds in Doubler and Core (5 Total)	2-0.75 dia Inserts in Doubler 2-0.75 dia Inserts in Skin 1-0.75x2.0 dia Inserts in Skin	X X X	X X X		
4	Aluminum Skin Aluminum Honeycomb Core	F/A-18 Leading Edge (Doubler to Core Section)	Simulated Unbonds in Doubler (2 Total)	0.75 x 4.5 0.25 x 4.5	X X	X X		
5	Carbon/Epoxy Skins Aluminum Honeycomb Titanium Closure	F/A-18 Horizontal Stabilizer Tip	Flat Bottom Holes to Simulate C/E to Ti Unbond in Closure (3 Total)	Diameter Depth 0.125 0.085 0.250 0.085 0.50 0.085	X X X	X X X		
6	Polymer Matrix Composite	Leading Edge Radius Section	Flat Bottom Holes (7 Total)  Slots (4 Total)	Diameter Depth 0.25 0.20 & 0.080 0.125 0.20 & 0.080 0.25 x 1.0 x 0.02 Deep 0.125 x 1.0 x 0.080 Deep	X X X X	X X X X	X X X X	
7	Kevlar/Epoxy	Laminate	Flat Bottom Holes (9 Total)	Diameter Depth 0.125 0.007 0.25 0.015 1.0 0.025	X X X	X X X	X X X	
8	Carbon/Epoxy	Cocured Structure With Hat Stiffeners	Flat Bottom Holes (6 Total)	Diameter Depth 0.125 0.040 0.25 0.040 0.50 0.040	X X X	X X X	X X X	
9	Glass/Epoxy	Laminate Large Radius	High Degree of Porosity Flat Bottom Holes (9 Total)	Diameter Depth 0.125 0.030 0.50 0.125 1.00 0.165	X X X	X X X	X X X	
10	Carbon/Epoxy	Laminate With T-Stiffener Cocured and Kevlar Stitched	Flat Bottom Holes (5 Total)	0.125, 0.25 dia and 0.375 dia at 0.050 and 0.080 Depth	X	X		
11	Kevlar/Epoxy and Carbon/ Epoxy Spliced Skins, Fiberglass/Phenolic Core	Honeycomb Assembly With Tapering Spliced Skins	Shims Between Skin and Core (8 Total)	0.125 Wide 1.25 and 6.75 Long	X	X		
12	Kevlar/Epoxy and Carbon/ Epoxy Spliced Skins, Fiberglass/Phenolic Core	Honeycomb Assembly With Tapering Spliced Skins	Shims Between Skin and Core (6 Total)	0.125 Wide 1.25 and 7.87 Long	X	X		
13	Aluminum	Adhesively Bonded Assembly With Multiple Substructures (T & J-Stiffeners, Doublers)	Unbonds (18 Total) 8 - 1st Layer 3 - 3rd Layer 6 - 2nd Layer 1 - 4th Layer	0.5 Squares	X			
14	Aluminum	Adhesively Bonded Skins	Unbonds (3 Total)	0.5 Square 1.0 Square 1.0 x 2.0	X X X			
15	Aluminum	Adhesively Bonded Skins	Unbonds (3 Total)	0.5 Square 1.0 Square 1.0 x 2.0	X X X			
16	Aluminum	Adhesively Bonded Skins	Unbonds (3 Total) Slots (6 Total)	0.5 Square: 1.0 Square: 1.0 x 2.0 0.01 x 0.25 x 0.02 0.015 x 0.45 x 0.02 0.012 x 0.34 x 0.02 0.010 x 0.25 x 0.02 0.020 x 0.54 x 0.02	X X			
17	Kevlar/Epoxy Skins Fiberglass/Phenolic Core	Honeycomb Assembly	High Attenuation Skin Simulated Unbonds at Core (3 Total)	Diameter Depth 0.25 0.06 0.50 0.06 1.00 0.06	X X X	X X X	X X X	
18	Aluminum	2 in. Wide Doubler to Skin Section	Flat Bottom Holes (2 Total)	0.75 dia Each (1 - 0.062 Depth, 2 - 0.064 + 18 mils Adhesive Depth)	X			
19	Aluminum	Riveted Skin	Slots at Fasteners Represent Cracks (8 Total)	Lengths in First Layer: 0.05, 0.14, 0.25, 0.4 Lengths in Second Layer: 0.20, 0.35, 0.50, 0.75	X			
20	Aluminum	Riveted Skin	Corrosion at Fasteners (8 Total)	0.50 x 0.25 Area and 0.5 x 1.0 Area on Each Layer	X			
21	Aluminum	Skin	Flat Bottom Holes (5 Total) Around Fastener Holes	Percent Material Removed: 3, 6, 9, 12, 15 (All With 0.5 dia)	X			
22	Carbon/Epoxy	Laminate	Flat Bottom Holes (17 Total)	(14) 0.50 dia and (3) 0.75 dia Depth Ranges From 0.009 to 0.440	X	X	X	X
23	Carbon/Epoxy	Stepwedge Laminate	Flat Bottom Holes (28 Total) Inserts (21 Total)	0.25 and 0.50 dia 0.5 Square (at 10 mils From Front Surface and 10 mils From Back Surface)	X	X	X	X
24	Quartz/Epoxy Skins Bihacell Core	Bonded Assembly, Resin Transfer Molded	Flat Bottom Holes (6 Total)	0.25, 0.5, 1.0 dia 0.050 and 0.25 Depth	X	X	X	X
25	Quartz/Epoxy	Unidirectional Laminate	Flat Bottom Holes (9 Total)	0.125, 0.25, 1.0 dia, Depth Range from 0.007, 0.012, & 0.025	X	X	X	X
26	Thermoplastic	Laminate	Flat Bottom Holes (24 Total) Inserts (12 Total)	0.25, 0.312, 0.375, 0.50 dia 0.25, 0.312, 0.375, 0.50	X	X	X	X
27	Aluminum	Plate (Fatigue Specimens)	Fatigue Cracks (23 Total)	Ranging From 0.009 x 0.05 to (D/L) 0.053 x 0.121	X			
28	Aluminum	Plate (EDM Notch Specimens)	EDM Notches (29 Total)	Ranging From 0.005 x 0.017 (D/L) to 0.054 x 0.152	X			
29	Carbon/Epoxy	Laminate	Carbon Epoxy Patch	Voids With Various Sizes to be Compared With X-Ray		X	X	
30	Carbon/Epoxy	Laminate F-18 Wing Skin	Flat Bottom Hole (12 Total)	Diameter Depth 0.125 0.010 0.25 0.015 1.0 0.025	X X X	X X X	X X X	

GP94031027.cvs

Figure 2.1.4-5. Correlation Study Summary

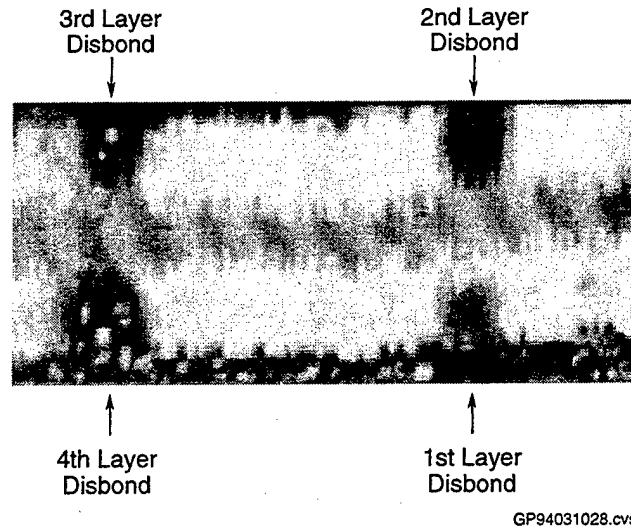


**Figure 2.1.4-6. Ultrasonic Resonance Scan of Multi-Layered Adhesive Bonded Aluminum Structure**

### **2.1.5 Prototype Design Concept**

#### ***Prototype LACIS/MAUS System***

The prototype LACIS/MAUS system concept was presented at the Preliminary Design Review at the Air Force Research Laboratory. The prototype system consisted of three main elements: signal conditioning, data management and interchangeable scanners. The development of this prototype built upon the proven capabilities of the breadboard system and incorporated many of the features offered in MAUS II and AUSS-based systems.

#### ***Signal Conditioning***

The goals targeted for the prototype signal conditioning package are presented in Figure 2.1.5-1. The signal conditioning hardware used in the breadboard development task was redesigned to achieve these goals. All of the functionality of the breadboard system was maintained, with the new hardware designed to achieve size, weight and power goals for the prototype system. The breadboard hardware was designed using a modular approach that resulted in 14 circuit boards required for multi-modal operation. The prototype hardware integrated the breadboard designs into a dedicated circuit that resided on two to three boards. Programmable logic devices (EPLIDS) were used to replace portions of the integrated circuits required in the hardware. In addition, the power saving features of these EPLIDS reduced the power drawn by the circuits to the minimum level required for operation. Advanced multiple function integrated circuits were used to replace existing circuits when possible.



- Size
  - 8 in. x 11 in. x 2 in.
- Weight
  - 10 lb
- Power Requirements
  - 5 V 2 amp
  - 12 V 1 amp
  - 24 V 1 amp
- Functionally
  - Pulse-Echo Time-of-Flight
  - Pulse-Echo Amplitude
  - Ultrasonic Resonance
  - Eddy Current
  - Ethernet Communications
  - Automatic Sensor Calibration

GP94031029.cvs

**Figure 2.1.5-1. Target Goals for LACIS/MAUS Signal Conditioning Package**

### ***Data Management***

The data management component consisted of a laptop computer workstation with data acquisition, manipulation, storage, retrieval and communication software. The commercial laptop computer market advances at a very rapid pace. New innovations routinely appear on the market with improved LCD displays and smaller packaging. Based on this, the selection of the computer for the prototype was delayed until the prototype development task. This delay ensured that the best commercially available system with the latest technologies was obtained for the prototype.

The data management software for the LACIS/MAUS prototype was an extension of the system software currently used in the AUSS/product line. This software required a UNIX-based operating system and was written entirely in the C-programming language. This allowed for easy transfer of the software to a wide range of computing platforms. The basic data acquisition, imaging, storage, retrieval and communication functions were already available through the existing software. Additional software functions that were incorporated in the prototype included an expert system database to support the operator in system set-up, and image reconstruction.

The inspection information catalogued during breadboard development identified the appropriate inspection method for a given structure. It defined the resolution, sensitivity, and inspection speed that can be expected when using a particular method. This information was incorporated into an expert system database to advise the operator in defining the approach to take at the beginning of an inspection. The operator may identify the type of structure to be inspected, the material type and the general configuration. The expert system will suggest an inspection mode, type of sensor to be used, and the required settings for the system variables.

The operator may use these settings as the basis for the initial set-up, or request the settings for an alternative approach. The operator will always make the final selection of the system parameters; however, the expert system will be available to support the operator during the selection.

Image reconstruction functions will allow the operator to build a complete image of a large structure from the individual strips of data collected by the scanner. Two approaches were provided for this image reconstruction. The first was a software capability that enabled the operator to identify reference points on two data images. The software merged the data in these two data images using reference points for the data overlay. The second approach was an extension of this software reconstruction capability where an external source was used to define the reference points. This external source used either non-invasive markers on the surface of the structure, or sensors to locate the overall position of the scanner on the structure.

### *Scanners*

Three interchangeable scanners were designed and built for the prototype LACIS/MAUS. One scanner was designed to inspect large, flat surfaces such as wing skins and control surfaces. These applications require simple scanner manipulation and maximum area coverage. The second scanner was designed to inspect areas with compound, complex curvature such as leading edges, nose cones and inlet ducts. The design goal for this scanner was to maintain sensor contact with the part surface despite constant changes in curvature. The third scanner was designed to inspect areas with limited access, such as internal ribs and spars and tight radius areas. The major consideration for this scanner is physical size.

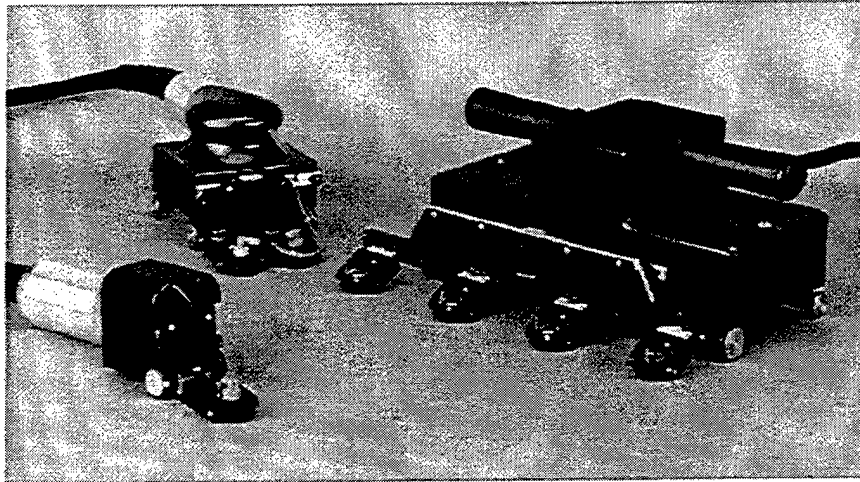
Several common features were incorporated into all three scanners to support the ability to interchange scanners. These include common drive mechanisms, position feedback, signal cabling and sensor mounting. A major design goal was to maximize the number of parts common to all three scanners to reduce the spare parts inventory required for maintaining the scanners. Design goals for each scanner included lightweight, balanced, high-speed operation, multiple sensors, easy sensor interchange and ergonomic operation.

## 2.2 Prototype Development

Assembly of the prototype MAUS III system was completed in May 1993. The system, shown in Figure 2.2-1, consisted of a laptop workstation computer, signal conditioning electronics and a curve-following scanner. Additional scanners are shown in Figure 2.2-2. The physical dimensions, weight and design goals of each component are listed in Figure 2.2-3. All of the major signal conditioning circuits were fully evaluated, system software check and refined and scanner mechanisms operated extensively. The final system specifications for the MAUS III are shown in Figures 2.2-4 and 2.2-5[2].



**Figure 2.2-1. Prototype MAUS III System**



GP94031031.cvs

**Figure 2.2-2. Additional Scanners for MAUS III**

Component	Physical Size (in.)	Actual Weight (lb)	Design Goal (lb/in.)
Laptop Computer	8.5 x 11 x 2	7 lbs	< 9/ 8.5 x 11 x 2
Signal Conditioner	11 x 11 x 5.5	14 lbs	< 20/ 8.5 x 11 x 2
Curve Follower Scanner	4 x 4 x 7	4 lbs	< 4/ 4 x 4 x 8
Tight Access Scanner	3 x 3 x 7	2 lbs	< 3/ 2 x 2 x 8
Large Area Scanner	12 x 9 x 4	8 lbs	6/ 12 x 12 x 4

GP94031032.cvs

**Figure 2.2-3. MAUS III Physical Parameters vs. Design Goals**

Feature	Specification
<b>Timing</b>	
Gate Triggers P/E Depth Gate P/E Amplitude Gate 1 P/E Amplitude Gate 2 Front Surface Discriminator Timing Resolution	Main Bang, 1st or 2nd Interface 0.10 to 50.0 microseconds 0.10 to 50.0 microseconds 0.10 to 50.0 microseconds 0.01 to 5.00 microseconds 0.01 microseconds
<b>Pulse-Echo Pulsar/Receiver</b>	
DC Excitation Voltage Peak Voltage into 50 Ohms Rise Time (10-90%) Input Maintenance Gain Frequency Response	475 VDC 300 VDC 20 nanoseconds 50 ohms 6 dB $\pm 1$ dB to 20 MHz
<b>Pulse-Echo Data Acquisition</b>	
Input Dynamic Range Frequency Range Threshold Range Filter Range	32 dB 2.25 - 15 MHz 0 - 100% 2, 4, 8, 12 MHz
<b>Pulse-Echo Data Conversion</b>	
Distance Amplitude Correction Modes Range Thickness Resolution Front Surface Resolution Back Surface Resolution Maximum Thickness	(DAC curves) Exponential (Defaults) or Programmable 32 dB 20 nanoseconds (0.001" in C/E) 0.02" in C/E 0.01" in C/E 40 microseconds (2.6" in C/E)
<b>Signal Digitizer</b>	
Clock Frequency Conversion Frequency Resolution Triggers Base Range Delay Range Channels Signal Channel Options Auxiliary Channel Options	40 MHz Up to 20 MHz 25 nanoseconds Main Bang or 1st Interface 20, 35 or 50 microseconds 0, 5, 10, 15, 20 microseconds 2 Video, Gated Amplitude, R/F Event Mark, Depth Gate, Amplitude Gates

GP94031033.cvs

**Figure 2.2-4. MAUS III Signal Conditioning Specifications**

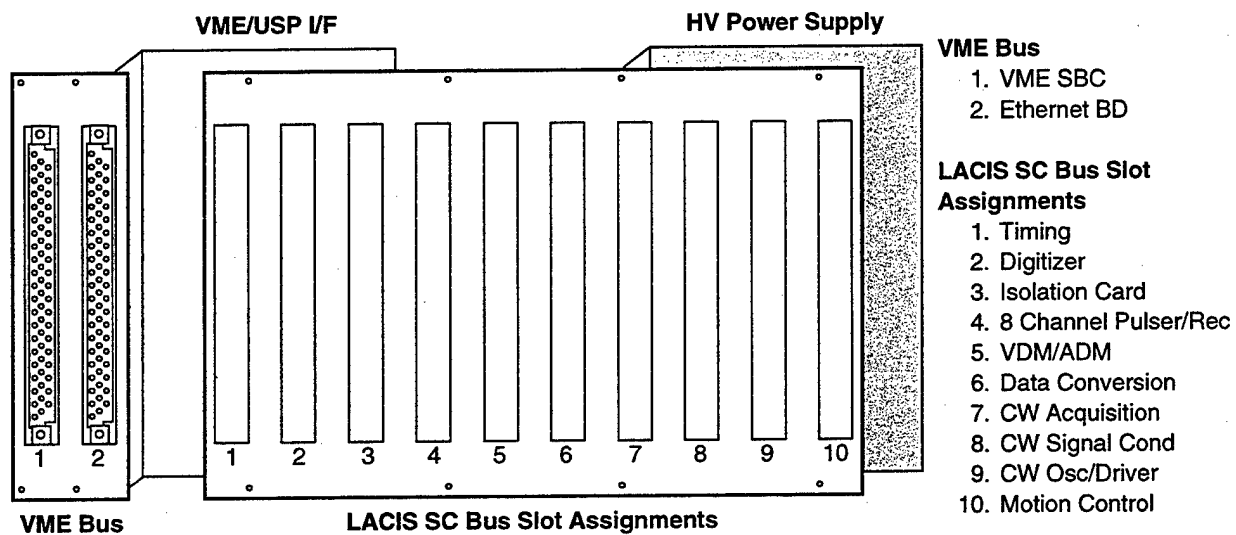
Feature	Description
<b>Computer</b>	
Processor Memory Hard Disk Drive Data Storage Capacity  Laptop Display Resolution External Resolution	40 MHz SPARC RISC 16 MB 500 MB 3,500 sq ft @ 0.04 in. Resolution 14,000 sq ft @ 0.08 in. Resolution 56,000 sq ft @ 0.16 in. Resolution 640 x 480, 1152 x 900 Emulation 1152 x 900
<b>Archive Data Storage</b>	
Optical Disk Storage Size Data Storage Capacity	Read/Write, 5.25 in. Removable Optical Disk 660 MB 7,680 sq ft @ 0.04 in. Resolution 30,760 sq ft @ 0.08 in. Resolution 123,000 sq ft @ 0.16 in. Resolution
<b>C-Scan Display</b>	Display Inspection Data as an Area Image
Point Measurement  Linear Measurement  Area Measurement Histogram  Defect Area  Annotations Text Measurements Histograms	Display the Data Value at Any Point on the C-Scan Image. Point Values in Inches for P/E Depth, dB for P/E Amplitude, and Counts for Resonance and Eddy Current Display the Linear Measurement Between User-Selected Points on the C-Scan Image Display the Measured Area Within a User-Selected Boundary Display the Histogram Analysis of the Data Located Within a User Selected Boundary Display the Area of Data Within the Histogram Boundary That Fulfills the Defect Criteria Defined By the User Store Operator Annotations With C-Scan Data Text Messages to Identify Sections of Data Results of Point, Measure, and Area Measurements Results of Histogram Analyses
<b>A-Scan Display</b>	Display Inspection Data as an Individual Signal
P/E Video Display P/E Gated Amplitude Timing Signals Resonance Freq. Sweep	Standard Flaw Detector Format - Video Video Signal Modified With the Amplitude Gates Auxiliary Signal to Display Gates or Event Marks Frequency Sweep of Resonance Sensors
<b>System Setup</b>	Systems Setups Stored in Disk Files for Fast Configuration Changes
Setup Files File Management P/E Depth P/E Amplitude Resonance Eddy Current Scanner Display	Setup Files are Recalled and Saved in a Simple Menu Menus for Setup File Copy and Delete Depth Gate, Filters, Threshold, Sensor Gains Amplitude Gates, Sensor Frequency, Sensor Gains Sensor Frequency, Gains, Auto-Null, Auto-tune Sensor Frequency, Gains, Auto-Null Configuration: Sensor Type, Width of Scan, Flaw Size Format Information for C-scan Display
<b>Data Archive</b>	Store and Retrieve Data Files From an Optical Disk
Store Restore Library	Store Data Files to the Optical Disk Retrieve Data Files by Name or With Template View Library of All Data Files Stored on Optical Disks

GP94031034.cvs

**Figure 2.2-5. MAUS III Data System Specifications**

### 2.2.1 Signal Conditioning Subsystem

The signal conditioning subsystem included all of the electronic circuits required to measure scanner position and to collect ultrasonic pulse-echo, resonance and eddy current data. A schematic of the MAUS III signal conditioning enclosure is shown in Figure 2.2.1-1. It was assembled using a standard VME-bus chassis and two VME-bus backplanes. A dual element backplane was used for the VME microprocessor cards that controlled the signal conditioning circuitry. The ten-element backplane provided the basic bus structure for the signal conditioning bus. The VME-bus format was selected for these backplanes since several vendors were available to supply ready-made hardware. However, the Signal Conditioning Bus (SCB) did not emulate the standard VME-bus pin assignments. The pin assignments were completed based on the requirements for the signal conditioning electronics. Figure 2.2.1-2 identifies each of the circuit boards and the functions they perform relative to the full system.



GP94031035.cvs

Figure 2.2.1-1. Schematic of MAUS III Signal Conditioning Enclosure

Circuit Board	Function	Type of Board	Location
Data System Processor (DSP)	Master Control for the Signal Conditioning Subsystem	Printed Circuit	DSP Backplane
Data Link Processor (DLP)	Data Link to the Data Management Computer	Printed Circuit	DSP Backplane
VME to SCB Interface	Signal Connection Between the DSP and the Signal Conditioning Electronics	Wire Wrap	Between DSP and SCB B/P
System Timing	Signal Gates, Sync Signals, Event Mark Timing	Wire Wrap	SCB Backplane
P/E Pulser/Receiver	Pulse-Echo Pulsers and Receiver Amplifiers	Printed Circuit	SCB Backplane
P/E Video and Amplitude Detection	Video Conversion and Detection Circuitry for P/E Depth and Amplitude Measurement	Printed Circuit	SCB Backplane
P/E Data Conversion	Convert Depth and Amplitude Measurements to Digital Values	Printed Circuit	SCB Backplane
Signal Digitizer	Convert Analog Signals to Digital Values for A-Scan Display	Wire Wrap	SCB Backplane
RES/EC Frequency Generation	Frequency Generator for Resonance and Eddy Current Sensors	Printed Circuit	SCB Backplane
RES/EC Signal Conditioning	Signal Converter for Continuous Waveform Sensors Such as Resonance and Eddy Current	Printed Circuit	SCB Backplane
RES/EC Data Acquisition	Convert RES/EC Measurements to Digital Values	Printed Circuit	SCB Backplane
Motion Control Processor (MCP)	Measures Scanner Position, Controls Scanner Motor	Printed Circuit	SCB Backplane
Scanner Switch Input	Reads Switch Inputs Lights Status LEDs	Wire Wrap	Scanner
Front Panel Switch Input	Read Front Panel Switches and Data Inputs	Wire Wrap	Front Panel
Power Supply Board	Power Modules For Scanner Control and High Voltage Pulser	Wire Wrap	SCB Backplane

P/E = Pulse Echo    SCB = Signal Conditioning Bus    RES/EC = Resonance/Eddy Current

GP94031036.cvs

**Figure 2.2.1-2. Summary of Signal Conditioning Subsystem Components and Their Functions**

### ***DSP and DLP Processors***

The Data System Processor (DSP) is the main processor for the signal conditioning electronics. The DSP configured all of the circuits based on configuration files received from the Data Manager (DM). The DSP also controlled the circuits which excited each sensor and processed the sensor responses during the data acquisition cycles. The DSP formatted the conditioned information into data packets and transferred them to the DM computer. An OR VCP706-DC16 single board computer was used for the DSP.

The Data Link Processor (DLP) controlled and monitored traffic on the data link between the DSP and the DM computer. All configuration files and data acquisition requests transferred to



and from the DM computer were processed through the DLP. An OR VLAN11C1 single board computer was used for the DLP.

### ***VME/SCB Interface Circuit***

The VME-to-SCB interface circuit included the data bus buffers and the interrupt functions that were used to convert the standard VME signals used with the DSP and the DLP into the standard SCB signals. All signal conditioning set-up information was passed to the acquisition circuits through this interface. All of the information collected from the signal conditioning electronics also passed through this interface card.

All data and address signals were stable as they were translated through the interface. The VME interrupt strategy was fully implemented with processor interrupts available for system set-up, switch inputs and data acquisition functions. The board performed the interface function completely, and no additional changes were required in the design.

This interface circuit design was fabricated as a wire-wrap board, allowing a fast transition from design to prototype. It was effectively used for digital circuits with a small number of components. The majority of the circuitry implemented in the VME/SCB interface resided in two programmable logic devices. All other components in the circuit were high-level digital circuits, so no performance limitations were created using wire-wrap for the fabrication. This board was ultimately replaced with a printed circuit board.

### ***System Timing Board***

The system timing board included the oscillators and timing circuits that were used to create a pulse-echo depth gate, two pulse-echo amplitude gates and a pulse-echo front surface discriminator data acquisition gate. In addition, the timing board included the counting circuits used to measure the pulse-echo depth time-of-flight parameter. The specifications for the timing functions are shown in Figure 2.2.1-3. Each gate included programmable start delays and widths that were set from the DM set-up software. The board performed the timing functions completely, and no additional changes to the design were required.

Feature	Specification
Gate Triggers	Main Bang, 1st or 2nd Interface
P/E Depth Gate	0.10 to 50.0 Microseconds
P/E Amplitude Gates 1 and 2	0.10 to 50.0 Microseconds
Front Surface Discriminator	0.01 to 5.0 Microseconds
Timing Resolution	0.02 Microseconds

GP94031037.cvs

**Figure 2.2.1-3. Timing Function Specifications**

### ***Pulse-Echo Pulser/Receiver Board***

The pulse-echo pulser/receiver board included the amplifier circuits used to excite up to eight ultrasonic sensors with a short/high voltage pulse and the amplifier circuits to measure the responses. The sensor responses were measured and processed as RF signal waveforms. A nominal 6 dB pre-amplifier signal gain was added. The signals from all eight sensors were multiplexed into one RF signal line. This multiplexed RF waveform was connected to the pulse-echo video and amplitude detection board. Figure 2.2.1-4 included the specifications for the pulser-receiver board.

Feature	Specification
D.C Excitation Voltage	475 VDC
Peak Voltage Into 50 Ohms	300 VDC
Rise Time (10-90%)	20 Nanoseconds
Input Impedance	50 Ohms
Gain	6 dB
Gain Frequency Response	+/- 1 dB to 20 MHz

GP94031038.cvs

**Figure 2.2.1-4. Pulser/Receiver Board Specification**

### ***Video and Amplitude Detection (VAD)***

The Video and Amplitude Detection board included the amplifier circuits used to convert the RF signals supplied from the pulser/receiver into video signals. This board also included the circuits used to detect the threshold crossings for depth measurement and the peak signal heights for amplitude measurements. These measurements were detected as analog signals that were transferred to the pulse-echo data conversion board. Figure 2.2.1-5 lists the specifications for the video and amplitude detection board.

Feature	Specification
Input Dynamic Range	32 dB
Frequency Range	2.25 – 15 MHz
Threshold Range	0 – 100%
Filter Range	2, 4, 8, 12 MHz

GP94031039.cvs

**Figure 2.2.1-5. Specifications for the Video and Amplitude Detection Board**

The conversion from RF to video signals was verified for each sensor response. The threshold crossing detector circuits were used to generate timing event marks. The amplitude peak detectors were used to detect peak values and the filter circuitry was subsequently verified. The components for these filters were adjusted with a simple hardware change after the prototype system evaluation was completed. No additional changes were required in the design.

### ***Pulse-Echo Data Conversion Board***

The pulse-echo data conversion board included the circuit used to digitally measure the time between the depth event marks generated on the VAD board. It included the analog conversion circuits used to enhance signal strength when the Distance Amplitude Correction (DAC) function was used. This function included additional amplification for the video signal as a function of time. It was used to compensate for signal losses that were often encountered in thick or attenuative materials. Figure 2.2.1-6 includes the specifications for the pulse-echo data conversion board.

The distance-amplitude correction circuit was adjusted to add a software programmed DAC curve to the video signals. Two DAC curves were programmed for the prototype system. Eight additional curves were included.

Feature	Specification
Distance Amplitude Correction Modes Range	(DAC Curves) Exponential (Default) Programmable 32 dB
Thickness Resolution	20 Nanoseconds (0.001" in C/E)
Front Surface Resolution	0.02" in C/E
Back Surface Resolution	0.001" in C/E
Maximum Thickness	40 Microseconds (2.6" in C/E)

C/E = Carbon Epoxy

GP94031040.cvs

**Figure 2.2.1-6. Specifications for the Pulse-Echo Data Conversion Board**

The counter circuits to measure the time between the threshold crossing event marks were analyzed. A significant amount of noise was identified in these circuits directly after the first event mark signal. The noise affected the near surface detection capability of the system and increased the minimum depth of detection to 0.04 inches below the surface or greater. Minor modifications were made to the circuit in an attempt to reduce this noise level; however, only marginal improvements were attained. An additional evaluation was performed on this board to determine the complete cause of the noise. It appeared that the two-layer printed circuit board layout was causing the problem and a new four-layer design was required to reduce this noise.

### ***Signal Digitizer Board***

The signal digitizer board included circuits used to translate an analog signal to a digitized representation of the analog signal. The specifications for the digitizer functions are shown in Figure 2.2.1-7. Each channel includes programmable start delays and widths that may be set from the DMA A-scan software. The board performed the digitizing functions completely, and no additional changes were required in the design.

Feature	Specification
Clock Frequency	50 MHz
Conversion Frequency	Up to 20 MHz
Resolution	0.04 Microseconds
Triggers	Main Bang or 1st Interface
Base Range	20, 35, or 50 Microseconds
Delay Range	0, 5, 10, 15, 20 Microseconds
Channels	2
Signal Channel Options	Video, Gated Amplitude, RF
Auxiliary Channel Options	Event Mark, Depth Gate, Amplitude Gates

GP94031041.cvs

**Figure 2.2.1-7. Specifications for the Signal Digitizer Board**

### ***Resonance/Eddy Current Frequency Generation Board***

The resonance/eddy current (RES/EC) frequency generation board included the circuitry to generate the drive frequency signals for four resonance or eddy current sensors. Frequencies were set from the DM set up software. Figure 2.2.1-8 presents the specifications for the frequency generator board. The drive signals were measured throughout the frequency range for each sensor channel. No additional changes were required for the final design. This frequency generator circuit was fabricated as a printed circuit board. Several portions of this circuit were used for conditioning low level analog signals. A wire-wrap implementation of this board could have resulted in

Feature	Specification
Drive Voltage	8 Volts P/P
Frequency Range	100 Hz to 3 MHz

GP94031042.cvs

**Figure 2.2.1-8. Specifications for RES/EC Frequency Generation Board**

### ***RES/EC Signal Conditioning Board***

The RES/EC signal conditioning board included the amplifier circuitry to measure the amplitude and phase changes across the conditioning bridge circuit. This board included a null-balance circuit with a controlled D/A converter to perform automatic bridge nulling on a

software request. A peak amplitude detection circuit and a phase detector circuit measured signal changes that occurred in the sensor signal. These circuits resulted in analog voltage signals that represented the amplitude or phase changes. The signals for all sensors were multiplexed into two voltage signals, amplitude and phase. These signals were transferred to the RES/EC data acquisition board. Figure 2.2.1-9 shows the specifications for the RES/EC signal conditioning board.

Feature	Specification
Probe Type	Resonance EC Absolute EC Differential EC Reflection
Inputs	RES - Coaxial Microdot EC - 8 Pin Burndy
Input Range	+/-20 Volts P/P
Gain Range	40 dB (Gain of 200)
Null Balancing	Software Controlled

GP94031043.cvs

**Figure 2.2.1-9. Specifications for the RES/EC Signal Conditioning Board**

The amplitude and phase conversion circuits were adjusted and verified. Minor changes were required in the software timing for the multiplexed signal. Additional time was added to stabilize the detection circuits before the digital signals were converted. The circuit was fabricated as a printed circuit board and no additional changes were required in the design.

### ***Motion Control Processor (MCP) Board***

The motion control processor (MCP) board included the microprocessor, memory and amplifiers used to dynamically control the scanner motor and to measure position information. Standard control software was used to control the scanner motor. Software configuration files were identified for each scanner so that the MCP could optimize scanner performance. Figure 2.2.1-10 lists the specifications for the MCP board. This board was checked with all three scanners, multiple sampling/control intervals and the switch box interface. The MCP was fabricated as a printed circuit board and no significant changes were expected relative to board design.

Feature	Specification
Control Profiles	Sinusoidal Trapezoidal
Sampling Intervals	0.04 in., 0.08 in., 0.16 in.
Control Intervals	1 in., 2 in., or 4 in.
Switch Inputs (2)	Scanner Active RES/EC Null
LED Outputs (3)	Scanner Status Null Status Data Alarm

GP94031044.cvs

**Figure 2.2.1-10. Specifications for the Motion Control Processor Board**

### ***Scanner Switch Input Board***

The scanner switch input board was a small circuit that contained two momentary switches and three LED status lights. A "hot foot" connector was mounted on the board to allow a quick connect/disconnect on the scanners. This board was fabricated as a wire-wrap board and was checked using the prototype system. It was subsequently replaced with a printed circuit board during the Field System Development/Evaluation phase of the program.

### ***Front Panel Switch Input Board***

The front panel switch input board was a small circuit that routed the front panel switch and connector signals to the signal conditioning boards. Cables were connected to this board to carry the scanner signals from the front panel to the board locations. This board was fabricated as a wire-wrap board and was subsequently replaced with a printed circuit board during the Field System Development/Evaluation phase of the program.

### ***Power Supply Board***

The power supply board was a small circuit that contained the power supplies and power transistor circuits required for high-voltage pulses on the pulser/receiver board, scanner motor power on the MCP board and -5 volt power on the frequency generator board. This board was fabricated as a wire-wrap board and was subsequently replaced with a printed circuit board during the Field System Development/Evaluation phase of the program.

## **2.2.2 Data Management Subsystem**

The data management subsystem included all of the software designed for the MAUS III system. The data display portion of this software combined the data collected from the

DSP/DLP into high-resolution C-scan and A-scan images. These images were evaluated to determine the depth, size, length and/or area of a feature that appeared in the data. These images were stored on the computer hard drive for further evaluation, archived to an optical disk for long-term storage, or sent through an ethernet/model link to a remote site for evaluation. Figure 2.2.2-1 identifies the variety of functions that were included in the DM subsystem.

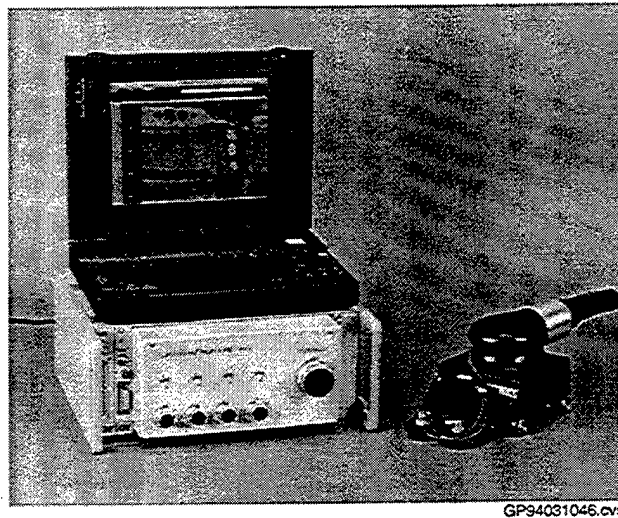
Feature	Description
<b>C-Scan Display</b>  Point Measurement  Linear Measurement  Area Measurement  Histogram  Defect Area  Annotations Text Measurements Histograms	Display Inspection Data as an Area Image  Display the Data Value at Any Point on the C-Scan Image. Point Values in Inches for P/E Depth, dB for P/E Amplitude, and Counts for Resonance and Eddy Current Display the Linear Measurement Between User-Selected Points on the C-Scan Image Display the Measured Area Within a User-Selected Boundary  Display the Histogram Analysis of the Data Located Within a User-Selected Boundary Display the Area of Data Within the Histogram Boundary That Fulfills the Defect Criteria Defined By the User Store Operator Annotations With C-Scan Data Text Messages to Identify Sections of Data Results of Point, Measure, and Area Measurements Results of Histogram Analyses
<b>A-Scan Display</b> P/E Video Display P/E Gated Amplitude Resonance Freq. Sweep	Display Inspection Data as an Individual Signal Standard Flaw Detector Format - Video Video Signal Modified With the Amplitude Gates Frequency Sweep of Resonance Sensors
<b>System Setup</b> Setup Files File Management P/E Depth P/E Amplitude Resonance Eddy Current Scanner Display	System Setups Stored in Disk Files for Fast Configuration Changes Setup Files are Recalled and Saved in a Simple Menu Menus for Setup File Copy and Delete Depth Gate, Filters, Threshold, Sensor Gains Amplitude Gates, Sensor Frequency, Sensor Gains Sensor Frequency, Gains, Auto-Null, Auto-tune Sensor Frequency, Gains, Auto-Null Configuration: Sensor Type, Width of Scan, Flaw Size Format Information for C-scan Display
<b>Archive</b> Store Restore Library	Store and Retrieve Data Files From an Optical Disk Store Data Files to the Optical Disk Retrieve Data Files by Name or With Template View Library of All Data Files Stored on Optical Disks

GP94031045.cvs

**Figure 2.2.2-1. Data Management System Features**



A Tadpole laptop computer was used for the MAUS III prototype system. Figure 2.2.2-2 shows the computer sitting on top of the signal conditioning enclosure with the contour following scanner in the foreground. The data management software was installed in this system and the data imaging and system set-up functions were evaluated.



GP94031046.cvs

**Figure 2.2.2-2. Prototype MAUS III System with Laptop Computer**

The MAUS III menus were located on the corners of the computer workspace as shown in Figure 2.2.2-3. The general administrative menus were located in the lower left-hand corner. The A-scan menu appeared in the lower right-hand corner. The set-up menus appeared in the upper right-hand corner, while the c-scan menus appeared in the upper left-hand corner. Typically, the display zoom was set so that one quarter of the workspace was visible at any given time. The operator simply moved the cursor into one of the workspace corners to view the desired menus.

Additional software was added to the subsystem for the communication link between the motion control processor in the signal conditioning subsystem and the data management software. A connection was established between the existing Ethernet link between the MCP and DM. When a new scanner was detected by the MCP, a scanner request was sent through the link to the DM. An array of scanner configuration and control variables was sent back to the MCP. A second array of variables was transferred to the MCP at the start of each C-scan. These variables included a number of sensors, width of inspection strip and minimum flaw size. The MCP used these variables to control the scanner for the C-scan and to control data acquisition to guarantee that the minimum flaw is detectable.

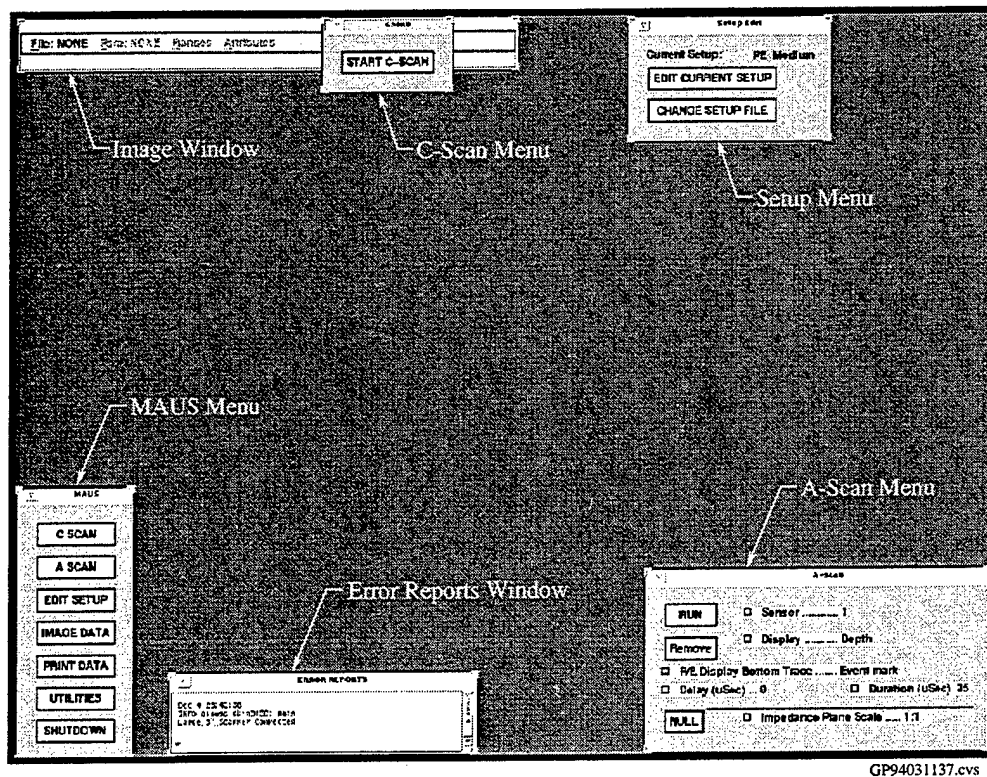


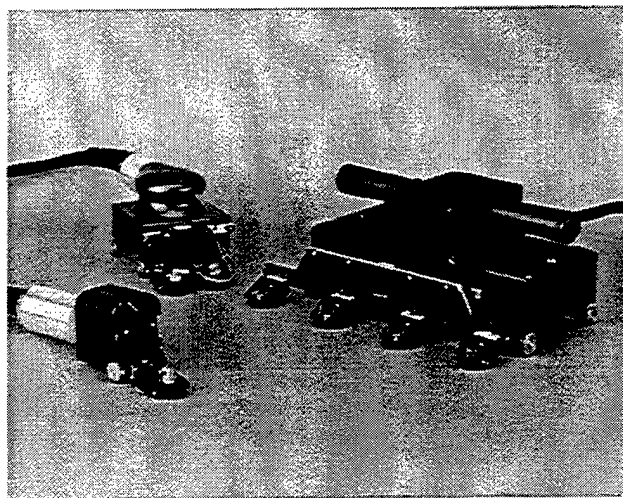
**Figure 2.2.2-3. MAUS III Computer Workspace - Complete Menus**

The format of the C-scan display process was modified to accommodate the MCP variations as well as the data reconstruction software. The original C-scan display allowed the operator to assign data parameters to specific screen locations. This approach was used to allow a mixed C-scan display of depth and amplitude data. This was a fine approach to use if the C-scan data width was set to eight inches and the sample interval was fixed at 0.04 inches. The revised MCP capabilities allowed variations in data width from two to 16 inches with sampling intervals of 0.04, 0.08 and 0.16 inches. The actual settings were defined by the set-up variables described above.

The C-scan display software was revised so that the depth/phase data was always displayed on one of the C-scan screens while the amplitude data was always displayed on a second screen. A revised view option displayed both parameters on a single screen at half scale. This allowed a dual view when both parameters had to be evaluated at the same time. The overall sale of the C-scan display was based upon the maximum expected width of he inspection strip. The display was scaled so that the entire inspection strip was displayed on the computer screen at one time.

### 2.2.3 Scanner Subsystem

Three scanners were included in the scanner subsystem to allow the inspection of a wide variety of geometries. A tight access scanner was designed to allow inspection access to tight areas and very tight curvatures. A curve-following scanner was designed to allow inspection of surfaces with complex curvature changes. A large scanner was designed to cover inspections of large, relatively flat surfaces. The three scanners are shown in Figure 2.2.3-1. The design goals for these scanners included easy handling, rapid scanning, adjustable mounts, removable sensors, interchangeable parts, reliable operation and minimal maintenance. The number of moving parts and wear surfaces were minimized to provide reliability and reduce maintenance requirements. The scanners were also designed for easy access and assembly when maintenance is required. Features common to all three scanners are described in Figure 2.2.3-2. Features unique to each scanner are shown in Figure 2.2.3-3.



GP94031047.cvs

**Figure 2.2.3-1. MAUS III Scanner Subsystem**

Features	Description
<b>Scanner Operation</b> No Attachment to Surface Sensor Motion Automatic On/Off	Scanners Are Rolled Over the Part Surface Sensors Are Mechanically Oscillated Across the Surface Motion Is Automatic With Forward Movement
<b>Position Measurement</b> Absolute Sensor Position Relative Scanner Position	C-Scan Data Is Collected in Data Strips. The Width of the Data Strip Can Be 2 in. - 16 in., the Length of the Data Strip Can Be Any Length Sensor Position Measured as Sensors Are Moved Across the Inspection Surface Scanner Position Measured as Scanner Is Moved Forward or Backward. Measured Position Is Relative to Starting Position on the Inspection Surface
<b>Drive Mechanisms</b> Motors Control Approach User Configuration	Scanner Mechanical Motions Are Computer Controlled DC Gear Motors Used in All Scanners Software Controlled Mechanical Motion Control Configurations Defined Through User Setups Parameters Include Scan Speed, Stroke Length, Data Sample Interval, Control Variables
<b>Sensor Holders</b> Gimble Mechanisms Interchangeable Sensor Mounts Fast Adjustment	May Be Exchanged Between Scanners. Common Mechanisms and Sensor Mounts Excellent Curve Following Capability Easy to Change Between Different Types of Sensors No Tools Required to Adjust Sensor Holders
<b>Cabling</b> Scanner Connection Automatic Scanner ID Couplant Delivery Cable Length Extender Cable	Common Cables for All Scanners One Connection at Main Case for All Scanners Automatic Detection of Attached Scanner Couplant Delivery Tubing Built Into Cables 12 Feet Standard Cable Length 15 Feet Extender Cable Length

GP94031135.cvs

**Figure 2.2.3-2. Common Scanner Subsystem Features**

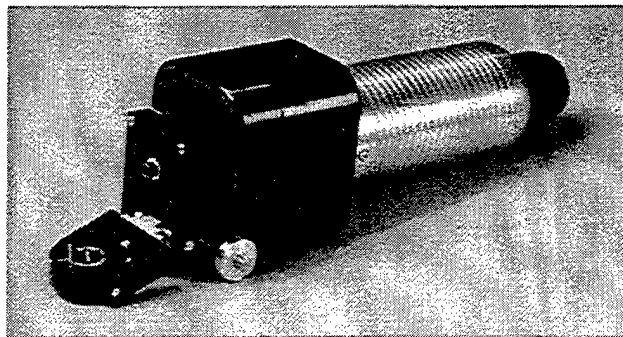
Feature	Description
<b>Tight Access Scanner Features</b> Small Footprint Additional Small Sensor Mount Scan Stroke Limitations Maximum Scan Width	Allows Operation in Narrow or Low Profile Areas Used for Small Radii Applications Scan Stroke Is Set to 1 in. Only 2 in. Maximum Width
<b>Curve Follower Scanner Features</b> Average Footprint Scan Stroke Limitations Maximum Scan Width	Useful for Moderate Size Surfaces Variable Scan Stroke From 1 in. to 2 in. 8 in. Maximum Width
<b>Large Area Scanner Features</b> Large Footprint Scan Stroke Limitations Maximum Scan Width	Useful for Large Area Surfaces Variable Scan Stroke From 1 in. to 4 in. 16 in. Maximum Width

GP94031048.cvs

**Figure 2.2.3-3. Unique Scanner Subsystem Features**

The motor and resolver components are identical in each scanner. Common bearings, belts, couplers and wheels were used whenever possible. The goals in this phase were to reduce the number of unique parts on each scanner and to reduce the number of spare parts required for long-term maintenance. In the final designs, 12 components were common between scanners and four were specific to only one scanner.

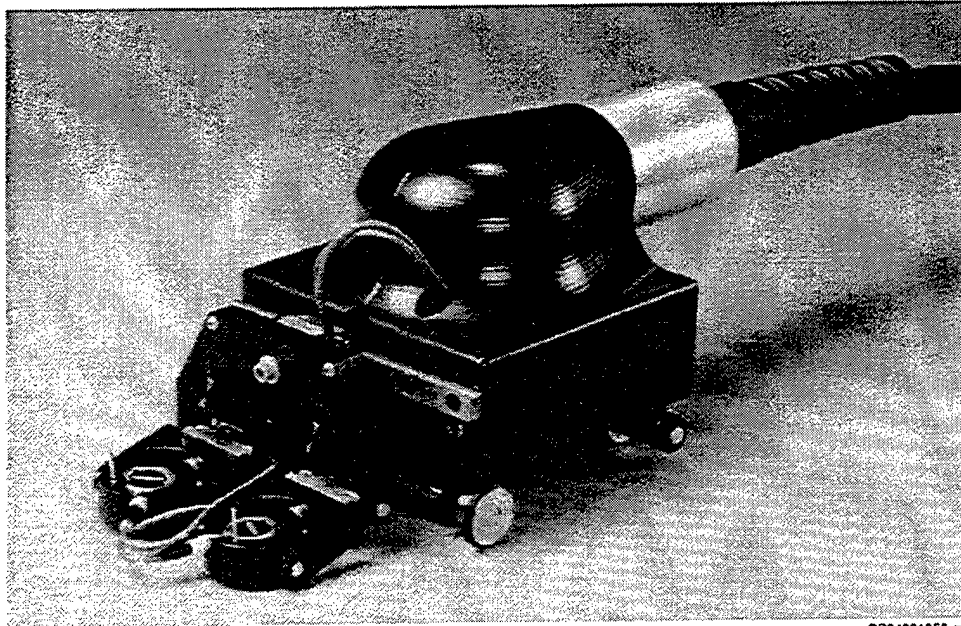
A photograph of the tight-access scanner is shown in Figure 2.2.3-4. This scanner is capable of manipulating sensors over a very small radius or in a tight access location. It measures 3 x 4 x 6 inches and weighs two pounds. The sensors in this scanner were moved using a scotch yoke design; therefore, the motor rotates in one direction. The velocity of rotation was controlled by the MCP and provided an even velocity for the sensor oscillation. As the motor rotates, the scotch yoke oscillates across this one-inch range. The sensor mount and sensors were attached to the scotch yoke mechanism and to a linear bearing that guided the motion of the sensor mount over the sweep.



GP94031049.cvs

**Figure 2.2.3-4. Tight-Access Scanner**

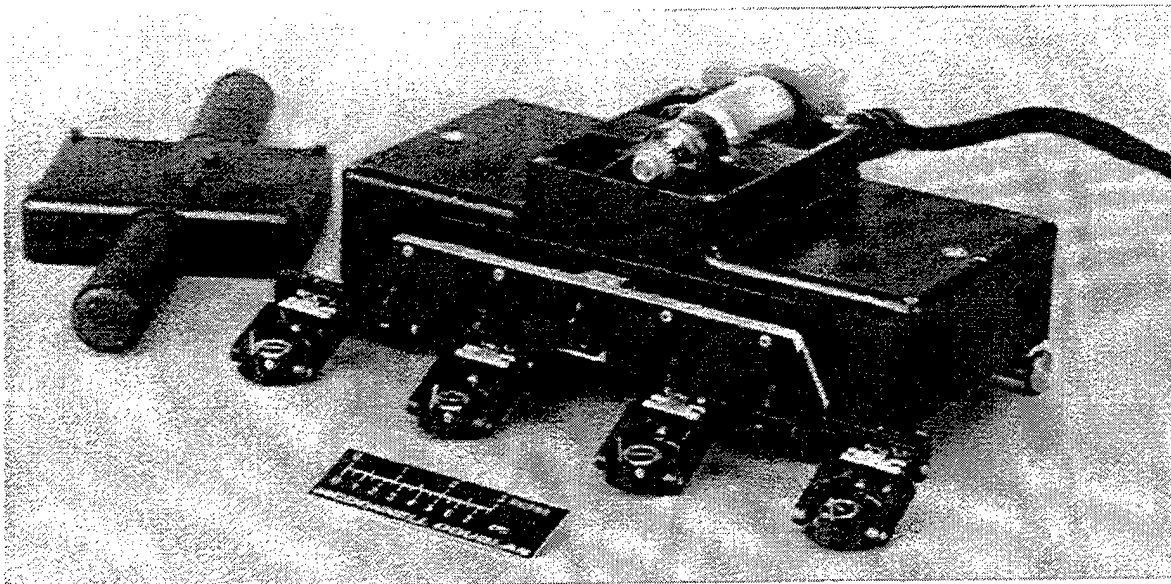
Figure 2.2.3-5 shows the curve following scanner. This scanner was capable of moving sensors over a convex or concave surface with a minimum radius of five inches. It measured 4 x 4 x 6 inches and weighed three pounds. The sensors in this scanner were moved with a direct-drive belt design. The motor oscillation was controlled by the MCP, which was located in the signal conditioning subsystem. The sensor mount and sensors were attached directly to the drive belt. A linear bearing was used to guide the motion of the sensor mount over a two-inch sweep. As the motor oscillated, the belt was moved across the two-inch range, moving the sensor mount and sensors as well. The MCP may control the motor to oscillate at shorter intervals to reduce the full sweep of the sensor mount.



GP94031050.cvs

**Figure 2.2.3-5. Curve Following Scanner**

Figure 2.2.3-6 shows the large area scanner. This scanner was capable of moving sensors over a large, relatively flat surface. It measured 12 x 4 x 6 inches and weighed approximately five pounds. The sensors in this scanner were moved with the same direct drive belt design used in the curve following scanner. The sensor mount and sensors were directly attached to the drive belt. Two linear bearings guided the motion of the sensor mount. The maximum length of the drive belt oscillation, as controlled by the MCP, was extended to four inches relative to this



GP94031051.cvs

**Figure 2.2.3-6. Large Area Scanner**

scanner. The maximum width of the inspection strip that may be covered with this scanner was 16 inches. The MCP controlled the motor to oscillate at shorter intervals to reduce the full sweep of the sensors if desired.

Figures 2.2.3-7 and 2.2.3-8 show the interiors of the tight access and curve following scanners. The scanner construction was similar for all three scanners, although each has unique drive mechanisms. The scanner bodies consisted of two shell sections that contain precision boards to house the motor, resolvers, bearings and gears used for the sensor drive mechanisms. The electrical components were placed in position and held in place by the pressure exerted when the two sections were fastened together. All wiring within the scanner was terminated with quick-release connectors. The connections to the scanner cable were made inside of the circular handle in the back of the scanner. This method of assembly made field replacement of any component a relatively quick procedure. If any component needed to be replaced, the operator simply opened the scanner, disconnected the component wiring, removed and replaced the component.

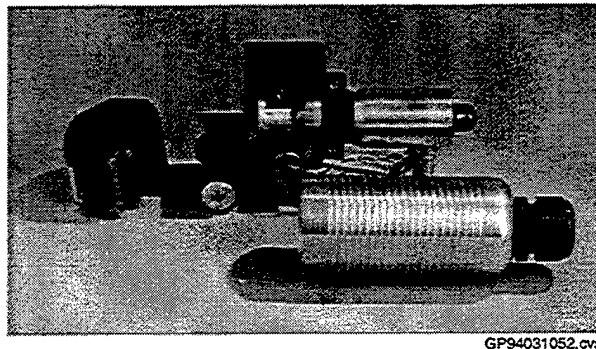


**Figure 2.2.3-7. Small Scanner (Disassembled)**

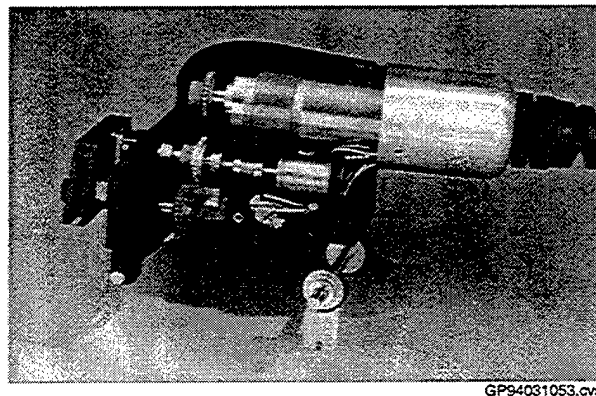


**Figure 2.2.3-8. Curve Following Scanner (Disassembled)**

Figure 2.2.3-9 shows the sensor mount clamps for the tight access and curve following scanners. The sensor mounts were designed to hold several combinations of sensor gimbals. The sensor gimbals slid into the sensor mount and were held in place with thumb-screws on the front of the mount. In addition, the height of the sensor mount relative to the part surface was adjusted with a thumb-screw located in the center of the mount. The design concept for the large area scanner sensor mount was similar; about two inches longer than the curve following scanner mount. The sensor mounts were designed with common dimensions at the attach point so that the mounts could be interchanged between the scanners.

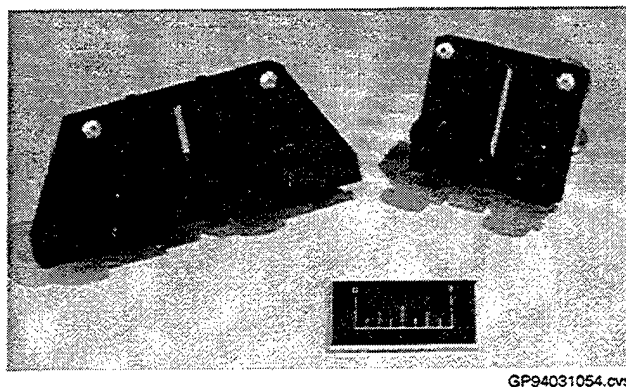


**Figure 2.2.3-9. Sensor Mount Clamps for Small and Curve Following Scanners**

Figure 2.2.3-10 shows the different types of sensor gimbals that were placed in the sensor mounts. The gimbal on the left included the standard sensor holders used with the curve following and large area scanners. The gimbal on the right included a modified sensor holder design that allowed for severe curve following and small sensors only. This gimbal was typically used with the tight access scanner, but could also be attached to the larger scanners. The dual transducer gimbals in the center of Figure 2.2.3-10 were intended for use on the curve following and large area scanners only. These gimbals positioned the two sensors exactly two inches apart. A second version of the dual gimbal was designed for the large area scanner and positioned the sensor's four inches apart.



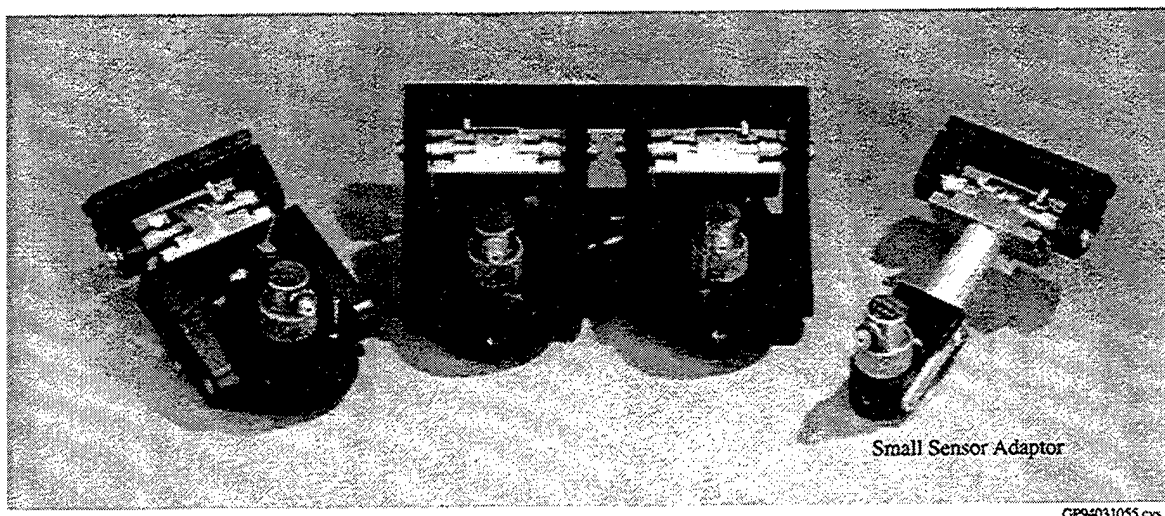


**Figure 2.2.3-10. Available Sensor Gimbals**

The sensor gimbals may be combined to allow a variety of inspection applications. Two four-inch dual gimbals held four sensors, resulting in sixteen inches of inspection coverage. Two two-inch dual gimbals resulted in eight inches of inspection coverage. One two-inch dual gimbal and one single gimbal resulted in three sensors that provided six inches of coverage. Two single sensor gimbals may be placed at 1.5 or 2.0 inch intervals to provide three or four inches of inspection coverage, respectively. Finally, only one gimbal may be placed in the sensor mount to provide minimal coverage.

Sensor adapters were designed to attach several different types of sensors to the gimbals. Figure 2.2.3-11 shows the normal sensor adapters with four different types of sensors. A pulse-echo delay-line sensor, two types of resonance sensors and an eddy current probe are shown. The sensor gimbals were installed and removed by applying a small amount of finger pressure to the back of the gimbal. This method allowed for a complete sensor change in less than one minute.

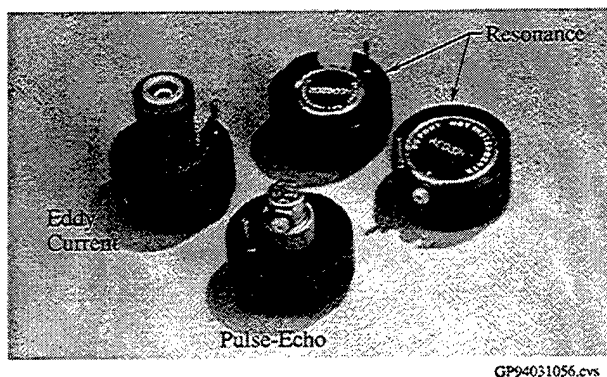


**Figure 2.2.3-11. Sensor Adapters with Sensors Installed**

A small sensor adapter is shown on the gimbal on the right in Figure 2.2.3-10. Its small diameter allows the sensor to follow a very tight curvature. This small adapter could only be used with pulse-echo delay line sensors or pencil-point eddy current probes.

Each scanner had a 15-foot cable that attached the scanner to the signal conditioning subsystem. Each scanner cable was terminated with a common connector so that the scanners could be interchangeably connected to the signal conditioning box. Since each scanner had unique capabilities and control parameters, the MCP in the signal conditioning subsystem was programmed to automatically recognize each scanner. When a scanner was attached to the signal conditioning box, the MCP identified the scanner and communicated the scanner information to the DSP and data management subsystem.

### **2.3 Demonstration and Validation**

The demonstration and validation phase of the program was intended to introduce the prototype system to the end users and to solicit comments on the strengths and weaknesses of the system[2]. These comments were addressed and many were implemented in the final MAUS III configuration to ensure that the system addressed the customers needs. The demonstration/validation schedule included one-week evaluations at C-17 and B-2 manufacturing facilities in Long Beach (Boeing) and Pico Rivera (Northrop-Grumman), respectively. The schedule also included two-day evaluations at each of the five Air Logistics Centers (Oklahoma City, OK, Ogden, UT, Warner-Robins, GA, Sacramento, CA and San Antonio, TX).

Several positive responses to the system's capabilities were repeated throughout the demonstration/validation trips. These centered on the portability, set-up, flexibility and versatility of the system. The strength of the system was that the only parts required for portable inspection were the signal conditioning package, laptop computer and scanner. These parts were easily transported to the inspection site and set-up within five minutes. All of the inspection modes were included within the small signal conditioning package so that any mode was available to the inspector. No additional equipment or parts were required to change from one inspection mode to another other than a change in sensors. Finally, the system menus were straightforward and relatively easy to learn.

The evaluations were very useful in identifying strengths and weaknesses in the prototype MAUS III design. The comments generated from the ALC evaluations provided insight into the portable inspection needs in current Air Force maintenance environments. Existing inspection applications were identified that could be improved using a MAUS III system. These applications were not specifically large area composite applications, but tended to be bonded and aging metallic applications. It was recognized in the ALC organizations that large area composite structures will be an inspection concern in the near future; however, detection of bondline flaws, cracks and corrosion appear to be the major inspection issues in current maintenance programs.

Existing inspection applications that were investigated at each ALC are discussed in the following section. Constructive feedback that was provided during these investigations is included in the application descriptions.

### **2.3.1 Delamination and Laminar Flaw Detection**

Laminated structures, including carbon/epoxy and fiberglass materials must be fully consolidated to ensure the integrity of the structure. Typical flaws that can occur in these structures include manufacturing defects such as porosity or foreign object inclusions, and in-service defects caused by impact damage and water entrapment. These defects are typically associated with laminar separations at specific locations within the material. The ultrasonic pulse-echo depth inspection technique can be used to accurately detect, locate and size defects found in composite laminates. The ultrasonic resonance technique can also accurately detect and size laminar defects. However, it is limited in its ability to locate the depth of a defect.

#### ***Laminar Defects in Carbon/Epoxy Laminates***

Figure 2.3.1-1 shows a MAUS III C-scan of delaminations in a carbon/epoxy laminate test standard. Laminar flaws were located at several depths within the laminate. The depth of each flaw is identified by a gray shade. Darker gray indications represent defects that are located near the top surface of the laminate. Lighter gray indications represent defects that are located deeper in the laminate. The defect sizes ranged from 0.25 to 0.50 inches. This C-scan was collected during a demonstration at Northwest Airlines using the standard, which was developed by Boeing for commercial aircraft composite inspections. This standard is similar in layout to a standard reviewed by SA-ALC that was used for composite rotor blade inspection. This was an

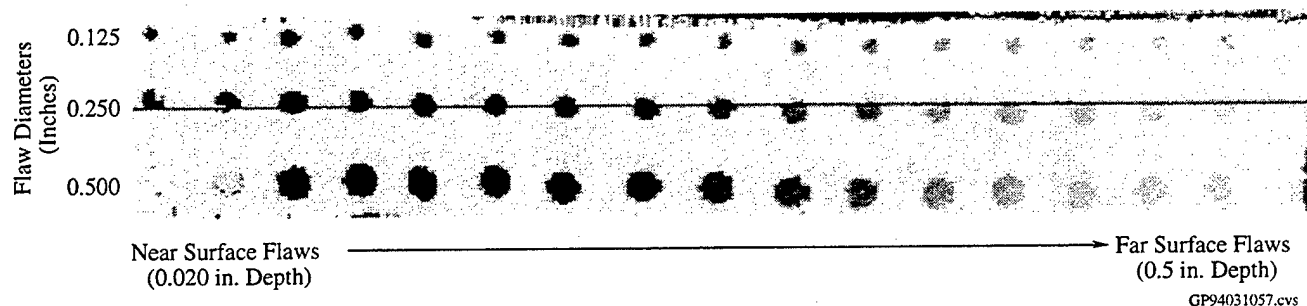


**Figure 2.3.1-1. MAUS III Pulse-Echo depth C-scan of Carbon/Epoxy Test Standard**

experimental program that required full-area inspection to detect flaws as small as 0.125 inches. This inspection was extremely difficult to accomplish using manual inspection techniques. The MAUS III pulse-echo depth C-scan capability could improve the flaw resolution and inspection speed relative to this application.

#### ***Impact Damage in a Carbon/Epoxy Wing Skin***

Figure 2.3.1-2 shows a C-scan of the ply separations that occurred after a carbon/epoxy wing skin was damaged when a British Royal Air Force GrMk5 aircraft rolled from the runway into a canal upon landing. The location of the damage within the skin occurred at a ply build-up where the skin thickness was changing dramatically. Several areas of the laminate skin were punctured in the accident and were detected visually. However, the damage shown in Figure 2.3.1-2 did not result in a puncture and was not visible from the outer surface of the skin. The multi-layer damage was shown using various shades of gray. Near-surface damage is shown as dark gray, while separations deeper in the laminate are shown as light gray. The MAUS III was used to scan the entire upper and lower surfaces of the wings. The size of the inspection area was approximately 400 sq. ft. All scanning was either inverted or vertical, and was separated into discrete sections. Inspection rates averaged approximately 75 sq. ft./hr. in the inverted position and 150 sq.ft./hr in the vertical position. The users were impressed with the clarity of the pulse-echo images, the measurements and analysis capabilities for data evaluation, and the general ease of set-up and use. Particular difficulties were encountered on the underside of the wings just aft of the engine exhausts. Areas that were coated with a film of oil from the engine exhaust were difficult to scan due to wheel slippage. These areas were cleaned with a solvent before the scans could be completed.

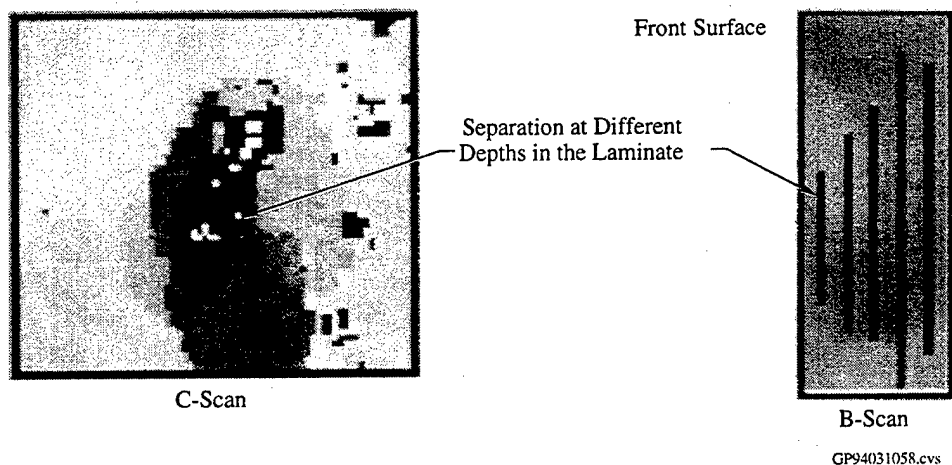


**Figure 2.3.1-2. Impact Damage in a Carbon/Epoxy Laminate Structure**

### ***Delaminations in a Milstar Radome***

Figures 2.3.1-3 and 2.3.1-4 show ultrasonic pulse-echo amplitude and resonance C-scans, respectively, of a delaminated area in a Milstar radome structure evaluated at SM-ALC. This structure consisted of a relatively porous fiber/resin combination, which, due to its porous nature, attenuated ultrasonic energy. This inspection was usually performed using a portable C-scan imaging system. The pulse-echo amplitude image correlated well with the images collected using the existing C-scan system. Since this was a porous structure, the ultrasonic resonance technique was also used to detect the delaminations because it was less susceptible to porosity. The resonance C-scan image duplicated the pulse-echo image, but appeared to provide different levels of detail in the delaminated area.



**Figure 2.3.1-3. MAUS III Pulse-Echo Amplitude C-scan of Milstar Radome**

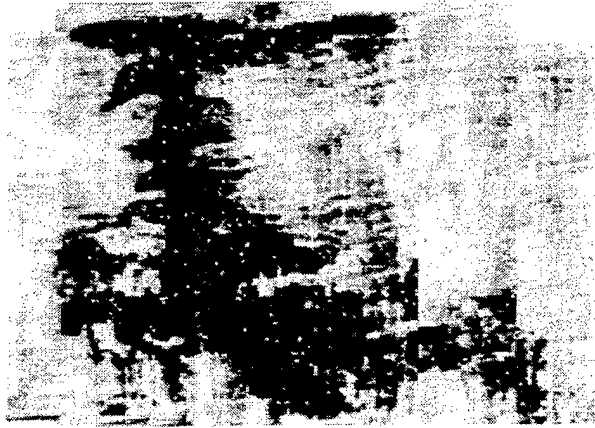
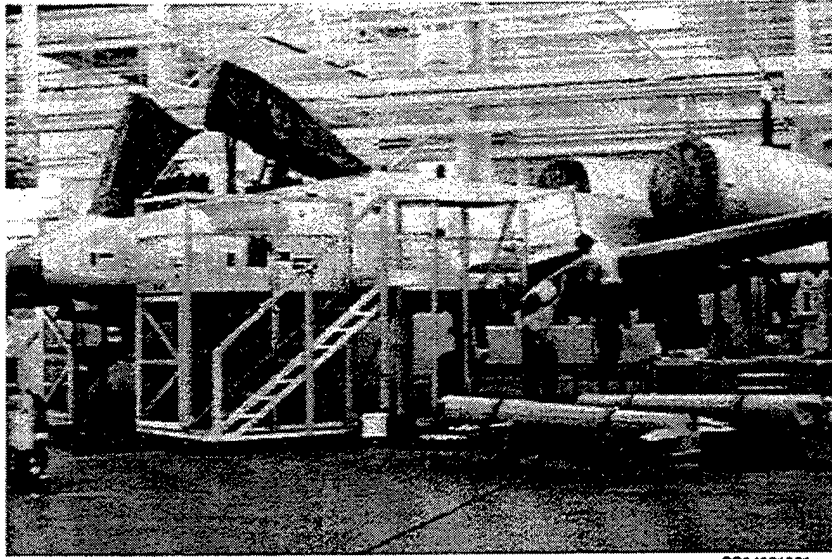


**Figure 2.3.1-4. Resonance Phase C-scan of Milstar Radome**

The inspection rate using the MAUS III system was approximately six times faster than that using the current system. System set-up was accomplished in approximately 10 minutes as compared to a one-hour set-up for the existing equipment. A significant amount of discussion was held regarding the pulse-echo set-up parameters. Several parameters that were provided in the existing equipment were not included in the MAUS III prototype. These included adjustable pulser power and damping and full RF waveform data collection. In addition, an impedance plane display for resonance scan set-up was recommended to provide an easier transition from manual inspection techniques to the automated MAUS III system.

#### ***Voids in A-10 Composite Leading Edge***

Several experimental composite leading edges were installed on A-10 aircraft to investigate replacements for the metallic structures normally used. The MAUS III was taken to a hangar at SM-ALC to evaluate the system performance on one of these composite leading edges. This exercise provided the opportunity to evaluate the system during an on-aircraft inspection. The area of interest was on the curved portion of the leading edge, thus providing a good test for the contour following capabilities of the scanner. Figures 2.3.1-5 and 2.3.1-6 show photographs of the A-10 in the hangar and the scanner positioned on the leading edge, respectively. Figure 2.3.1-7 presents an ultrasonic resonance C-scan of one section of the leading edge. Changes in structure geometry were represented as changes in gray shade as the scan approaches the leading edge. Voids in the leading edge appear as dark indications on the C-scan.



GP94031061.cvs

**Figure 2.3.1-5. MAUS III Evaluation of A-10 at SC-ALC**



GP94031062.cvs

**Figure 2.3.1-6. MAUS III Scanner Positioned on A-10 Leading Edge**

The system was easily transported around the hangar. A delay in system set-up was encountered, which was caused by trying to find extension to provide the AC line power. A support stand was required to access the leading edge from below. The leading edge could be reached from above, but it was difficult to scan below the apex of the edge while positioned on the top of the wing. The scanner was able to follow the leading edge very closely when it was moved from the upper wing surface into the leading edge. The curvature was too severe for the scanner to be moved down the length of the edge.

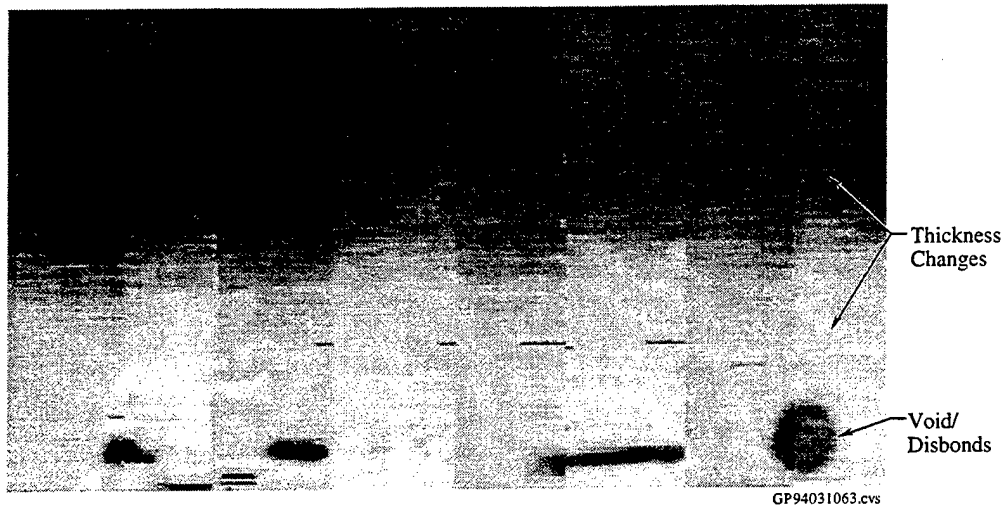


**Figure 2.3.1-7. Ultrasonic Resonance C-scan of an A-10 Leading Edge**

It was straightforward to collect the inspection data in strips positioned along the leading edge and to reconstruct the data into a full C-scan using the image processing package included with the system.

### **2.3.2 Adhesive Bondline Flaw Detection**

Many aircraft contain adhesive bondlines to join sections of composite or metallic structure. The transmission of loads between the bonded sections determines the strength and stiffness of the structure. These sections include outer surfaces, inner surfaces to increase support in specific areas, ribs and spars to transfer loads over specific paths and core sections to provide overall support to the outer surfaces. The adhesive bondlines must be intact to ensure expected structural performance. Ultrasonic through-transmission techniques are typically used to detect bondline voids when access is available to both sides of the structure. This access is often only available during initial manufacturing. Once all sections of the surface are assembled, inspection is usually limited to single-sided access. Ultrasonic resonance techniques are often used to detect the presence of bondline voids and to evaluate the extent of unbonded area. These techniques usually only require access from one side, but are limited to bondlines under thinner skin sections. The ultrasonic pulse-echo amplitude technique may be used to detect and size bondline voids in a small number of structures comprised of materials that allow strong ultrasonic reflections.

#### ***Bondline Voids in E-3 Radome***

The E-3 AWACS composite radome consisted of a thin glass/epoxy laminate coated with an anti-erosion coating and bonded to non-metallic honeycomb core. This structure is currently



maintained at OC-ALC and is inspected using a Sondicator<sup>®</sup> bond testing unit to detect impact damage due to bird strikes and/or hail. The Sondicator<sup>®</sup> was considered adequate for this inspection; however, the equipment was quite old and prone to failure. An alternative inspection system was desired to replace the aging equipment.

Figure 2.3.2-1 shows a MAUS III ultrasonic resonance C-scan of the E-3 standard that depicted several defects in the adhesive bondline between the glass/epoxy skin and the honeycomb core. The resonance sensors were used effectively to detect and size bondline voids in the radome. One drawback to this method is that water must be used to couple the resonance sensors to the radome. Other types of bond testing sensors that do not require couplant exist, but were not included in the MAUS III design. OC-ALC personnel requested that these sensors be investigated for use in the E-3 application to eliminate coupling requirements.

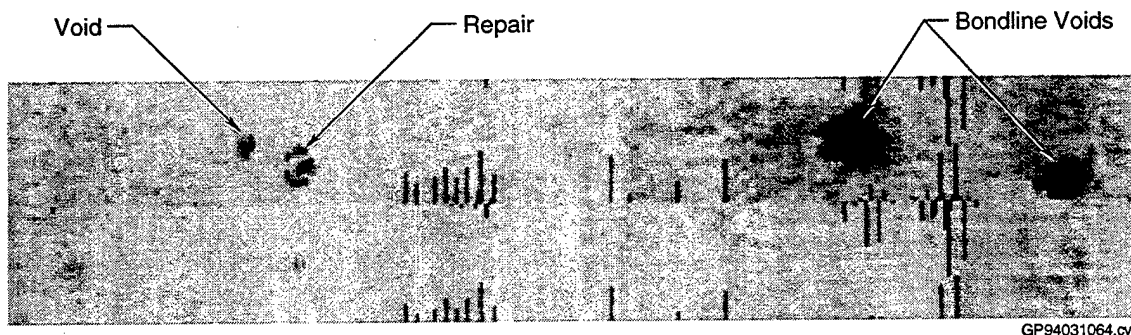


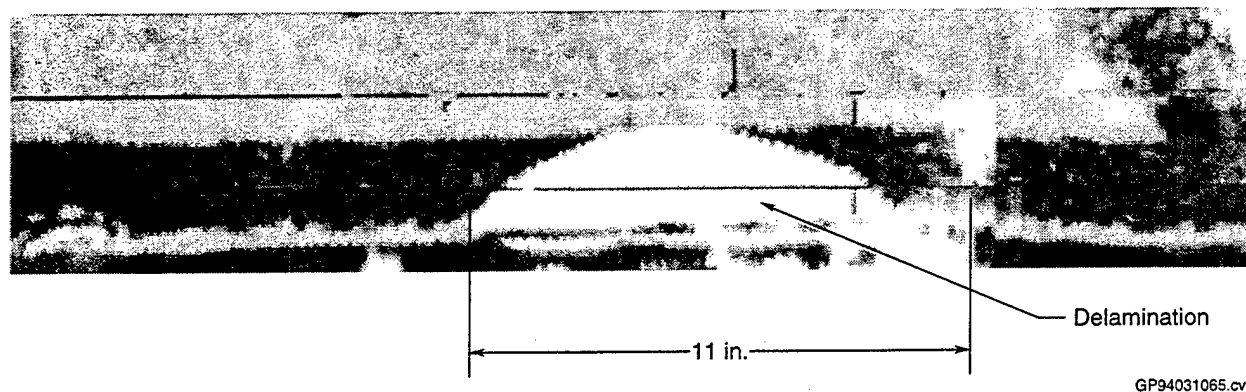
**Figure 2.3.2-1. MAUS III Resonance Phase C-scan of Bondline Defects in E-3 Radome Standard**

#### ***Delamination in B-1 Trailing Edge Flap***

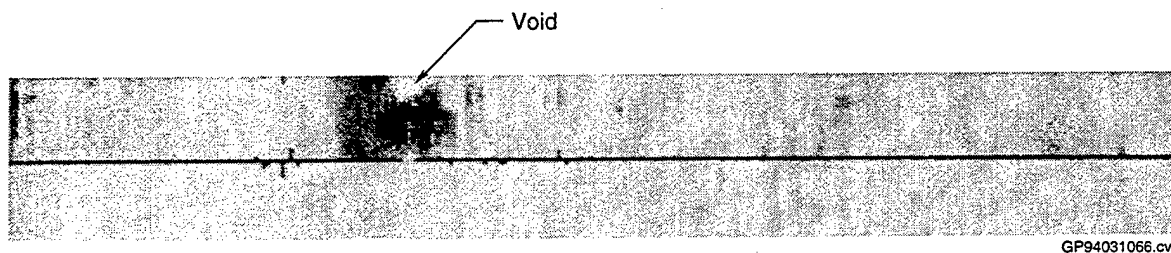
The B-1 maintenance activities at OC-ALC included the detection of bondline voids and impact damage in structures with composite skins bonded to metallic honeycomb core. These structures include trailing edge flaps, wing fairings, and weapon bay doors. The most effective method of inspection at that time was the manual tap test. This can be very tedious and difficult to reproduce over time. The MAUS III resonance method was used to demonstrate C-scan imaging capability for delaminations and disbonds relative to these structures.

Figure 2.3.2-2 shows an image of a skin delamination along the rib closure edge on a trailing edge flap. Figure 2.3.2-3 shows an image of a bondline void in the same structure. Figure 2.3.2-4 presents an image of a bondline void on an over-wing fairing. Each of these images illustrated the advantages provided by C-scan display to determine the exact size and location of the flaw.

The speed of scanning was considered to be beneficial. However, OC-ALC personnel preferred to use a non-coupling bond test sensor rather than the resonance sensors used with the MAUS III.



**Figure 2.3.2-2. MAUS III Resonance Phase C-scan of Edge Delamination at the Closure Rib on a B-1 Trailing Edge**



**Figure 2.3.2-3. MAUS III Resonance Phase C-scan of Bondline Void on B-1 Trailing Edge**

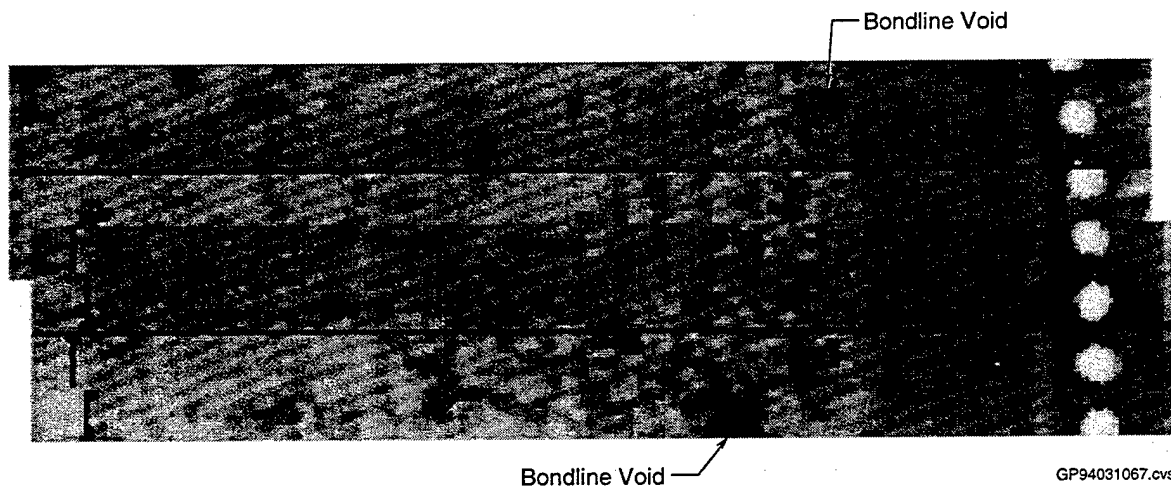


**Figure 2.3.2-4. MAUS III Resonance Phase C-scan of B-1 Outer Wing Fairing (Composite Skin/Non-Metallic Honeycomb Core)**

### ***Bondline Voids in T-38 Wing Tip***

The T-38 wing tip structure consists of metallic skin bonded to a metallic stiffening layer and to metallic honeycomb core. Bondline voids may be present in the bondline between metallic layers and between the skins and honeycomb core. Bondline defects in the standard represented both adhesive and cohesive bond failures. Figure 2.3.2-5 presents an ultrasonic resonance C-scan of selected portions of the wing tip standard.

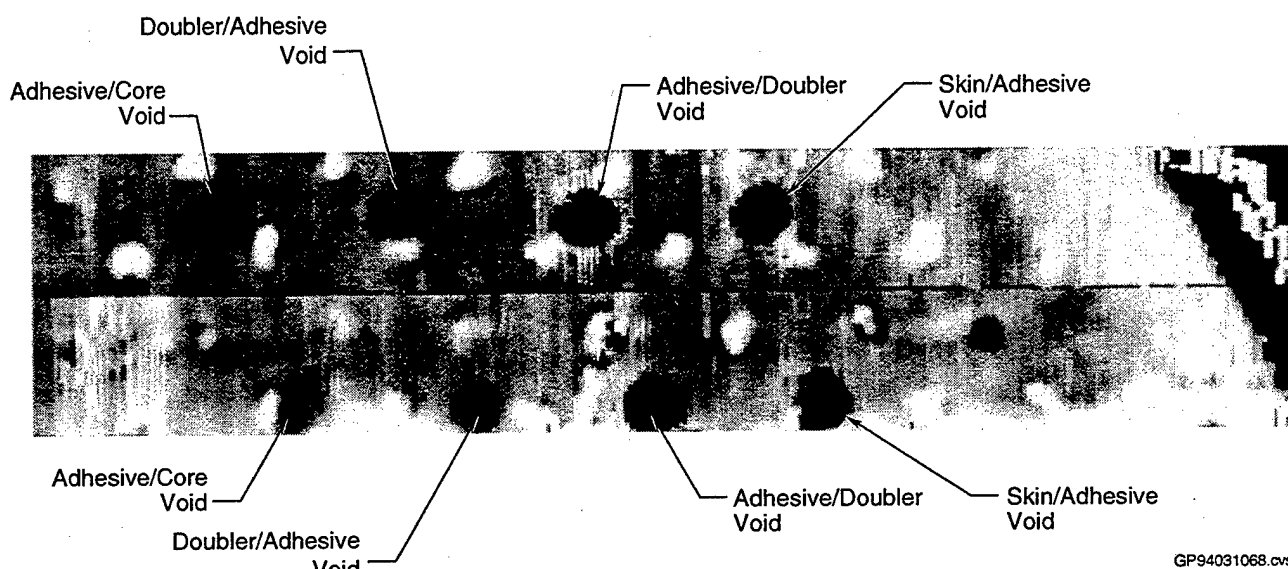


**Figure 2.3.2-5. MAUS III Resonance C-scan of Bondline Flaws in T-38 Wing Tip Standard**

Two difficulties were encountered while working with this structure. The first problem was due to the glossy painted surface of the wing tip. The water couplant for the resonance sensors tended to bead rather than uniformly wet the surface. A small amount of soap applied to break the surface tension of the water improved the sensor response. The second problem was due to the slick surface created by the soapy water. The scanner wheels had a tendency to slip on the surface, making it difficult to collect the C-scan information. An improved material for the scanner wheels was clearly needed.

### ***Bondline Voids in Boeing 727 Rudder Tab***

The Boeing 727 rudder tab was constructed with metal skins bonded to aluminum honeycomb core. Water intrusion into the structure can result in corrosion in the core and bondline failure between the skin and core. A rudder tab that was located in the repair shop at Northwest Airlines was provided for a MAUS demonstration. Figure 2.3.2-6 shows an ultrasonic resonance C-scan of a bondline void found in the rudder tab. This was a straightforward application where wheel slippage was the only difficulty encountered.

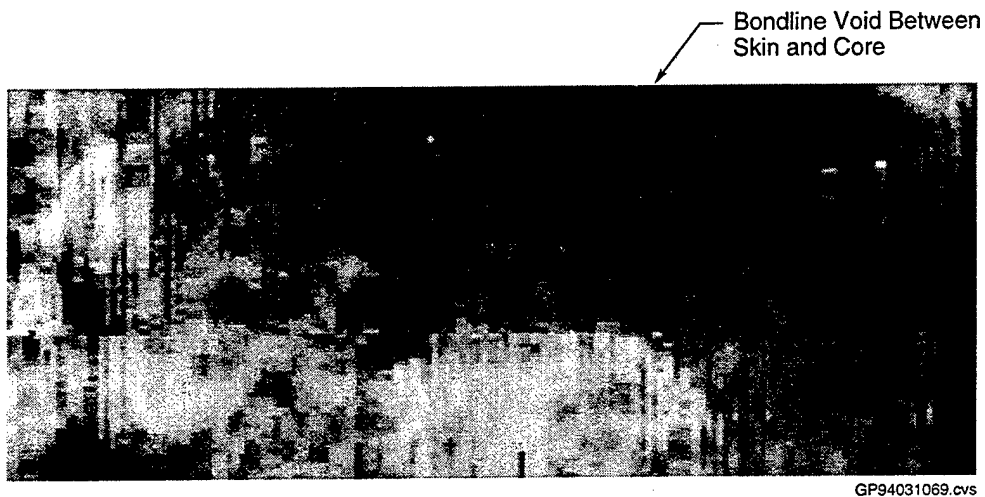


**Figure 2.3.2-6. MAUS III Resonance Phase C-scan of Boeing 727 Rudder Tab (Aluminum Skin/Aluminum Core)**

### ***Bondline Standard for Boeing Composite Spoiler***

The composite spoiler construction consisted of thin carbon/epoxy skins bonded to a non-metallic honeycomb material. The thickness of the core material varied from less than 0.25 inches to approximately 4.0 inches. Figure 2.3.2-7 shows an ultrasonic resonance C-scan of the bondline standard for the composite spoiler representing a core thickness of 0.25 inches. Bondline defects were located between the skin and core areas near both upper and lower surfaces. Note that both sets of defects were located in the C-scan, but back surface defects were not detectable on the sections of the structure where the core thickness was greater than 0.5 inches. For these areas, the inspections must be performed on both sides of the structure.



**Figure 2.3.2-7. Bondline Voids in a Bonded Composite Spoiler Standard (Composite Skins/Non-Metallic Core)**

### **2.3.3 Repair Verification**

Structural repairs are typically separated into two areas: bolted repairs and bonded repairs. When bonded repairs are performed, the quality of the repair is dependent primarily on the quality of the bondline. The adhesive bondlines within the repair must be inspected to detect the presence of unbonds and/or voids in the bondline.

#### ***Boron/Epoxy Repair of Metallic Structures***

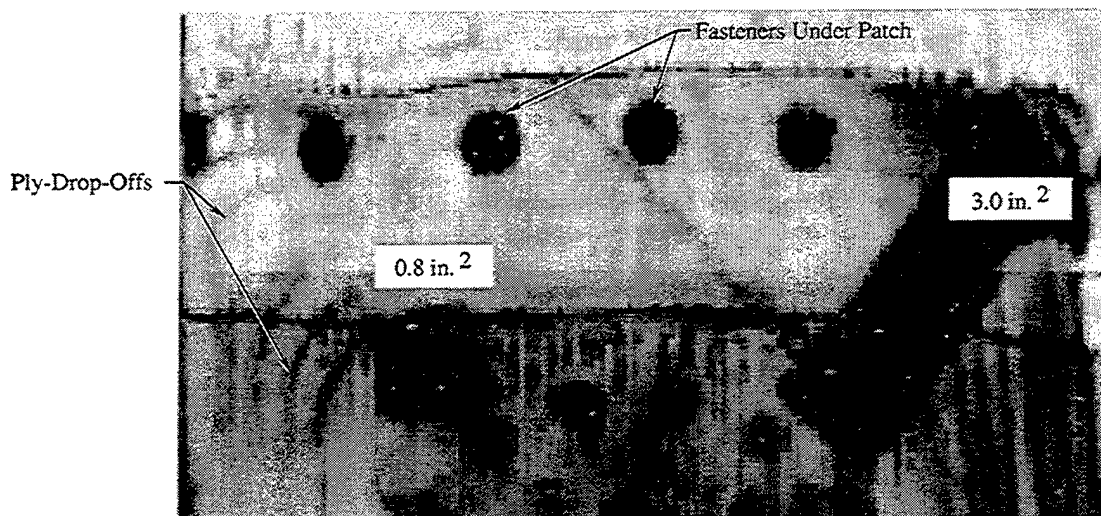
Boron/epoxy patches are currently being investigated for arresting and repairing cracks in metallic fuselage skins. The patches are adhesively bonded to the skins to provide alternative load paths for the structure at the crack location. Figure 2.3.3-1 shows a photograph of the boron/epoxy test patch on an F-16 lower wing skin. This patch was mounted by personnel at OO-ALC. The MAUS III pulse-echo amplitude method was used to image the bondline flaws and the cracks in a standard patch and also on the test patch. Figure 2.3.3-2 shows the pulse-echo amplitude C-scan of the patch standard. This patch was a layered structure with increasing thickness up to about 0.25 inches. The ply drop-offs are clearly visible in the C-scan as darker lines within the patch. The bondline voids were indentified by dark gray areas in the C-scan; the fasteners and crack in the metal skin were also visible.

The F-16 boron patch inspection was performed on the flight line at OO-ALC. This resulted in some significant observations. The power was supplied through a gas generator, and no



GP94031071.cvs

**Figure 2.3.3-1. MAUS III Inspection of Boron/Epoxy Patch on F-16 Lower Wing Skin**

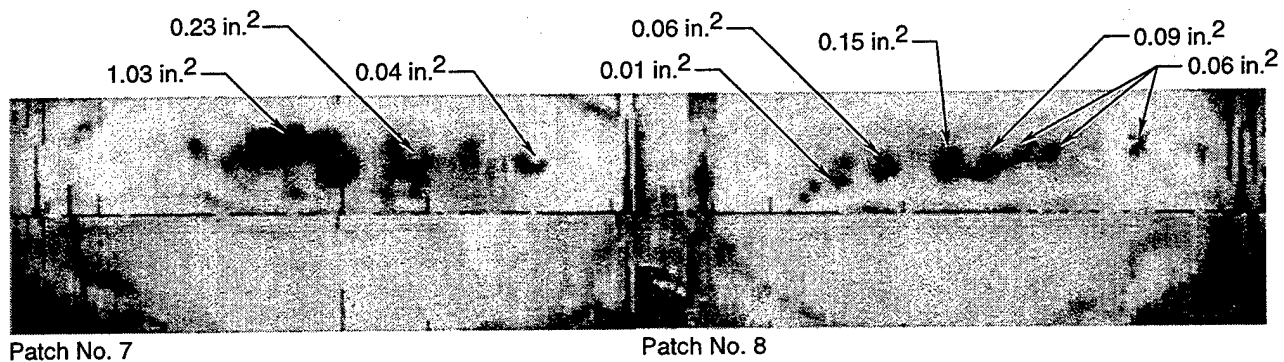


GP94031072.cvs

**Figure 2.3.3-2. MAUS III Pulse-Echo Amplitude C-scan of Boron/Epoxy Patch Standard**

problems were encountered by working under generator power. Bright sunlight caused a problem in viewing the laptop LCD display. It was difficult to see any detail in the display without providing some type of shading. A sun screen, anti-glare screen or heads-up display were candidate solutions to this problem. Finally, the surface of the wing skin was very slick with the water couplant, and, once again, the scanner wheels slipped on the surface.

Figure 2.3.3-3 shows an ultrasonic C-scan of a C-141 boron/epoxy patch standard that was evaluated at WR-ALC. This patch was designed to transfer load in a lower wing skin around a crack site located in an internal rib. The ultrasonic pulse-echo technique was difficult to apply due to excessive attenuation. The ultrasonic resonance technique was successfully used to identify and size bondline voids under the patch. Sections of good bond were represented by light gray shades; the bondline voids were represented by the dark gray shades. These data correlated very well with the thermography technique currently used to evaluate these patches.

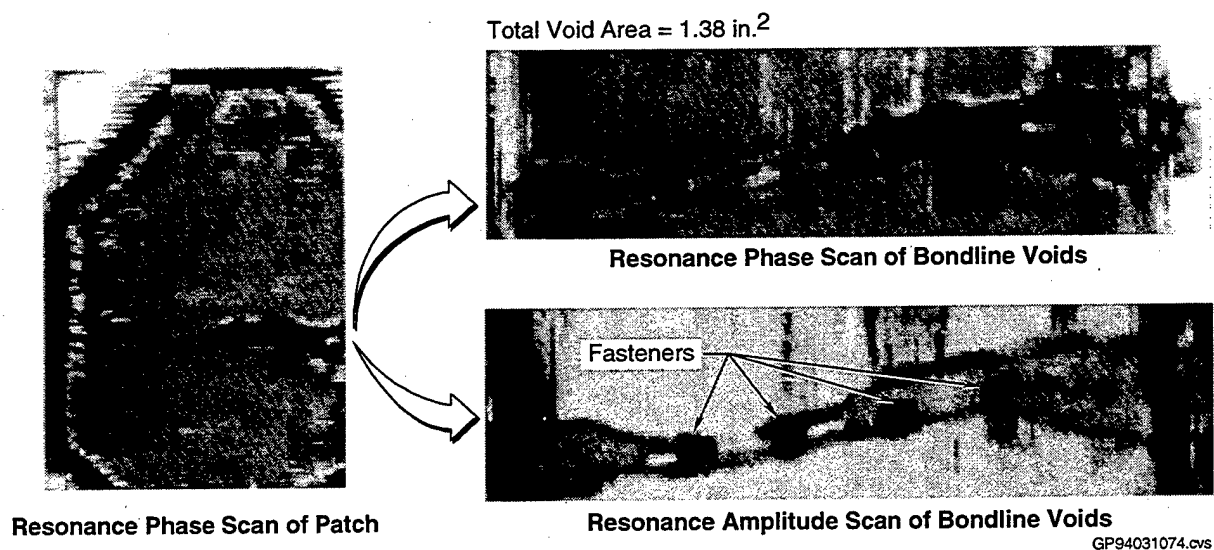


\*Dark areas indicate bondline voids

GP94031073.cvs

**Figure 2.3.3-3. MAUS III Resonance Phase C-scan of Boron/Epoxy Multiple Patch Standard**

Figure 2.3.3-4 shows an ultrasonic resonance C-scan of a test patch placed on a test fuselage at the Airworthiness Assurance NDI Center (AANC) operated by Sandia National Laboratories. It provided another example of the image consistency that was accomplished in evaluating bondline voids using the resonance technique.



GP94031074.cvs

**Figure 2.3.3-4. MAUS III Resonance C-scan of Boron/Epoxy Patch on Fuselage Panel**

### 2.3.4 Corrosion Detection

Corrosion in metallic structures is becoming a major problem as the airframe ages. In particular, when the corrosion initiates in a complex structure, it can be difficult to detect until substantial material loss has occurred. Ultrasonic pulse-echo methods may be used to detect material thinning, but may not be used to detect substructure corrosion in cases where there is no coupling between the skin and substructure. Eddy current techniques may be more useful in identifying corrosion thinning in these areas.

#### *KC-135 Pilot Drain Hole*

The KC-135 has become a major concern relative to corrosion detection and corrosion maintenance. One known site for corrosion was the pilot drain hole located directly below the pilot's window. Water entrapment and corrosion in the fuselage may occur when this hole becomes plugged. Figure 2.3.4-1 shows a photograph of the pilot drain hole location. Figure 2.3.4-2 presents a photograph of the SM-ALC evaluation of the MAUS III relative to this application. The eddy current phase C-scan that was generated relative to this application is shown in Figure 2.3.4-3. The dark gray areas between the fasteners and below the drain hole are suspect areas of corrosion. Portable C-scan equipment at SM-ALC was used to verify the results provided by MAUS III.



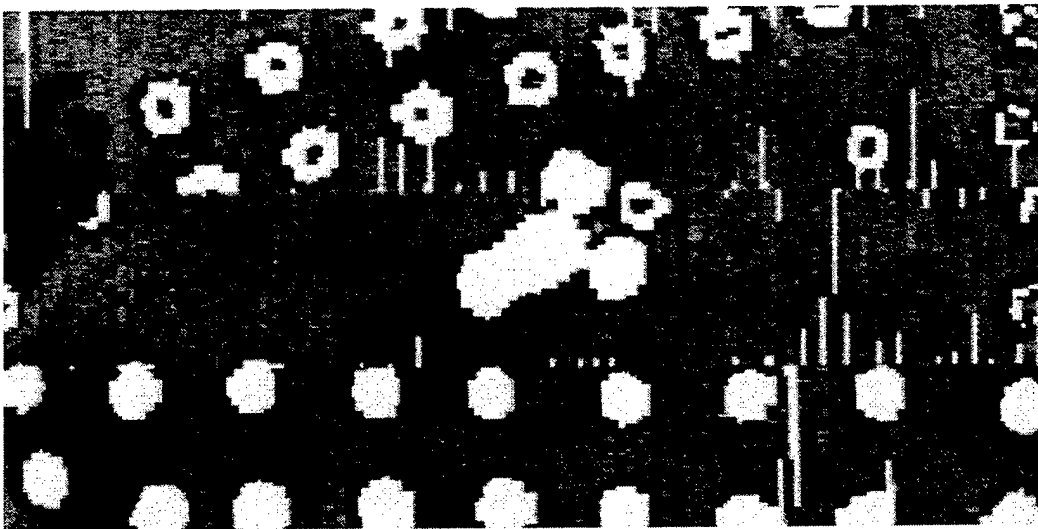
**Figure 2.3.4-1. KC-135 Pilot Drain Hole**





GP94031076.cvs

**Figure 2.3.4-2. MAUS III Inspection of KC-135 Pilot Drain Hole**



GP94031077.cvs

**Figure 2.3.4-3. MAUS III Eddy Current C-Scan of KC-135 Pilot Drain Hole**

This application provided another opportunity to showcase the portability and rapid set-up features of the MAUS III system. The ability to change configuration and easily was demonstrated. An impedance plane display for the laptop computer was requested by SM-ALC personnel to translate the manual set-up process used by most operators into MAUS III format.

#### ***Corrosion Thinning in KC-135 Lap Joint***

Lap joints in large aircraft fuselage skins connect large sections of continuous skin. Typically, the skin sections are overlapped at the lap joint and fastened together using three or

four rows of fasteners or spot welds. Problems that may occur in these areas include water intrusion, which may ultimately lead to corrosion. Figure 2.3.4-4 shows an eddy current C-scan of a KC-135 lap joint standard. This lap joint included a section of relatively severe corrosion that was accompanied by a thickness separation in the lap joint due to the corrosion. The change in gray shade from light to dark represents the lap separation, or pillowing, due to the excessive corrosion by-product.

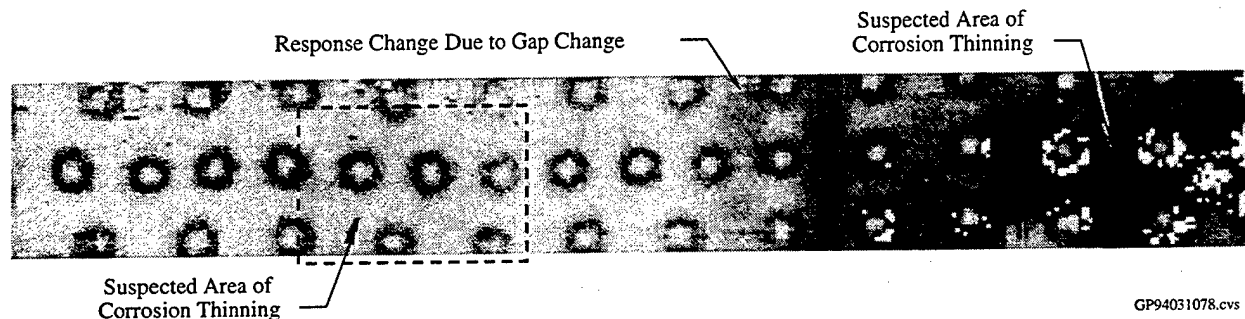


**Figure 2.3.4-4. MAUS III Eddy Current Phase C-scan of KC-135 Fuselage Lap Joint**

#### ***Corrosion Around Fasteners in Boeing 707 Wing Panel***

Galvanic corrosion may be a problem around steel fasteners installed in aluminum skins. This corrosion, caused by the galvanic effect created by dissimilar metals, causes intergranular attack in the aluminum material. This results in flaking and disintegration of the material. Occasionally, surface indications may be identified to locate the corrosion, but often the corrosion is below the surface and can only be detected when the fastener is removed. A pulse-echo amplitude C-scan of a wing panel with suspected intergranular corrosion is shown in Figure 2.3.4-5. Several areas in this panel appear to have been repaired, while several other fasteners show indications of galvanic corrosion.

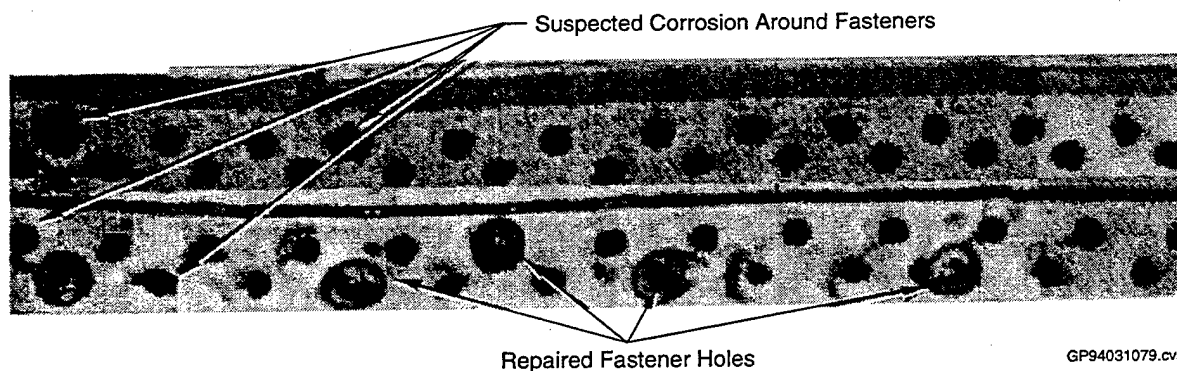


**Figure 2.3.4-5. MAUS III Pulse-Echo Amplitude C-scan of Boeing 707 Fuselage Skin With Suspected Exfoliation Around Fasteners**

### ***Corrosion Thinning in DC-10 Fuselage Skin***

Sections of aircraft fuselage may be exposed to fluids from leakage in galleys and lavatories. Corrosion caused by these effects typically occur on the inside of the fuselage skin and does not become visible from the outside until it is exposed as a hole or crack. Figure 2.3.4-6 shows an eddy current C-scan of corrosion in a section of fuselage skin that was removed from a DC-10 aircraft. The large white areas in the C-scan are the effects measured from a small crack and hole that developed when the corrosion extended through the skin thickness. The dark gray areas in the image represent less severe corrosion and pitting that was not visible from the surface.

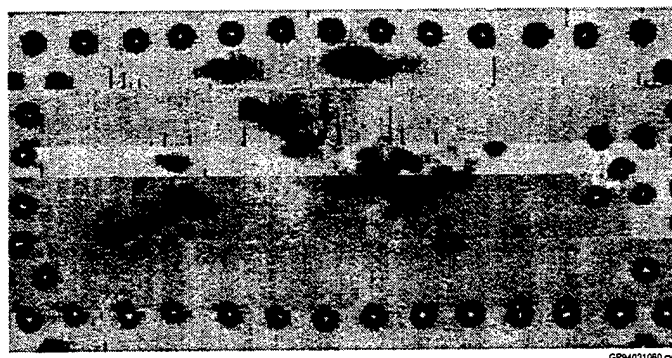


**Figure 2.3.4-6. MAUS III Eddy Current Phase C-scan of DC-10 Fuselage Skin**

### **2.3.5 Crack Detection**

A second inspection problem associated with aging structures is detection of fatigue cracks in first, second and third layers of airframe structure. Eddy current techniques may be used effectively to detect cracks in most areas. However, it is difficult to separate the sensor responses that are due to geometry from those caused by flaws. C-scan imaging helps to separate these sensor responses and to improve the reliability of the inspection.

#### ***F-4 Horizontal Stabilizer Cracking***

Fatigue crack growth can often occur between a series of fasteners. It is important to detect these cracks before they extend between several fasteners. The NDI group at OO-ALC had detected several cracks along the edge of an F-4 horizontal stabilizer using manual hand-scan techniques. They suggested using the MAUS III system to demonstrate the C-scan imaging capability for crack detection. Figure 2.3.5-1 shows an eddy current C-scan of a long crack that had extended between several fasteners before it was detected by the manual hand-scan. This figure also includes an image of a smaller crack that had just started to grow from another fastener.

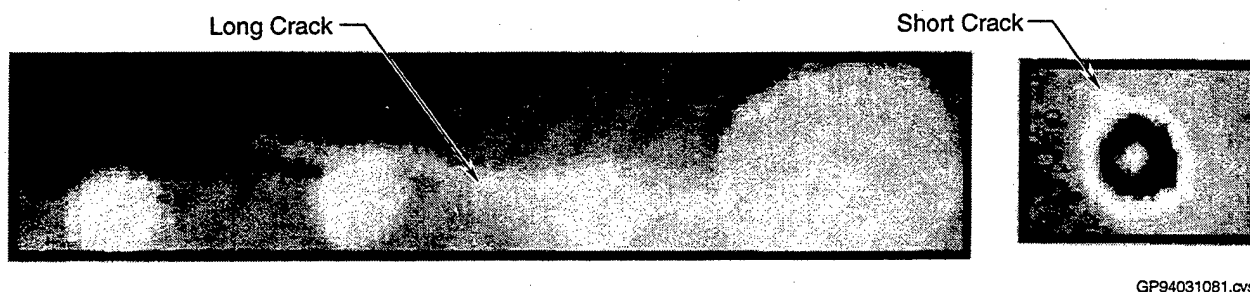


**Figure 2.3.5-1. MAUS III Eddy Current C-scan of Fatigue Cracks in F-4 Horizontal Stabilizer**

In general, eddy current hand-scanning is not difficult to perform on single-layer metallic structures with known fatigue crack sites such as the F-4 horizontal. An automated C-scan may not be necessary for these types of inspections. The greatest benefits of the C-scan approach are realized in complex metallic structures with widespread cracking.

### ***DC-10 Crown Skin Joint***

DC-10 crown skin joints include a metallic skin with finger doublers that are fastened to the inner surface of the skin. Eddy current techniques may be used to detect cracks emanating from the fastener holes in the finger doublers. Figure 2.3.5-2 shows an eddy current C-scan of a test standard developed for the crown skin joint. EDM notches were cut in the finger doublers at various locations along the joint. The finger doublers are shown as light gray areas on a dark gray background, which represents the skin. The fasteners appear as dark gray circles and the EDM notches appear as darker indications radiating from the fasteners. The C-scan image provides a clear picture in the eddy current scanning mode. It would be difficult and tedious to process this information manually without the use of the image.

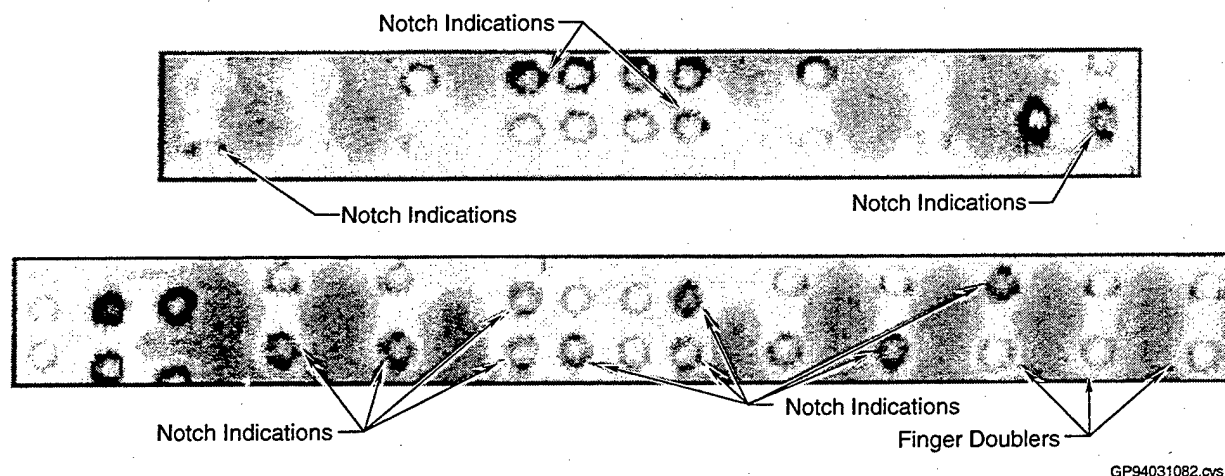


**Figure 2.3.5-2. MAUS III Eddy Current Phase C-scans of a DC-10 Crown Skin Joint Standard**

### **2.3.6 Requested Improvements**

A summary of the evaluation comments and suggested improvements are documented in the following subsections.

#### ***General System Operation***

Several changes in the system were requested to address safety and general usage concerns. Testing to determine if the equipment may be used in explosive or hazardous environments was requested. In addition, testing for adverse environmental conditions, such as temperature and humidity, was suggested.

Some concerns were expressed relative to the durability of the system when used for on-aircraft inspections. Suggestions included providing rubber feet for the signal conditioning package, develop a method to attach the laptop to the signal conditioning package and provide a "soft-pack" for transportation around a test site.

Additional operator support was requested to aid the operator while collecting data. Two scanner alarm lights were suggested. One scanner light could be used to alert the operator when the scanner was moved too quickly, or when the data was not being collected properly. The second scanner light could be used to signal the operator when the data was out of range. These lights would provide additional visual feedback to support the C-scan data images.

#### ***Pulse-Echo Improvements***

The pulse-echo inspection capability was optimized to enable accurate flaw detection in composite laminates. Additional inspection applications using pulse-echo techniques are frequently used to detect delaminations in porous materials and bondline voids in metal skin/core structures. These techniques were developed using equipment with adjustable pulser power, damping and large sensors. Requests were made by several ALC personnel to provide the same adjustments for the pulse-echo ultrasonics that are provided with conventional flaw detectors currently in use. These requests included additional pulser power, adjustments to select pulser power, adjustable damping, full R/F waveform display and waveform data collection.

### ***Resonance Improvements***

The ultrasonic resonance C-scan capability demonstrated with the MAUS III is an interesting feature relative to nondestructive testing. Typical bond testing applications are generally tedious manual inspections that are performed when no other option is available. The resonance C-scan demonstrations were quite impressive since the application of this method using the MAUS III is very easy. Given this, there were very few requests for changes to the resonance scanning mode since there wasn't much commercially available to compare. However, two requests were made to improve the system capability, including an impedance plane display for system set-up and an auto-balance function for the resonance phase circuit to balance the individual sensors. Although the resonance sensors were very effective in detecting bondline voids, water was still required to couple the sound into the structure. An investigation into non-coupling bond test sensors was requested.

### ***Eddy Current Improvements***

The eddy current inspection capability generated a great deal of interest during the ALC demonstrations. This method was not required for large area composite inspection, but was included in the original system to address inspection needs relative to metallic structures. One requested addition was a multi-frequency data acquisition mode to provide enhanced multiple layer detection capabilities. It was possible to mathematically combine the data collected at multiple eddy current frequencies to reduce the effects of gap changes, fasteners and multiple layers in sensor signals. Inclusion of these functions in the MAUS III system could improve the detection capabilities.

## **2.4 Field System Development**

Specific changes to the MAUS III system as defined during the Critical Design Review and the actions taken relative to system modification are summarized in the following sub-sections.

### **2.4.1 General System Operation**

The MAUS III prototype designed and developed during Phase II included four circuit boards that were built as wire-wrapped prototypes. These boards included the VME/SCB interface board, the system timing board, the signal digitizer and the HV power supply board. The circuit designs for these three boards were transferred to printed circuit format and

fabricated as PC boards. The circuits for the system timing and signal digitizer were combined into one circuit board layout in order to reduce the number of circuit boards[3].

Two operator support functions were requested during the demonstrations. Operator feedback on the scanner was suggested to indicate when the scanner was moved too quickly or when a flaw was encountered. The motor power light feature indicated when the scanner was moved too fast. The green power light indicated when the scanner was ready to scan and remained lit during the scan. If the scanner was moved too fast, the light flashed to alert the operator to decrease the scanner movement. The red alarm light was used to indicate when a flaw was detected. The signal levels that triggered the alarm light were adjusted in the "SETUP EDIT - SCANNER" menu in the system software. The light was only illuminated when data was outside the trigger levels that the operator established.

#### **2.4.2 Pulse-Echo Improvements**

The ultrasonic data conversion circuit that was originally included in the MAUS III prototype proved to be susceptible to electronic interference that resulted in relatively poor resolution of near surface reflection indications in the ultrasonic signals. The layout of this circuit was modified by changing the printed circuit board to a multiple layer design and improving the signal layout on the board.

The ultrasonic pulser/receiver circuit was redesigned to provide greater adjustment and flexibility for thin structure[3]. These changes included adjustable pulse width and dampening filters for each channel. This enabled the operator to tune each channel for the sensor frequency, and to adjust the signal response to optimize the signal sensitivity. The filters on the response signals were also adjusted to correspond to the standard sensor frequencies that are typically used in ultrasonic pulse-echo applications. Two requested improvements that were not implemented were adjustable pulser voltages and a square wave pulser option. These changes would require a substantially larger pulser power supply that would have resulted in a major design change in the circuit layouts. It was determined that a more useful future alternative for additional pulser power would be to design an external pulser circuit that could complement the existing circuitry in applications that would require more power.

### **2.4.3 Resonance Improvements**

An investigation into alternative bond test sensors that do not require couplant was requested during the demonstrations. Mechanical impedance analysis (MIA) and pitch/catch resonance were sensors that have been used successfully to detect bondline flaws at low frequencies without the use of couplant. Preliminary evaluations of the MIA sensors showed that they may be used to generate C-scan data by moving them slowly across the surface. Additional work in this area is described in Section 4 of this report.

### **2.4.4 Eddy Current Improvements**

The eddy current circuitry was modified slightly to reduce the cut-off frequency for the signal filters on the data conversion board[3]. This modification allowed the MAUS III system to drive very low frequency eddy current sensors. These sensors were typically used for second/multiple layer corrosion/crack detection in metallic structures. Typical frequencies that were used with the modified circuit range from 400 Hz to 2 MHz.

The mechanical design effort focused on designing a sensor mount for eddy current sensors that can protect the sensor from surface discontinuities such as raised rivets, pillowing and surface corrosion. A prototype eddy current sensor mount was fabricated and evaluated. Short brushes were added to the base of the sensor mount to compensate for surface irregularities and to hold the sensor at a constant distance from the surface. The standard gimbal design used for the MAUS III scanner mounts was modified to hold the brush mount. Evaluations of this approach were very successful as most surface inconsistencies were completely neutralized when the mount was used.

### **2.4.5 External Equipment Inputs**

The continuous waveform data acquisition board design was modified to include the option to select up to four inputs from an external instrument[3]. These inputs may be any signal with a voltage range between -10V and +10V. The external inputs were selected for each channel using the same software menu that was used to select the pulse-echo, resonance or eddy current inspection modes. Each channel could be selected independently so that any combination of pulse-echo, resonance, eddy current or external inputs may be selected from the four available channels.



## 2.4.6 Mechanical Scanner Improvements

The design for the transducer gimbal mechanism was modified to improve the lateral curve-following capability of the scanner[3]. The yoke arm in this gimbal mechanism was rotated 90 degrees to provide greater stability in the lateral axis. Figures 2.4.6-1 and 2.4.6-2 illustrate the original and modified gimbal designs, respectively. Evaluations indicated that this modified mechanism did improve the lateral curve-following capability; however, small compromises in the forward/aft movement ability were observed. Based on this, it was recommended that this modified mechanism should only be used in applications where lateral curvature was a problem.

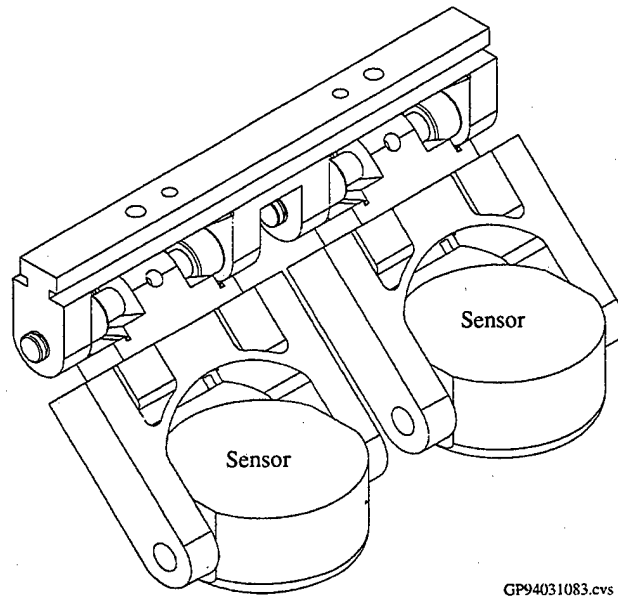


**Figure 2.4.6-1. Original Gimbal Design**

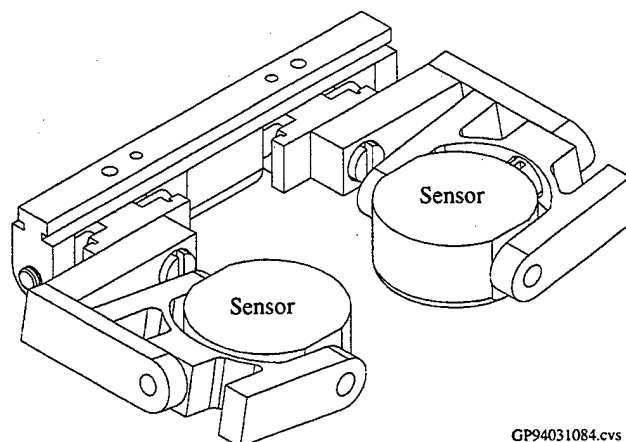


**Figure 2.4.6-2. Modified Gimbal Design**

An adjustable edge guide was designed to attach to the medium scanner. This edge guide was used to position the scanner at a constant distance from an edge or protrusion. A prototype edge guide was fabricated and it appeared that the guide aided in scanner positioning and will substantially reduce the operator effort required to follow an edge.

A spring-loaded scan marker concept was developed to attach to the scanner. The intent was to mark the scan path as the scanner was moved over the part surface. The marks placed on the part indicated the area of inspection and were used to reference the scanner for the next scan. Figure 2.4.6-3 illustrates the pen marking concept.

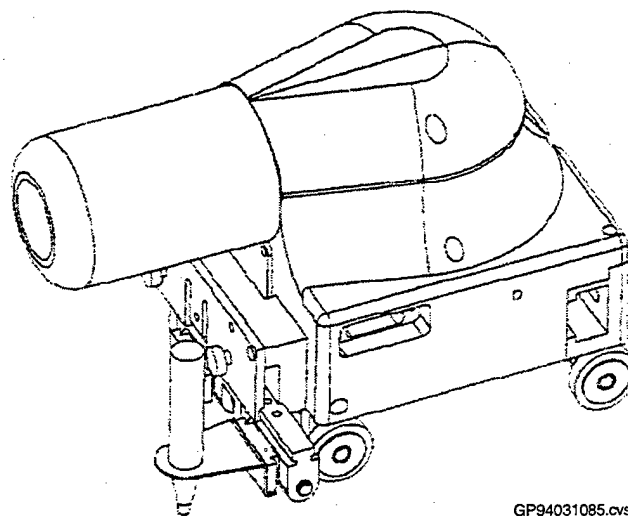
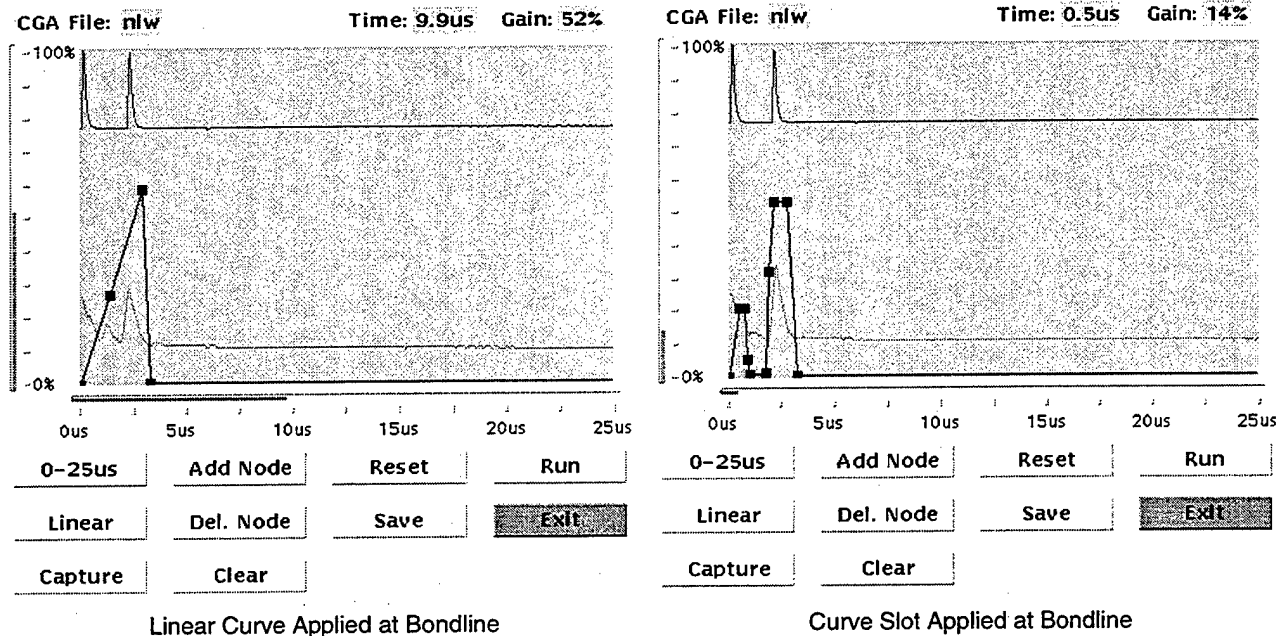


**Figure 2.4.6-3. Pen Marking Concept**

#### **2.4.7 Software Improvements**

The MAUS III software package was refined to eliminate the minor software concerns that were identified during the system evaluations[4]. System crashes were virtually eliminated and initial problems with scanner calibrations were resolved.

The programmable DAC software was improved to provide an easy interface for the DAC curve designer. The DAC curve may be programmed by drawing the DAC/time graph on the computer screen. The RF signal was overlaid on the graph to provide a convenient reference point for the curve designer. The curves contain up to 512 distinct nodes that were set using either a linear or spline curve fit. Figure 2.4.7-1 shows the DAC curve menu with the RF signal underneath the DAC curve representation. Any number of DAC curves may be stored in the computer and recalled for a specific inspection.



GP94031086.cvs

**Figure 2.4.7-1. DAC Curve Menu**

An impedance plane display option was added to the A-scan menu to aid the operator in equipment set-up. The format of this display option was intended to duplicate the standard display formats that were used in manual eddy current and bond-testing instruments. The initial implementation of this software did not directly duplicate the standard formats since the measured parameters of amplitude and phase were not directly compatible with impedance components that are typically measured in manual instruments. Figure 2.4.7-2 shows the MAUS III impedance plane display.

Data reconstruction software was developed and was used to create a single data file that combined the MAUS III data strips into a C-scan of the entire inspection area. The reconstruction process starts with the operator selecting the sections of MAUS III data strip that will be included in the reconstructed data. These sections are subsequently merged into a single data file. The operator can move, rotate, group and scale the data sections within the merge file. A flip function was also requested during the software evaluation and was included in the package. Figures 2.4.7-3 through 2.4.7-5 illustrate this reconstruction process.

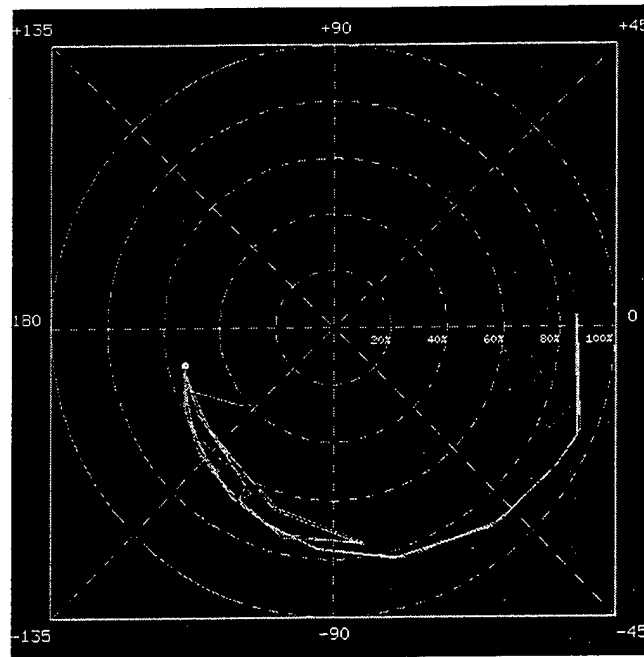


**Figure 2.4.7-2. MAUS III Impedance Plane Display**

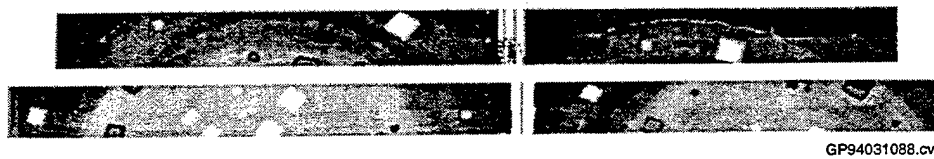


**Figure 2.4.7-3. Original Inspection Data Collected in Strips**

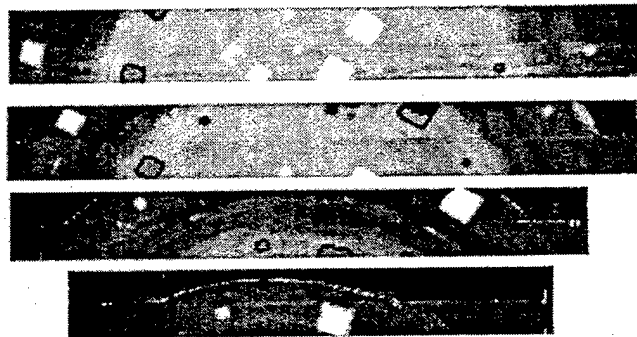
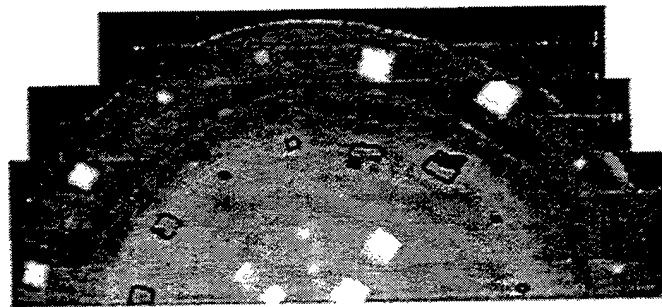


**Figure 2.4.7-4. Data Strips Selected from Original Data File**



GP94031090.cvs

**Figure 2.4.7-5. Data Strips Repositioned to Create Full Image Data File**

### **2.4.8 Portable Soft-Pack Carrying Cases**

A soft-pack carrying case was designed to incorporate several of the change requests in one item[4]. The case, shown in Figures 2.4.8-1 and 2.4.8-2, contained the electronics box, laptop computer, power supply, computer mouse and cables. All of the system cables, with the exception of the scanner cable, may remain connected when the equipment is stored in the case. A velcro strap was provided to hold the electronics box in the case. A second velcro strap was provided to attach the laptop computer to the electronics box and case. Two access flaps were included in the front and the back of the case to allow access to the system front panel and the power input module on the system back panel.



GP94031091.cvs

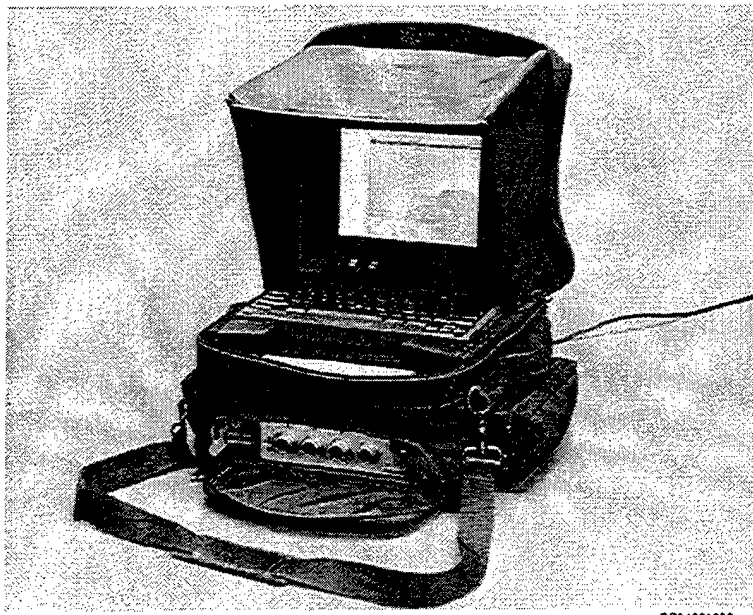
**Figure 2.4.8-1. Soft-Pack Case for MAUS III**



GP94031092.cvs

**Figure 2.4.8-2. Soft-Pack Case Showing Storage Capability for MAUS III Components**

A screen shield was included in the top of the soft pack case. The sides of the shield may be unfolded, as shown in Figure 2.4.8-3, and velcro-attach to the sides of the case. The shield effectively blocked external sunlight from reflecting directly on the computer screen and improved visibility. Glare or indirect reflections from the sun were not eliminated using the shield; however, a small, commercial, non-reflective screen appeared to have solved the visibility problems caused by the glare. The screen was stored with the shield in the top of the case.



GP94031093.cvs

**Figure 2.4.8-3. MAUS III Soft-Pack Carrying Case Showing Anti-Reflection Screen Shield**

The combined weight of the equipment in the soft-pack case was 25 pounds. A padded shoulder strap was included with the soft-pack case. Handles were also provided on both sides of the case to aid in carrying. Rubber feet on the bottom of the case firmly held the equipment in place, even on slightly curved surfaces. Four external pockets were added to hold probes, reference standards, paper and miscellaneous items.

A second soft-pack was also designed to hold the system scanner and additional support equipment that may be needed for an inspection. The second case was similar to the case previously described, but did not have the zipper access panels. Two shipping containers were added to the system so that the soft-pack cases may be placed directly in the containers for storage or shipment. This proved to be very useful for on-site inspections since the equipment was already packed in the soft-pack cases and pre-assembled upon arrival at the site.

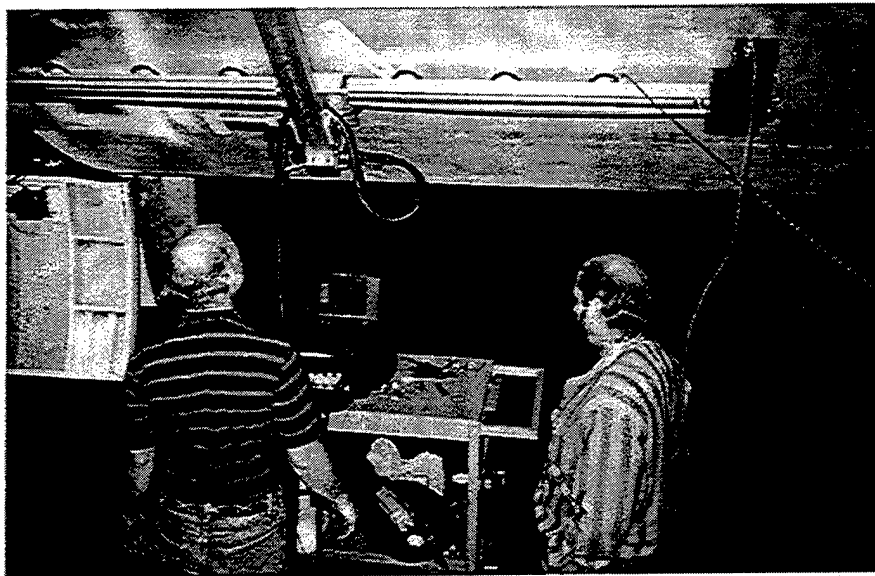
### 3.0 FIELD SYSTEM DEPLOYMENT (MAUS III)

A total of 10 MAUS III systems were procured under additional program funding in January 1995. These systems were placed at various Air Force and Navy installations to evaluate system capabilities. The following section summarizes the results of the evaluations and the variety of applications investigated

#### 3.1 Oklahoma City Air Logistics Center (Tinker AFB, OK)

The MAUS III system was used extensively by Oklahoma City Air Logistics Center (OC-ALC) personnel to evaluate KC-135 lap seams, as shown in Figure 3.1-1. The dual frequency eddy current inspection mode was used to collect inspection information over areas that contained suspected corrosion. Substantial efforts were expended to develop the inspection approach, validate the data results, and develop a wide experience base on in-service aircraft. Many suggestions were generated by the OC-ALC personnel and implemented in the MAUS III software and hardware design. These suggestions were typically operational requests to simplify inspection functions.

Early feedback from this evaluation indicated that it was difficult to manually position the scanner across an inspection surface at the relatively slow speeds required for the dual frequency scanning. This was particularly a problem in overhead scanning applications on the belly of the



GP94031094.cvs

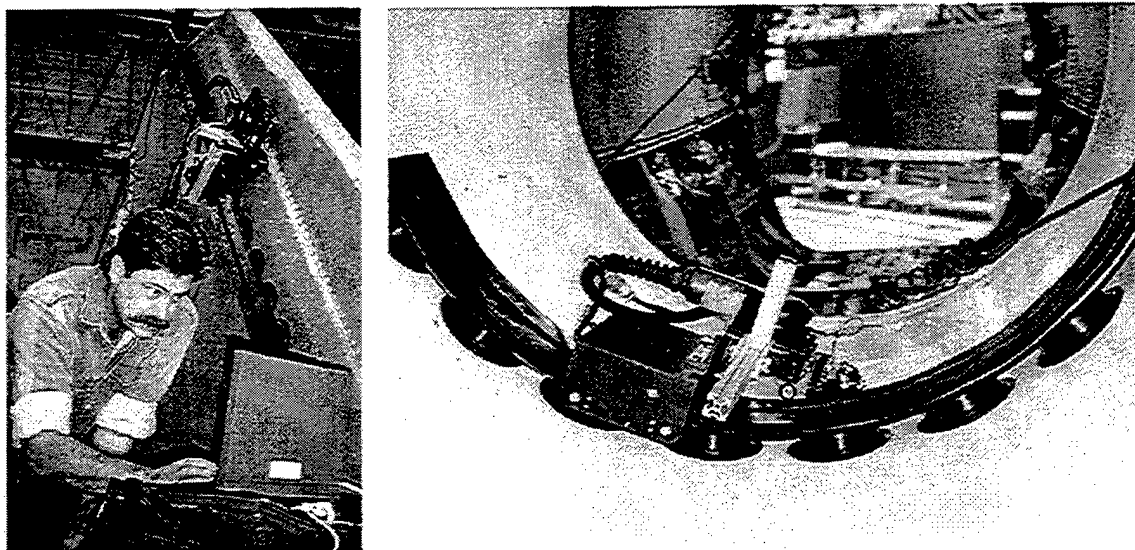
Figure 3.1-1. MAUS III Evaluation of KC-135 Lap Joints at OC-ALC



aircraft. A commercial positioning track was provided to supply automatic scanner positioning in these awkward inspection locations. This track improved scanning speed and reduced operator fatigue. However, it could not be used in some of the areas on the aircraft with substantial curvature changes. The system was used in a semi-production role for most of the evaluation period where it was used to check any suspect areas identified in visual inspections of the aircraft.

### **3.2 Ogden Air Logistics Center (Hill AFB, UT)**

The MAUS III was evaluated at the Ogden Air Logistics Center (OO-ALC) on several F-16 applications, as shown in Figure 3.2-1. In particular, coating bondlines in the inlet duct, cracking in wing spars, and cracking in vertical tail leading edges were investigated. Some limited production scanning was performed. Feedback from this evaluation centered on improvements to the operator interface for data collection and archiving.



GP94031095.cvs

**Figure 3.2-1. MAUS III Evaluation of F-16 Vertical Stabilizer Leading Edge and Inlet Duct at OO-ALC**

### **3.3 Sacramento Air Logistics Center (McClellan AFB, CA)**

Sacramento Air Logistics Center (SM-ALC) personnel evaluated MAUS III functions extensively, particularly for composite structure applications. Many comments were generated regarding signal conditioning functions, software data collection and display capabilities, and scanner improvements. Many of these comments were incorporated in system changes during the evaluation period. Several C-17 inspection applications were investigated. A formal technique was drafted for inspection of the landing gear door. MAUS training was provided to the personnel at Charleston AFB by the personnel from SM-ALC.

### 3.4 Air Force Research Laboratory (Wright-Patterson AFB, OH)

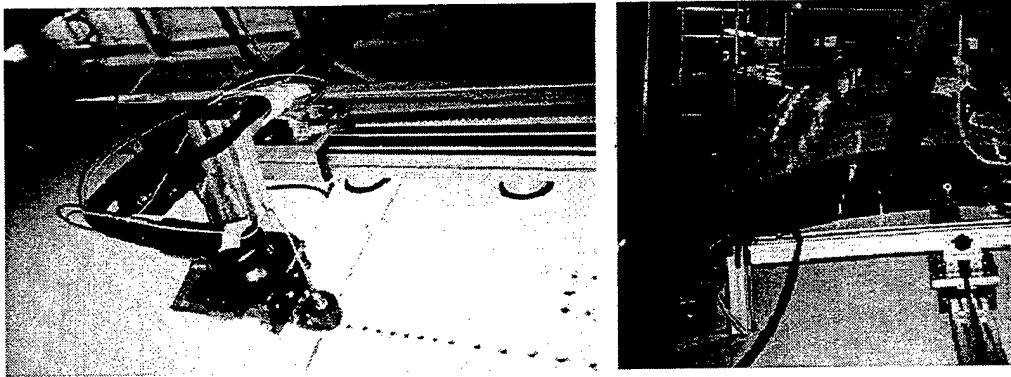
The MAUS III system use at the Air Force Research Laboratory (AFRL/MLLP) centered on general research and development applications and system demonstrations. Non-military technology transition applications were investigated in the automotive and marine racing industries, as well as in the commercial aircraft maintenance industry. As an example, the MAUS III was used to scan a composite car body at the Indianapolis Motor Speedway, as shown in Figure 3.4-1.



GP94031096.cvs

**Figure 3.4-1. Evaluation of MAUS III at the Indianapolis Motor Speedway**

Also, one of the AFRL MAUS III systems was placed at Northwest Airlines in Minneapolis, MN for evaluation relative to commercial aircraft maintenance inspections. A DC-10 Crown skin inspection was developed to identify cracks in multiple layers of the crown skin structure. This inspection, shown in Figure 3.4-2, replaces a costly and time-consuming radiographic inspection. The alternative means of compliance was granted by the FAA in June 1996. Fifteen aircraft have been inspected to date at several airlines using the MAUS III. Additional work was performed to evaluate MAUS III for corrosion detection in DC-9 belly skins. This work is contributing to current efforts to gain FAA acceptance for these applications.



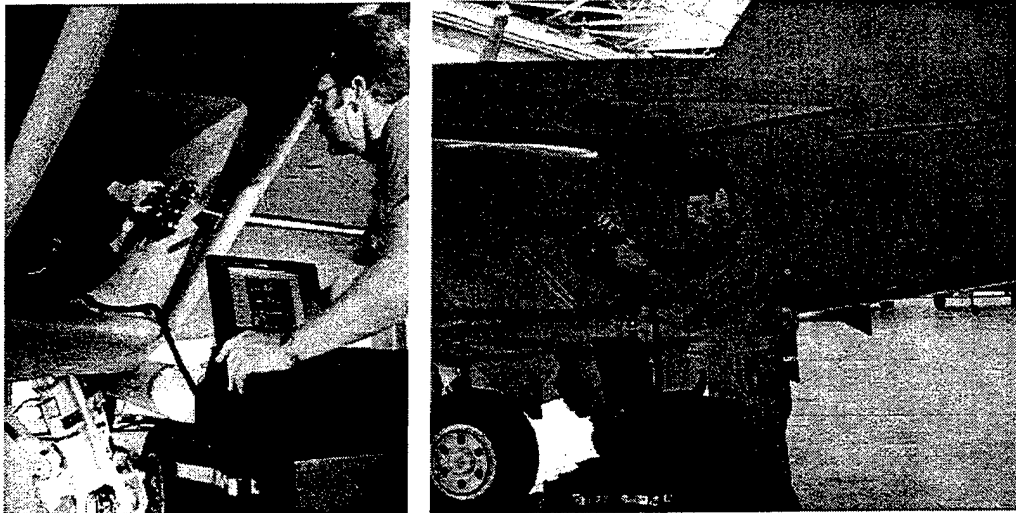
GP94031097.cvs

**Figure 3.4-2. MAUS III Evaluation of DC-10 Fuselage Structure at Northwest Airlines**

Significant feedback on user interface difficulties contributed to the human factors considerations in the MAUS IV development described in Section 4. In addition, the scanning experience developed during the DC-10 inspections contributed to the ergonomic design factors included in the flexible track development.

### **3.5 Naval Aircraft Applications**

Two MAUS III units were procured by the U.S. Navy under the contract and initially placed at Patuxent River Naval Air Station and at Cherry Point Naval Air Station. Both units were eventually transferred to the Patuxent River site due to substantial inspection requirements during the F-18 E/F flight test program. MAUS III evaluations of F/A-18E/F structures are shown in Figure 3.5-1. Three structures are inspected periodically on all flight test aircraft. Feedback from operators performing these inspections focused on the need for a simplified operator interface, and for improvements in scanner ergonomics. This feedback contributed to the design considerations for the MAUS IV program.



GP94031098.cvs

**Figure 3.5-1. MAUS III Evaluation of F/A-18E/F at Patuxent River, MD**

### **3.6 Warner-Robins Air Logistics Center (Robins AFB, GA)**

Usage of the MAUS III at Warner-Robins Air Logistics Center (WR-ALC) was limited and as a result, feedback was limited.

### **3.7 San Antonio Air Logistics Center (Kelly AFB, TX)**

Usage of the MAUS III at San Antonio Air Logistics Center (SA-ALC) was limited and as a result, feedback was limited.

## **4.0 PRODUCTION PROTOTYPE DEMONSTRATION/VALIDATION (MAUS IV)**

The MAUS III program transitioned to the Manufacturing Technology Directorate (ManTech) at AFRL to develop a productionized system, known as MAUS IV. ManTech modified the existing MAUS III research and development effort and initiated Task 4, Production Prototype Demonstration/Validation, in November 1996. Specific objectives included expansion of the bond detection capabilities, improved operational ergonomics, and simplified system operation.

The bond detection methods included in the original MAUS III design were ultrasonic pulse-echo and resonance. These methods are effective for many bondline voids particularly in composite structures consisting of skin/skin bonds or skin/metal core bonds. These methods are less effective on structures that include skin/non-metallic core bonding. Alternate inspection methods for these structures were evaluated and selected for inclusion in the productionized system.

Human factors and system ergonomics issues were raised after extensive use of the MAUS III system in production applications. In particular, overhead operation was difficult while using a relatively slow detection method such as dual frequency eddy current. Operator fatigue was a major concern as well as data quality. A straight track was used to hold the MAUS scanner on the part surface and this improved the operator fatigue and data quality issues. However, this track was cumbersome, difficult to position, and could not be used in many of the areas that required inspection. Efforts to enhance system ergonomics centered on improving the track positioning concept and scanner design changes.

A relatively experienced operator was required to use the MAUS III system effectively. In particular, it was difficult for an operator who used the system infrequently to remember the procedures to start, operate and shutdown the system. In addition, training efforts were substantial to qualify an operator for system operation. Efforts to simplify system operation were aimed at easing confusion by reducing the system setup tasks, eliminating multiple menus, and using industry standard operator interfaces.

Technical efforts required to accomplish the program objectives were concentrated in five areas:

1. Sensor evaluation to define additional bond test methods
2. Circuit card modifications to integrate additional methods and simplify system operation
3. Mechanical design to address human ergonomic concerns
4. Software development to simplify system operation
5. System evaluation and feedback

#### **4.1 Bondline Inspection Sensor Evaluation**

Conventional inspection methods were evaluated to identify advantages for bondline detection and to determine suitability for inclusion in the MAUS system. Commonly used methods such as Pitch/catch (Sondicator design), Mechanical Impedance, and tap test were examined. Less common methods such as Eddy sonics and Microwave were also considered.

##### **4.1.1 Pitch/Catch Resonance**

The Pitch/catch sensor includes two sensing elements. A sine wave burst is applied to one of the elements to generate a surface wave in the material. The signal frequencies for the excitation frequency are in the 10-40kHz range. The surface wave is detected by the second element. Changes between the excitation and receive signals indicate changes in the stiffness of the structure or bondline. This method is quite effective for examination of bonding between thin skins and non-metallic core. Defects in the core as well as bondline voids are easily detected with this method.

Initial evaluations of the method showed that the signals obtained from areas representing unbonds were substantial in both the amplitude and phase components of the signal. The signal-to-noise ratio was quite good. Limitations with the method include a large detectable defect size of 0.5 inches and relatively slow sensor movements required to maintain a stable signal.

##### **4.1.2 Mechanical Impedance Analysis (MIA)**

The Mechanical Impedance sensor includes one excitation/sensing element. A sine wave burst is applied to the element to generate a vibration in the material. The signal frequencies for the excitation frequency are in the 5-20kHz range. When the element is placed on the surface, the structure creates a change or load that is measured in the receive signal. Changes between the

excitation and receive signals indicate changes in the stiffness of the structure or bondline. This method is also quite effective for examination of bonding between thin skins and non-metallic core. Defects in the core as well as bondline voids are easily detected with this method.

Initial evaluations of the method showed that signals obtained from areas representing unbonds were moderate in both the amplitude and phase components of the signal. High level voltages resulted in an acceptable signal-to-noise ratio. Limitations with the method include a large detectable defect size of 0.5 inches and very slow sensor movement necessary to maintain a stable signal.

#### **4.1.3 MIA – Bondcheck**

The Bondcheck instrument is a commercial product with an approach similar to conventional Mechanical Impedance(MIA) sensors. The original plan was to evaluate the Bondcheck sensors to determine the advantages over conventional MIA approaches. After some investigation it was clear that the manufacturer optimizes the instrument for each sensor and that the two cannot be separated. This becomes a major disadvantage when more than one sensor is used, or if a sensor is damaged and requires replacement. Therefore, this approach was not considered for inclusion in the system.

#### **4.1.4 Tap Test**

The most common technique used for bondtesting is the tap test. It is a crude method of identifying bondline voids by inducing sonic energy into the structure with a tap and listening for changes in the sound. It is very subjective, somewhat unreliable, and difficult to determine actual flaw size. Advantages in tap testing are that it is simple to perform and that it requires no instrumentation to tap or listen.

Boeing has developed a method to improve tap test results by measuring the energy in the tap and correlating this measurement to changes in the bondline. It is a simple approach to quantifying the energy changes that are detected aurally in conventional tap testing. This method was evaluated for inclusion in the MAUS system. It appeared to be a good fit for the excitation and measurement of the energy in the tap. However, a significant technical barrier was that a tap test sensor was not commercially available. Therefore, this method could not be considered for the productionized MAUS IV system until a commercial sensor is offered.

#### **4.1.5 Eddy Sonics**

The eddy sonic sensing approach creates an excitation in the material using an eddy current field. Ultrasonic surface waves resulting from this excitation can indicate bondline changes in the structure. Evaluations of this technique showed moderate success in detecting bondline voids in thin metal/metal bonds and poor results on composite materials. In addition, a large amount of energy is required to generate the excitation signal. This would require a very high-level power supply that would not fit within the form factor of the MAUS equipment. With no distinct detection advantage over other sensing methods, this approach was abandoned.

#### **4.1.6 Microwave**

A microwave approach was investigated where a low frequency ultrasonic resonance based transducer was used to generate displacements in the surface of the material and a Ku-band waveguide was used to detect the surface displacements. The results of an investigation showed that hardware for millimeter wave measurements would be required to detect displacements on the order observed during a resonance inspection. This would increase the cost of the system dramatically, and therefore, this approach was not pursued.

#### **4.1.7 Summary of Signal Conditioning Improvements**

The selected sensor/detection methods for inclusion in the MAUS equipment were Pitch/catch and Mechanical Impedance. The Boeing Tap Test method was considered in the implementation of the system changes to allow the use of tap test sensors when they become commercially available.

Specific considerations required for these sensing techniques included adjustments for excitation signal strength and the duration of the excitation signal burst. Excitation signals may vary from 0.1 to 50 volts depending on the type of sensor that is used. The signal burst may vary from 1-10 cycles or a continuous wave signal may be applied to the sensor. Adjustable time delays between signal excitation and data sampling were specified to optimize signal-to-noise characteristics. Finally, modifications to the Phase/Amplitude detection circuitry were also specified to allow for direct detection of the impedance and reactance components between the excitation and receive signals.



## 4.2 Circuit Board Enhancements

Changes in the MAUS circuitry were necessary to address the signal conditioning requirements that resulted from the bond testing evaluation. In addition, several changes were initiated to enhance system performance and to simplify the system operation. Specific changes centered on the CPU board, the front panel, the timing/digitizer board and the continuous wave circuit boards. Small changes were also anticipated for the Motion Control Processor (MCP). Figure 4.2-1 illustrates the circuit card changes that were accomplished in this program.

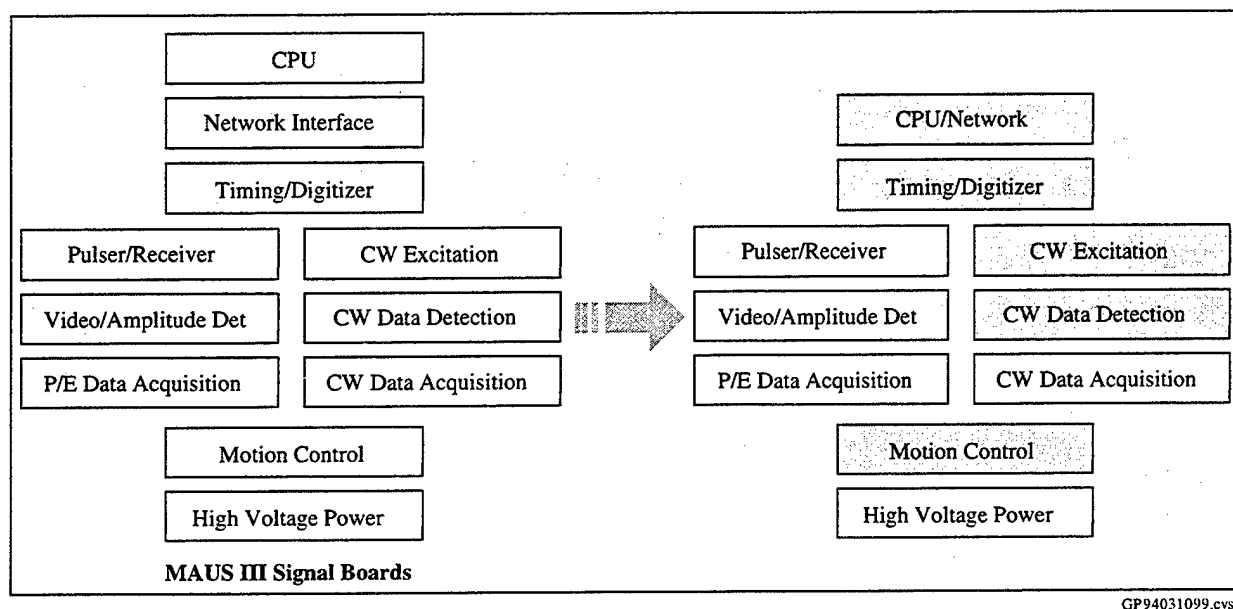


Figure 4.2-1. Summary of Circuit Card Changes Implemented in MAUS IV

### 4.2.1 CPU board

The CPU is the supervisor of the signal conditioning circuitry. This card coordinates the scanner motion control and data acquisition functions. The scanner position and data values are formatted into data buffers that are transferred through a network connection to the laptop for display and storage.

Several improvements in CPU capability were specified to improve system performance and operation. These included reducing startup and connection time, increasing data collection rates, reducing board count, and implementing a Remote Process Command (RPC) protocol for communication with the PC laptop. The original CPU functions on the MAUS III were accomplished using a two-board set procured through a commercial vendor. Production control

was difficult to accomplish due to changes imposed by the manufacturer/distributor every few years. A PowerPC chip was selected to replace the functions performed by the two-board set. This chip increases the CPU speed from 20 MHz to 40 MHz, and includes all of the network functions required for communication to the laptop computer. A new board design and layout was performed to combine all of the CPU capability into a single board. This board design includes flash memory to retain the software programming for the CPU board. The flash memory allows the program to start immediately on power up but it can be reprogrammed for software updates. Additional memory was added to the board to allow for larger buffer sizes when transferring data between the CPU and the laptop computer.

#### **4.2.2 Front Panel**

The original front panel for the MAUS III included switches to select the sensor type and to route the signal information to the correct circuitry. These switches created problems for an operator when they were switched inadvertently or when they were forgotten. Also, additional switching was required to integrate the pitch/catch and MIA methods. These sensors require different signal energy levels, and the cabling is unique for each sensor type. A new front panel was designed to remove the manual switches and to provide automatic switches and adjustments for all of the sensors. Transformers were added to increase voltage levels up to 48 volts for the MIA probes. The front panel was also designed to accommodate the connectors and switches for the new CPU board. The signal inputs for the eddy current, pitch/catch, and MIA sensors were combined into a single receptacle labeled "Sensors". The resonance and pulse-echo ultrasonic signals are combined with the position feedback and motor signals in a single receptacle labeled "Scanner".

#### **4.2.3 Timing/Digitizer Board**

The CPU board controls the data acquisition process using the timing/digitizer circuit board. This board was re-designed to couple directly to the new CPU board allowing for faster data transfer between the two boards. The circuit clock was increased from 32MHz to 100MHz resulting in improved depth resolution for pulse-echo data readings and increased resolution for digital waveforms. In addition, precise control of the timing for acquired waveforms results in reduced sizes for waveform data files.

#### **4.2.4 Continuous Wave Circuit Boards**

The continuous wave excitation circuit board required modification for the pitch/catch and MIA sensor modes to allow for adjustable signal bursts. New frequency generator chips were incorporated to allow for specific alignment of the sine wave signal at the start of the signal burst. Circuitry to control the exact length of the signal burst was also added. The continuous wave signal conditioning circuit board was changed to provide data information in similar formats to conventional impedance plane instruments. Impedance and reactance measurements (X/Y) are measured directly from the circuit in the new design. Phase rotation is available to the operator to position the X/Y data in the desired orientation. The Phase and Amplitude readings are calculated from the X/Y data values.

#### **4.2.5 Motion Control Processor**

The planned changes for the Motion Control Processor (MCP) were minor intending only to accommodate the new variable stroke scanner. Unfortunately, the functional changes in scanning approach introduced by the variable stroke scanner resulted in substantial modifications to the circuit board firmware – software stored in programmable logic chips and programmable memory chips. These firmware changes were required to allow for speed, offset, and stroke adjustments before and during a C-scan. In addition, the data resolution settings also required additional accommodation in the firmware. Many of the issues raised during the initial evaluation period were addressed through these changes.

#### **4.3 Ergonomic Enhancements**

Human factors and ergonomic improvements in the MAUS scanner were accomplished through the mechanical design tasks. The most significant difficulty encountered while using the MAUS III scanners was operator fatigue, particularly when scanning in awkward positions with slower inspection methods such as dual frequency eddy current. It was hard for the operator to hold the scanner in position, and to move the scanner at an even speed for long periods of time. In some cases, slick surfaces also created a problem when the wheels of the scanner would slide rather than roll on the surface resulting in position detection problems. Optimal inspection speeds are obtained when the scanner is moved at an even speed leaving just enough time to allow data collection at each data point. When the MAUS scanners are positioned manually, it is difficult for an operator to maintain this optimal speed. Valuable inspection time is lost when the operator

must reverse the scanner position to fill in data points that are missed when the scanner is moved too quickly.

A commercial track mechanism was successfully used to alleviate manual-positioning problems, however, it was time-consuming to set up and could not be used on many of the complex surfaces encountered on an aircraft. Improvements on this concept were initiated to address these human factors concerns. Some concerns relative to the ruggedness of the hand scanners were also expressed. In particular, the wheel mounts on the hand scanners were vulnerable to impact when the scanners were dropped. In many cases, the wheel mount would snap off if the scanner orientation allowed the wheel mount to absorb the entire impact. A design review of the hand scanners was requested to improve on impact resistance for these scanners.

#### **4.3.1 Flexible Track Concept**

A flexible track concept had been developed at Boeing to provide the scanner positioning advantages of the commercial rigid track while conforming to the complex curvatures encountered on fighter aircraft. A positioning carriage was fabricated and a prototype track section was machined from neoprene rubber to demonstrate the positioning concept. This prototype positioning system successfully demonstrated the feasibility of the concept however it was extremely expensive to manufacture. Over one hundred machining hours were required to cut each half of the track section from a solid rubber piece. The two rubber half sections were bonded together using a rubber adhesive. Mechanical design efforts in the project were directed towards creating a flexible track design that could be produced for a reasonable cost.

#### **4.3.2 Flexible Track Production**

The initial conceptual development for the flexible track included internal plenums for the vacuum chambers so that no external tubing or cabling was required. The suction cups remained separate from the track section so that torn or damaged cups could be easily replaced. A rack was included in the center of the track to drive the carriage and provide position information for the carriage/scanner. Angled edges were used to provide bearing surfaces for the carriage. A quick release vacuum feature was identified to allow easy removal of the track section. Finally, a leap-frog approach was requested to enable continuous positioning of two track sections. One track section could be added to the current track section. Once the scanner carriage had moved to the

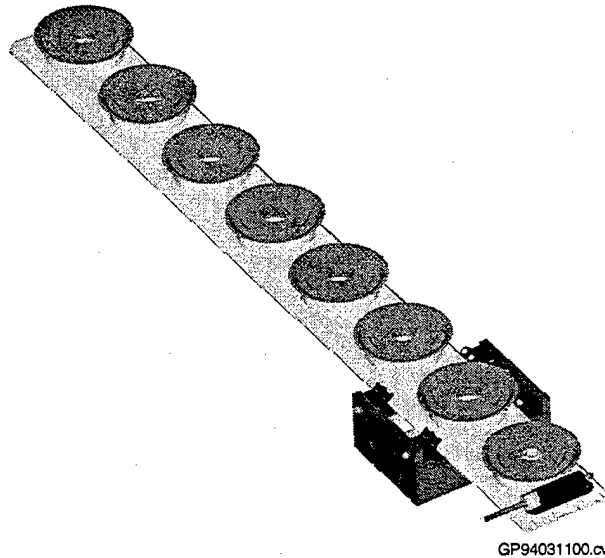
new track section, the previous section could be removed and added to the front of the new section.

A direct implementation of this design required molding the track with a poured mold or injection mold process. These processes require a substantial investment to create the mold but result in relatively inexpensive final products once the mold is in place. An outside vendor with extensive experience in molded urethane products was selected to build the track sections. Consultations with the vendor resulted in several modifications to the initial track design. The durometer of the urethane was increased to improve local stiffness along the track. The track thickness was reduced from 1.0 inch to 0.75 inches to improve flexibility and to reduce weight by 20%. Recesses were added to hold the hex nuts for all screws flush with the surface. Two concepts for linking track sections together were discussed. A hard link would allow longer permanent track section lengths, but would require tooling to attach the track sections together. A soft link concept would allow two sections to be aligned using a pin/hole approach and would allow for repositioning of the track sections. The second concept was selected for the simplicity of the design and for the leap-frog capability.

The initial track design was translated to a mold design by the outside vendor and submitted to Boeing for approval in April 1997. The mold was manufactured by a subcontractor and delivered to the vendor for the initial pour in early May. The first molded track sections were delivered to Boeing in early June. Initial manufacturing problems encountered in these first sections included poor surface quality due to tooling marks left on the surface of the mold, and air bubbles on the end of the track section. Minor changes in the pin/hole design were made to improve on the leap-frog position capability. In addition, the hex nut recesses were too deep. The mold was reworked and a second set of track sections was poured.

The prototype track sections were sent to the OC-ALC evaluation team in August 1997. Evaluations of the functional capability of the flexible track were very favorable. Substantial improvements in inspection speeds were accomplished using the leap-frog position capability.

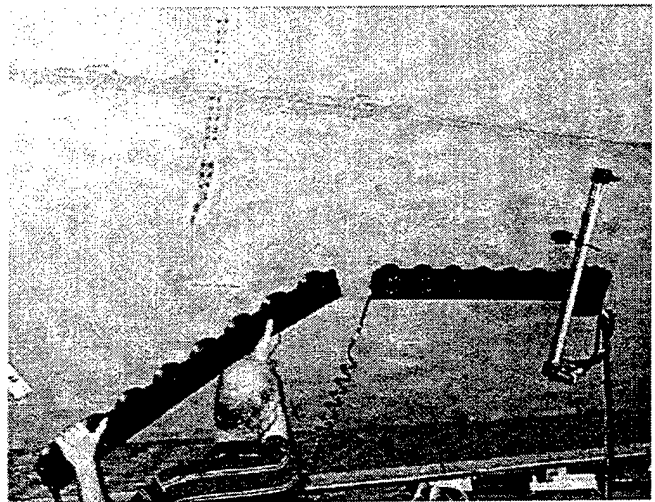
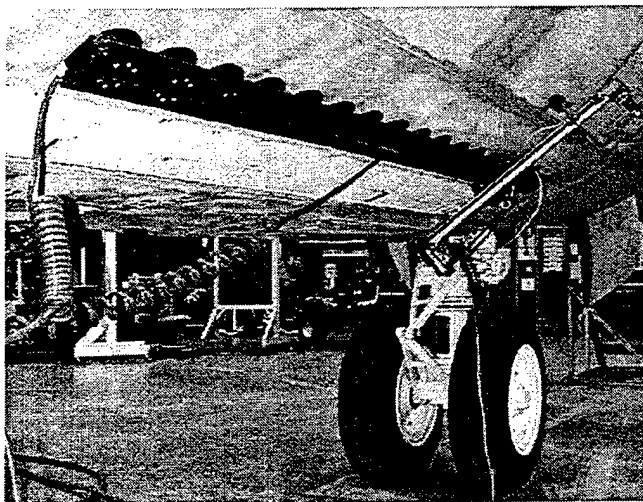
In the final design, shown in Figure 4.3.2-1, each track section is 5.0 inches wide, 2.5 inches high, and 43 inches in length. Eight suction cups attach the track section to a surface using vacuum pressure. Each suction cup has an individual shut-off valve so that the vacuum pressure is not affected if a cup is not in contact with the surface. One quick release valve is positioned at



GP94031100.cvs

**Figure 4.3.2-1. Flexible Track Design**

one end of the track section so that the vacuum can be released with slight finger pressure to remove the section from a surface. A drive rack is molded in the center of the track providing positive positioning for the track carriage. Each section contains alignment pins on one end and holes on the opposite end to allow for easy accurate alignment when one section is added to a second section, as shown in Figure 4.3.2-2. Safety line attachments are optionally added at one end of each section.



GP94031101.cvs

**Figure 4.3.2-2. Flexible Track Attached to KC-135 Fuselage**

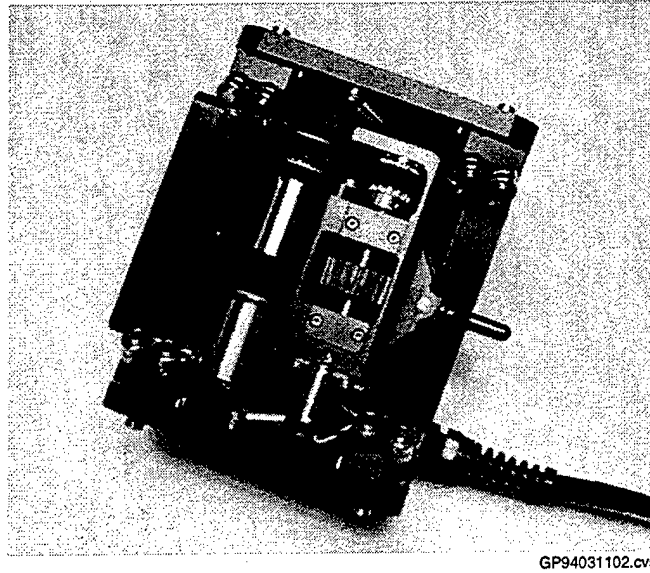
A significant stumbling block for the OC-ALC personnel was the lack of safety backup if the vacuum was lost. Evaluation continued without a safety backup but they were clear that the track could not be used in production without additional safety considerations. A manual safety system was designed to provide safety backup for the flexible track, carriage, and scanner. Two suction cups are manually placed above the inspection area. A safety line connects between the two suction cups. Lanyards attach to the carriage, and optionally to each track section, connecting the components to this safety line. When the vacuum is interrupted, the safety line holds all of the attached components until the operator can recover the vacuum or remove the components. This manual safety system has been tested many times with good results. Some care is required when the system is attached to the aircraft to determine where the components will swing when the vacuum is released.

A venturi pump is used to convert standard shop air to the vacuum required to hold the track sections on the surface. In some instances, when substantial leakage around the suction cups existed, the vacuum supply to the track sections was insufficient. The sections would hold on the surface but could be easily pulled away. Analysis of these conditions led to replacement of the supply lines between the pump and the track sections, increasing the line diameter from 0.375 inches to 0.5 inches. In addition, the pump was re-designed to remove energy saving devices that were limiting the air-flow through the pump. These changes resulted in a simpler, more rugged vacuum supply system.

#### **4.3.3 Track Carriage Design**

The flexible track provides an attachment to the part surface. The track carriage automatically positions a scanner along the track to perform an inspection. The track carriage design considerations included positive drive and position encoding, low-friction carriage movement along the track, and quick connections for the MAUS scanners and cabling.

The carriage motor and resolver are mounted in a bracket that maintains the relative position of the position system components. Figure 4.3.3-1 illustrates the bracket. The carriage motor rotates at controlled speeds while the drive belt translates this rotation to the drive gear and to the position resolver. A single adjustment for drive belt tension is included in the bracket. All other components remain in a fixed position.



GP94031102.cvs

**Figure 4.3.3-1. MAUS IV Carriage Motor/Resolver**

The carriage housing measures 7.0 x 5.5 x 3.0 inches. It holds the bearing surfaces for the carriage as it rides along the track. Four bearing assemblies are located at each corner of the carriage. The cross section of these bearing assemblies duplicates the cross section of the track. Each bearing assembly is free to rotate through approximately twenty degrees to provide self-alignment as the carriage slides onto a track section.

The drive bracket is positioned in the carriage housing using two shoulder screws. These screws provide a pivot point for the drive bracket that allows adjustment for the drive gear position. Two tension springs are located on either side of the drive bracket to provide positive spring force. These springs hold the drive gear in a lowered position to engage the gear with the molded rack in the track section. A handle is present on the drive bracket to release the spring tension, and lock the bracket in the released mode if desired.

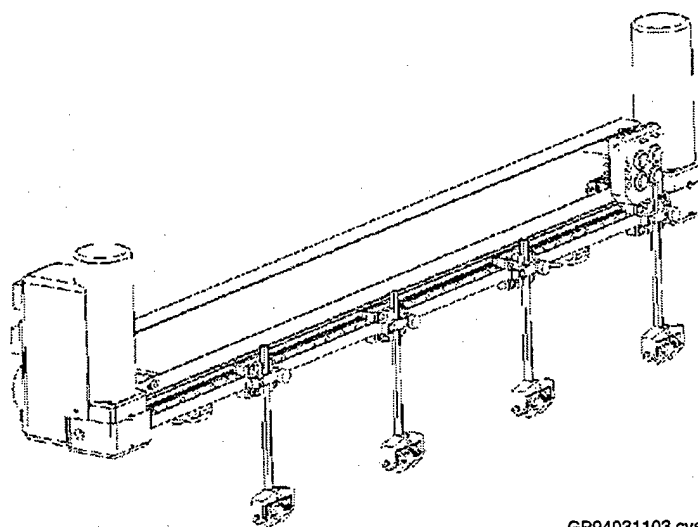
The original carriage design contained two limit switches on the forward and aft edges of the carriage. These limit switches were designed to detect when a track section was present. If a track section was not present, the limit switches prevented motor movement in that direction. This scheme worked very well when the track sections were relatively straight and flat. However, when the track sections were used on complex curvatures, the limit switches would not work reliably. It was impossible to adjust the switches correctly for all of the potential curvature ranges that the flexible track could accommodate. Therefore, the limit switches were disabled and removed from the final design.



The front of the carriage holds a scanner attachment bracket. This bracket includes two mounting holes for a scanner quick release attachment. A rotational position adjustment is included in this bracket to adjust the orientation of the scanner relative to the carriage. The motor and resolver are wired together in the carriage cable. This cable has a spring release connector that is plugged into the variable stroke scanner or the scanner cable adapter for MAUS III scanners.

#### 4.3.4 Variable Stroke Scanner Design

A new scanner was designed to take full advantage of the improved data acquisition capabilities in the new system. In addition, this scanner was designed using a modular concept to increase design flexibility and reduce costs. The variable stroke scanner design is shown in Figure 4.3.4-1. The motor is housed at one end of the scanner while the resolver is positioned at the opposite end. A linear bearing, mounted to the center extrusion, holds the sensor attachments and carries the sensor load. The length of the linear bearing and center extrusion is insignificant to the total design, allowing this design to work for a very short ( $\approx 6$  in) stroke scanner or for an extremely long stroke (up to 4 ft) scanner. A drive belt translates the motor rotation to the position resolver and the sensor attachments. A connection block is located next to the motor allowing for cable connections between the electronics cardcage, track carriage, and the variable stroke scanner.



GP94031103.cvs

Figure 4.3.4-1. MAUS IV Variable Stroke Scanner

An adjustable stroke using multiple sensors is the defining feature in this scanner. Four sensors moved over a short stroke result in optimal inspection speeds. However, a single sensor moved over a wide stroke is preferred for eddy current, pitch/catch, and MIA inspections. In addition, when a single sensor is used, changes in the stroke length are commonly requested during a scan to allow for changes in the inspection area. A sensor connection block is located on the sensor #1 attachment. Two types of sensor connections are included in the block. Coaxial sensors, such as pulse-echo and resonance transducers, are attached to the coaxial connections on the left side of the block. Multiple signal connections such as pitch/catch, MIA, and eddy current are attached to the Lemo connections in the center of the block. A couplant manifold is also included in this block to control water supply for each of the four sensors.

The carriage attachment plate includes two quick release pins are mounted in the plate. These pins mate with the attachment holes on the carriage front bracket. An operator simply pushes the pins into the attachment holes until the button at the end of each pin pops out to lock the scanner onto the carriage. To release the attachment and remove the scanner, the operator simply presses the buttons at the end of each pin.

#### **4.3.5 Hand Scanner Design Review**

Specific issues raised with the hand scanner designs were the ergonomic issues of manually positioning the scanner, particularly in overhead scans, and maintenance concerns about scanner ruggedness. The ergonomic issues were addressed by designing an adapter to integrate the hand scanners with the flexible track design. An analysis of the history of maintenance service performed on the hand scanners showed that 80% of the maintenance work was related to typical component or cable wear issues. Impact damage resulting from dropping the scanner accounted for the remaining 20%. The impact damage items included removable parts and the wheel attachment brackets on the main body. The removable parts are easily replaced but the wheel brackets are an integral part of the main body and cannot be replaced. Design improvements were initiated to improve the impact resistance for the wheel brackets. The scanner body was changed to add a generous radius where the brackets extend from the main body. This reduces the point stress concentration around the base of the bracket.

## **4.4 Operator Interface Improvements**

Human factors improvements in the MAUS system were accomplished through the software design tasks. The most significant problem encountered while using the MAUS III system was difficulty in remembering how the software operated, and the specific steps required for system operation. Operators who used the system frequently were able to memorize these steps. Many inspections, however, are not performed daily but may occur monthly or every few months. Operators who used the system infrequently were unable to efficiently use the system without extensive efforts to re-learn system operation each time. Software efforts in this program centered on creating a simplified operator interface and menu structure to eliminate problems for the infrequent user.

### **4.4.1 Standard Windows NT/95 Features**

In general, if an operator has any previous computer experience it is on an IBM/Windows based computer. Observations of operators working with the MAUS III Unix-based software revealed that if they did not know the correct operating steps, they would try to use an equivalent operation used in standard Windows applications. For example, if an operator wanted to print an image, the tendency was to locate a Print entry in a File menu. Since the MAUS III was not structured in this manner, it was difficult for an operator to find the program steps required to print an image. The software efforts in this program started with the basic premise that all system functions would conform to Microsoft Windows standards whenever possible. This includes the look and feel of all menus, hot-keys, and system functions. Conformance to an industry standard allows an operator to figure out how to accomplish specific tasks without requiring unique steps that are difficult to remember. In addition, by adding to an existing knowledge base, training efforts are enhanced.

### **4.4.2 Program Layout**

The initial software design included three program windows: General configuration, data system setup, and data imaging. The general configuration functions included scanner control information and general data collection information such as sensor types, detection resolution and scanning mode. The data system setup functions included all variables that are specific to a sensor type such as excitation frequency, or sensor gains. The data imaging functions included displaying C-scan data and data analysis/annotation functions.

The final software design combined the general configuration and data system windows into a single setup window. This window, shown in Figure 4.4.2-1, as it appears when the program is started, includes tabs at the bottom of the window to select specific pages within the window. The Control and Overview tabs always appear since the variables defined in these pages are used for any inspection. The Sensor specific tabs are labeled P/E, PC, MIA, and EC. These tabs appear at the bottom of the screen only when a sensor type is set in the Overview page.

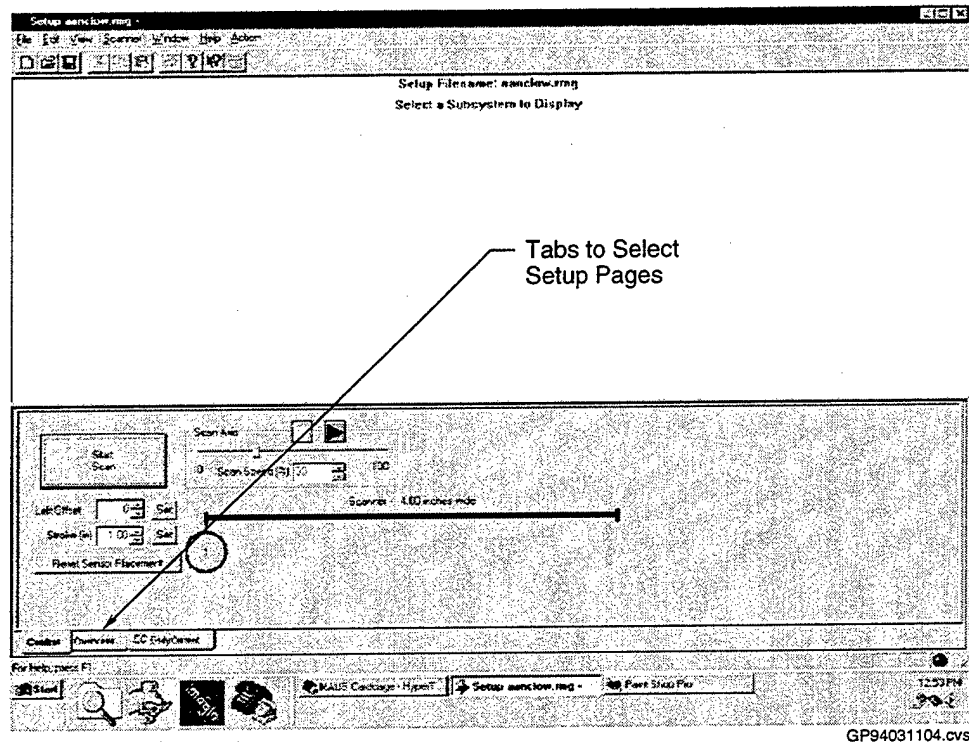
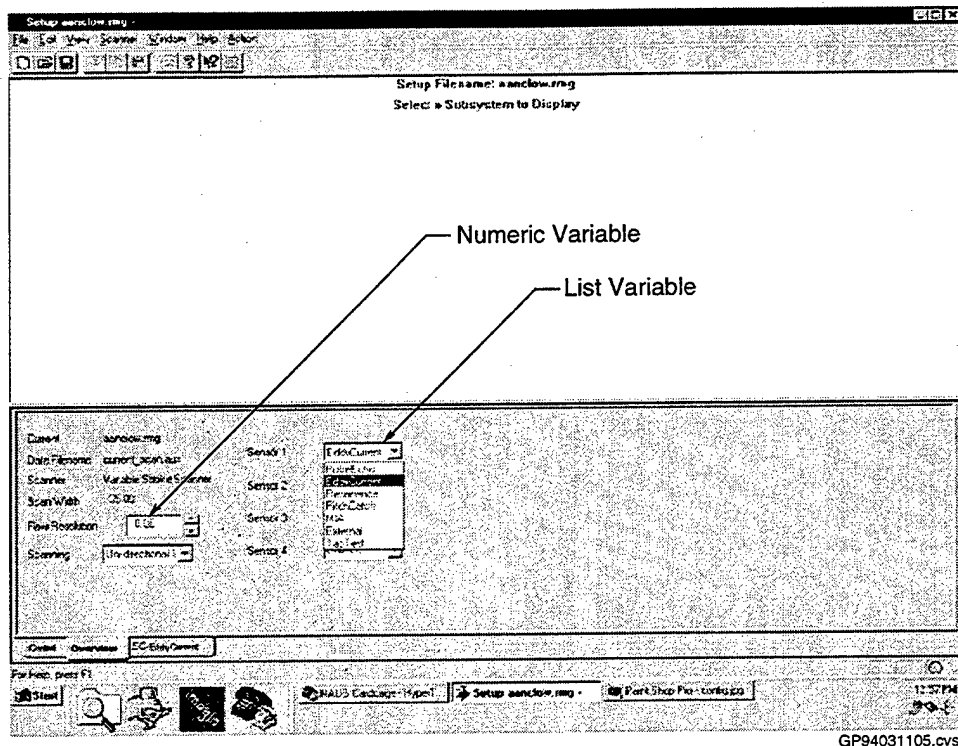


Figure 4.4.2-1. MAUS IV System Set-Up Window

### 4.4.3 Variable Adjustments

The setup variables include list selections and numerical settings. Examples of both types of variables appear in Figure 4.4.3-1. The list selections are accomplished using several standard methods. All list selections include a single arrow located to the right of the selection. The text for a selection can be typed directly in the variable, or the entire list can be shown using the single arrow key and the selection can be chosen from the list. In addition, once the variable is highlighted, the keyboard up/down arrow keys can be used to scroll through the list options.

Variables with numerical settings always appear with two up/down arrows located to the right of the variable. A number may be typed directly in the variable, or the arrow keys may be



**Figure 4.4.3-1. Set-Up Window Showing Numerical and List Variable Settings**

used to increment/decrement the number. In addition, some variables may be adjusted with a slide bar located below the variable. Slide bar adjustments are accomplished by selecting the slider and moving it smoothly to the right or left. Larger incremental changes can be accomplished by simply selecting to the right or left of the slider. Finally, some numerical adjustments can be made graphically within the A-scan signal display.

#### 4.4.4 System Startup

When the laptop computer is started, two programs are automatically started: the Setup window and the Hyperterminal. The Setup window appears full size on the screen while the Hyperterminal, used for system debugging, is minimized and appears as an icon in the task bar at the bottom of the screen. When the electronics chassis power is turned on, the Data System Processor (DSP) software is automatically started. If the network cable is connected between the chassis and the laptop computer, the Setup program initiates a scanner calibration. The scanner moves to the zero position, then to the maximum position to calibrate actual position with expected position. When the calibration is complete, the Setup window displays the scanner ID information above the sensor position graphic display. In addition, the red symbol in the lower right corner of the Setup window changes to a green symbol indicating that the system is ready

for use. Any change to a variable in the Setup window is communicated directly to the DSP software. If the setup program is restarted, or the electronics chassis is reset, the laptop and the DSP software automatically attempt to reconnect and repeat the scanner calibration process.

#### 4.4.5 Control Page

The "Control" page, shown in Figure 4.4.5-1, contains the setup variables that define the scanner motion and the C-scan start/stop control. This is the default page that always appears when the program is started. After the scanner calibration is performed, these variables are preset to the settings that were used previously for the scanner. The specific variables that control the scanner motion include Offset, Stroke, Scan Speed, and Index Speed (if a track axis is present). A graphic representation of the position of the selected sensors within the scanner width is shown in the center of the window. This graphic changes when the Offset or Stroke is adjusted, as well as when additional sensors are selected. Offset defines where the scanner stroke starts in relation to the zero position on the scanner. Stroke defines the length of the scanner stroke. When the hand scanners are used, the offset and stroke are typically set to fixed values. When the variable stroke scanner is used, the offset and stroke are changed as required during a scan to

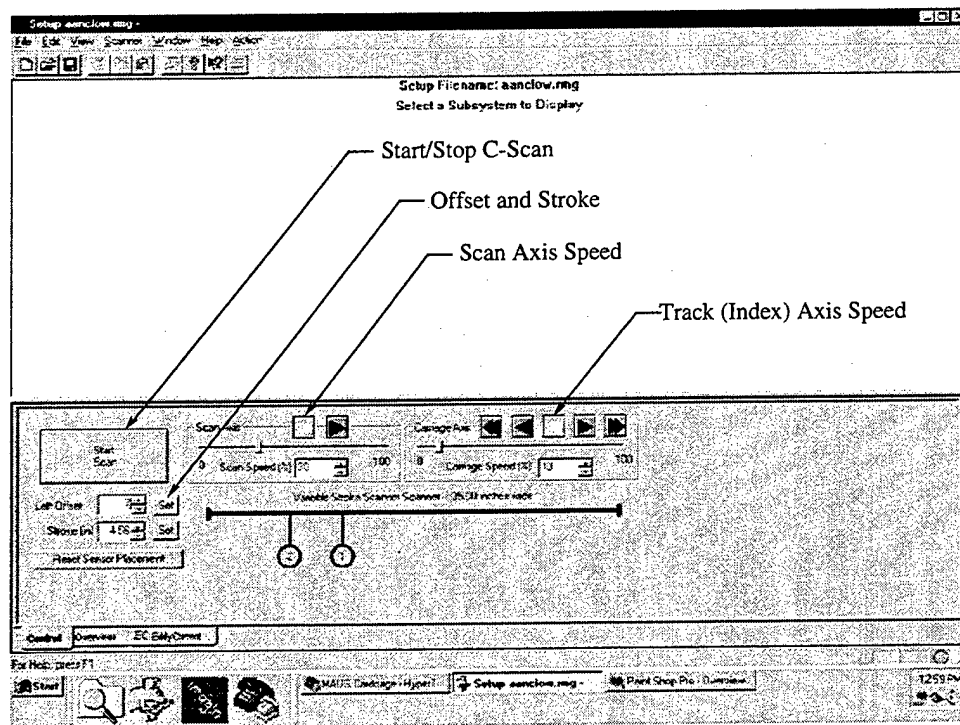


Figure 4.4.5-1. MAUS IV Control Page Window

provide full coverage of an inspection area. The Set buttons located next to the Offset and Stroke variables read the current position of the sensors within the scanner width and assign this position to either the Offset or the Stroke. This provides an easy procedure to relate these settings to actual positions on an inspection surface and is used frequently with the variable stroke scanner. The Scan speed variable adjusts the rate that the sensors are moved across the width of the scanner. The Index speed variable adjusts the rate that the carriage moves along a track section when a track is in use. The Index speed variable does not appear on the page when hand scanners are in use.

The C-scan Start button starts the C-scan data acquisition process. A file selection menu allows the operator to select the method of saving data either to a temporary file or a permanent file on the hard disk. After the data storage method has been selected, the C-scan ImagIn window automatically opens and is ready to collect data. When the C-scan is active, the button in the control window changes to C-scan Stop. This button is pressed to stop the active C-scan session. Alternatively, the stop C-scan tool in the ImagIn toolbar can also be used to stop the active C-scan session. When the session is ended, the Control page is returned to the laptop computer screen.

#### **4.4.6 Overview Page**

The "Overview" page, shown in Figure 4.4.6-1, contains the setup variables that define the general configuration of the inspection system. The variables included in this page are the sensor definitions for each channel, the data collection resolution, and the scanning mode. All four channels are displayed on the Overview page. A sensor type must be selected for at least the first sensor. All other sensors are optional. Choices for the sensor type include pulse-echo, resonance, pitch/catch, MIA, eddy current, and external input. When a sensor type is selected for at least one of the channels, a setup tab appears at the bottom of the window to access setup variables required for this sensor type. When multiple sensor types are selected, a setup tab appears for each type of sensor.

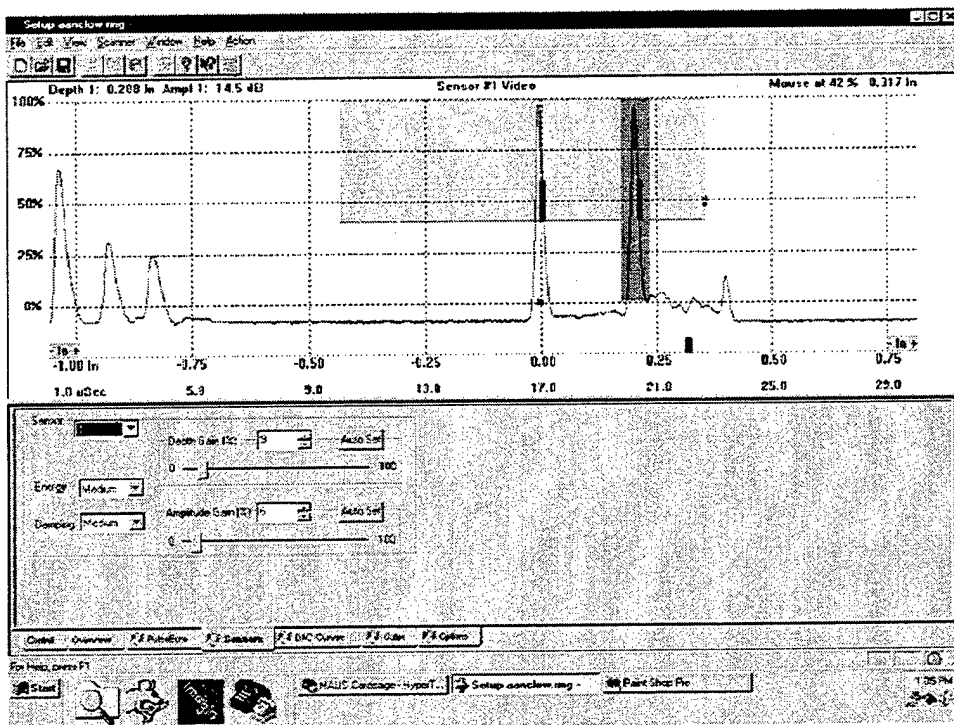
The data resolution defines the size of a pixel when data is collected and displayed in the C-scan window. Each time a sensor moves by one data resolution increment, a data point is collected. The scanning mode defines the scanning approach used to collect the C-scan data. A





#### 4.4.8 Pulse-Echo Data System Setup

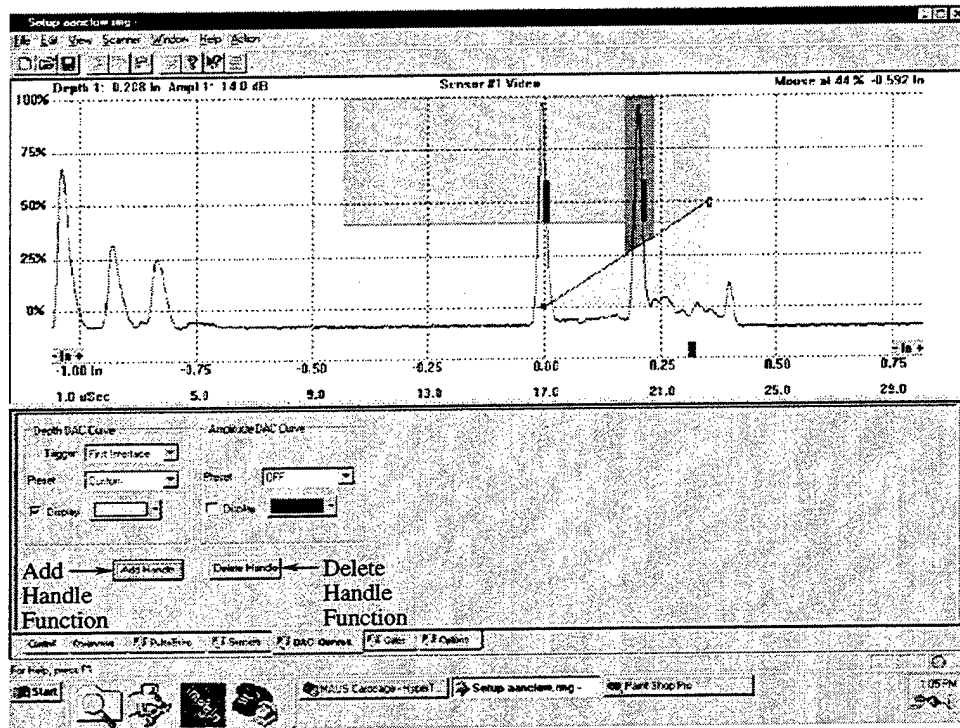
The Pulse-echo data system setup includes four pages: Sensors, DAC curves, Gates, and Options. The Sensors page, shown in Figure 4.4.8-1, contains the setup variables that define the pulser energy and damping, and the signal gain adjustments for depth and amplitude readings. The Sensors variable at the top of this page displays and changes settings for the selected channel. The sensor that is displayed in the A-scan signal trace is also selected by the Sensors variable.



GP94031108.cvs

Figure 4.4.8-1. MAUS IV Pulse-Echo Sensor Window

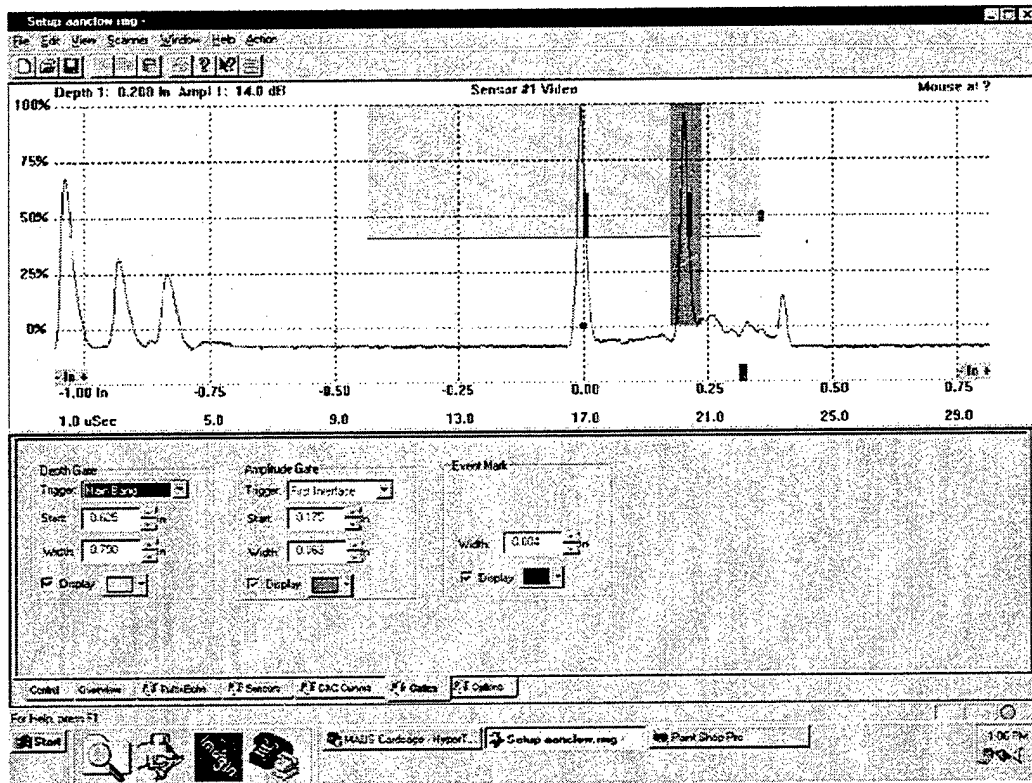
The "DAC curves" page, shown in Figure 4.4.8-2, displays the signal trigger and DAC functions for both Depth and Amplitude DAC curves. Several preset functions are provided in the variable lists under each parameter. In addition, Custom DAC curves can be defined using the Add Handle and Delete Handle functions. The curves are defined by moving the handles graphically on the A-scan display.



GP94031109.cvs

**Figure 4.4.8-2. MAUS IV Pulse-Echo Distance-Amplitude Curve Window**

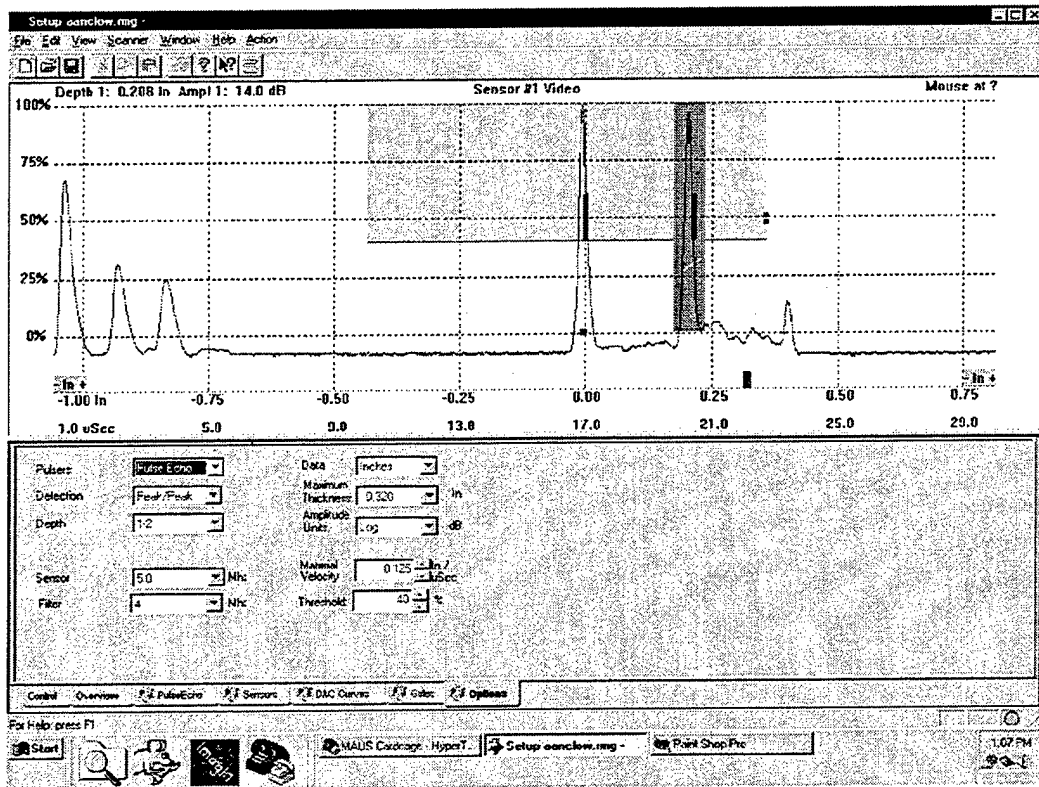
The "Gates" page, shown in Figure 4.4.8-3, shows the settings for the Depth, Amplitude, and Event Mark Width gates. Gate trigger, start, and width variables are included for the Depth and Amplitude gates. These gates can also be adjusted graphically on the A-scan display. The event mark width variable is the only adjustment for the event marks, it cannot be adjusted graphically.



GP94031110.cvs

Figure 4.4.8-3. MAUS IV Pulse-Echo Gate Window

The "Options" page, shown in Figure 4.4.8-4, shows settings that are infrequently adjusted. Typically, these settings are adjusted when a pulse-echo setup is established for a specific part and they are not changed over time. These settings impact the calibration coefficients used to calculate amplitude, and the variables used to calculate the depth readings.

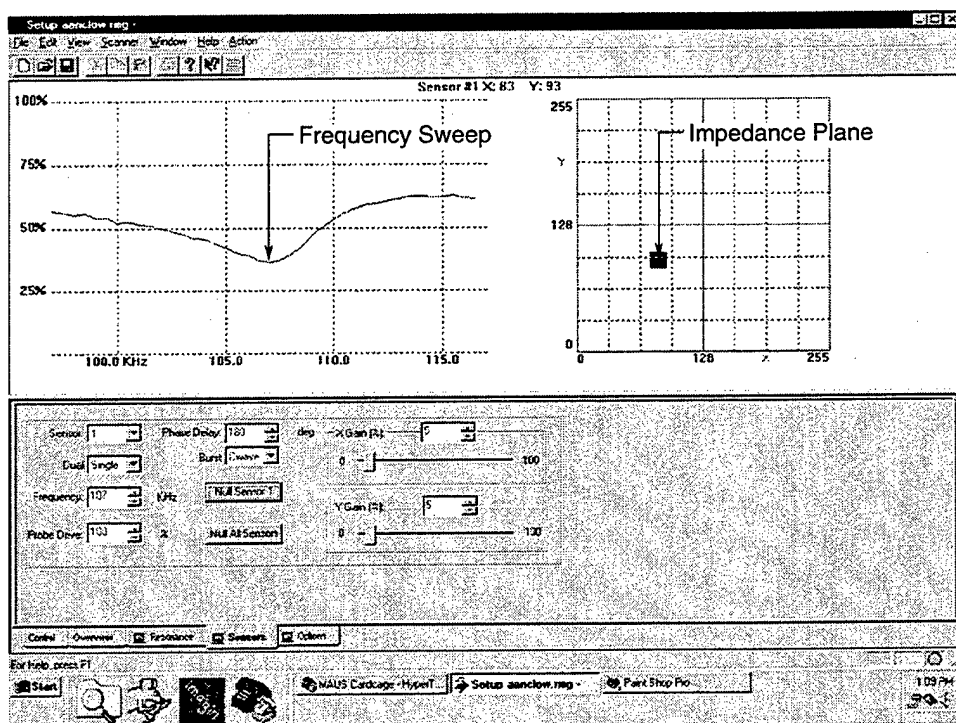


GP94031111.cvs

Figure 4.4.8-4. MAUS IV Pulse-Echo Options Pages

#### 4.4.9 Resonance Data System Setup

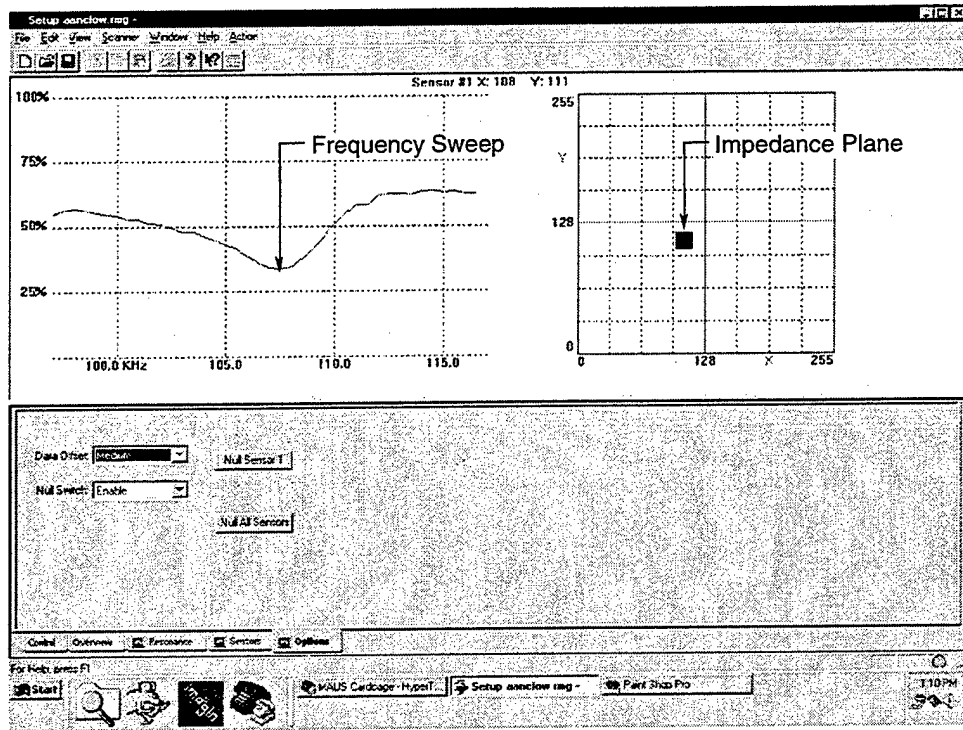
The Resonance data system setup includes two pages: Sensors and Options. The Sensors page, shown in Figure 4.4.9-1, contains the setup variables that define the excitation frequency, power level, signal duration, and the signal gain adjustments for X and Y readings. The Sensors variable at the top of this page displays and changes settings for the selected channel. Two displays are shown at the top of the window. The sensor that is displayed in the A-scan signal trace is also selected by the Sensors variable. The display on the left shows the signal response as the sensor frequency is changed from 10KHz below the setpoint frequency to 10KHz above. The lowest level of the signal responses represents the natural frequency of the sensor. This is the frequency that is typically selected for the center frequency. The display on the right shows the impedance plane representation of the sensor responses. Changes in the Y parameter appear as vertical movements in the impedance plane. Changes in the X parameter appear as horizontal movements in the impedance plane. Sensor null buttons are included on the Sensors page. One button nulls the displayed sensor only. A second button nulls all of the sensors at one time.



GP94031112.cvs

Figure 4.4.9-1. MAUS IV Resonance Sensors Window

The Options page, shown in Figure 4.4.9-2, includes adjustments for the sensor null. The data offset variable changes the null position between a low, middle, or high point in the data range. The scanner null switch can be enabled or disabled from this page.



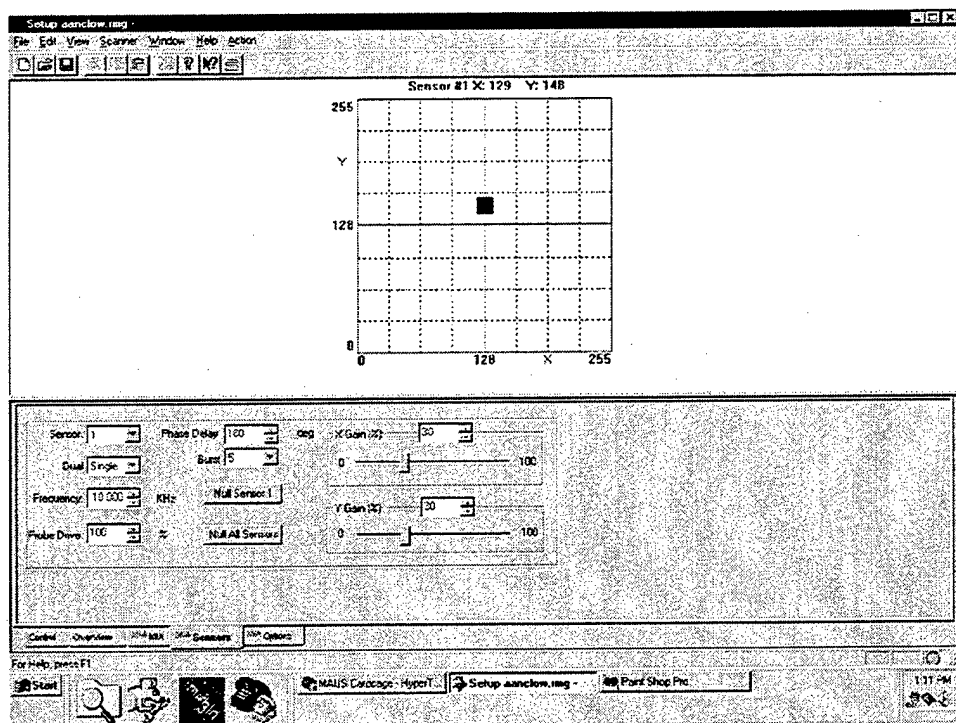
GP94031113.cvs

**Figure 4.4.9-2. MAUS IV Resonance Options Window**

#### 4.4.10 Pitch/Catch Resonance and MIA Data System Setup

The Pitch/catch and MIA data system setups include two pages: Sensors and Options. The Sensors page, shown in Figure 4.4.10-1, contains the setup variables that define the excitation frequency, power level, signal duration, signal burst cycles, and the signal gain adjustments for X and Y readings. The Sensors variable at the top of this page displays and changes settings for the selected channel. An impedance plane display is shown at the top of the window. Changes in the Y parameter appear as vertical movements in the impedance plane. Changes in the X parameter appear as horizontal movements in the impedance plane. Sensor null buttons are included on the Sensors page. One button nulls just the displayed sensor. A second button nulls all of the sensors at one time.

The Options page includes adjustments for the sensor null. The data offset variable changes the null position between a low, middle, or high point in the data range. The scanner null switch can be enabled or disabled from this page.



GP94031114.cvs

Figure 4.4.10-1. MAUS IV Pitch/Catch-MIA Sensor Window

#### 4.4.11 Eddy Current Data System Setup

The Eddy Current data system setups include two pages: Sensors and Options. The Sensors page, shown in Figure 4.4.11-1, contains the setup variables that define the acquisition mode for single or dual frequency applications. This page also includes the excitation frequency, power level, signal duration, signal burst cycles, and the signal gain adjustments for X and Y readings. When a dual frequency application is selected, separate variables are defined for each signal frequency. The Sensors variable at the top of this page displays and changes settings for the selected channel and frequency. An impedance plane display is shown at the top of the window. Changes in the Y parameter appear as vertical movements in the impedance plane. Changes in the X parameter appear as horizontal movements in the impedance plane.

Sensor null buttons are included on the Sensors page. One button nulls just the displayed sensor. A second button nulls all of the sensors at one time. When dual frequency mode is selected, both frequencies the null is set for both frequencies when either null button is selected.

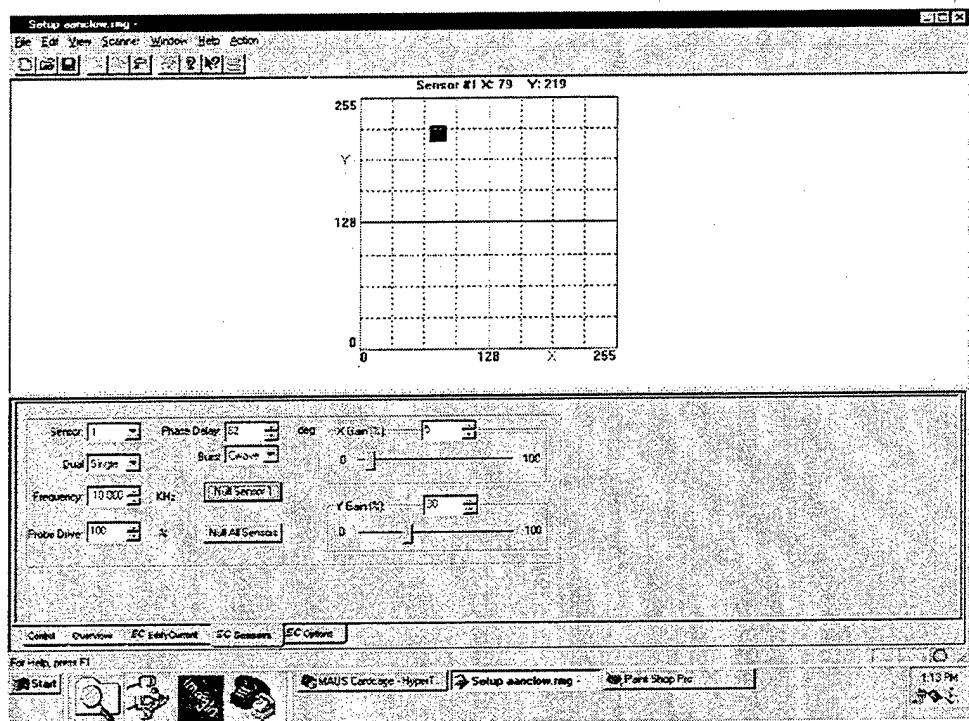


Figure 4.4.11-1. MAUS IV Eddy Current Sensor Window



The Options page includes adjustments for the sensor null. The data offset variable changes the null position between a low, middle, or high point in the data range. The scanner null switch can be enabled or disabled from this page.

#### **4.4.12 C-scan Data Display**

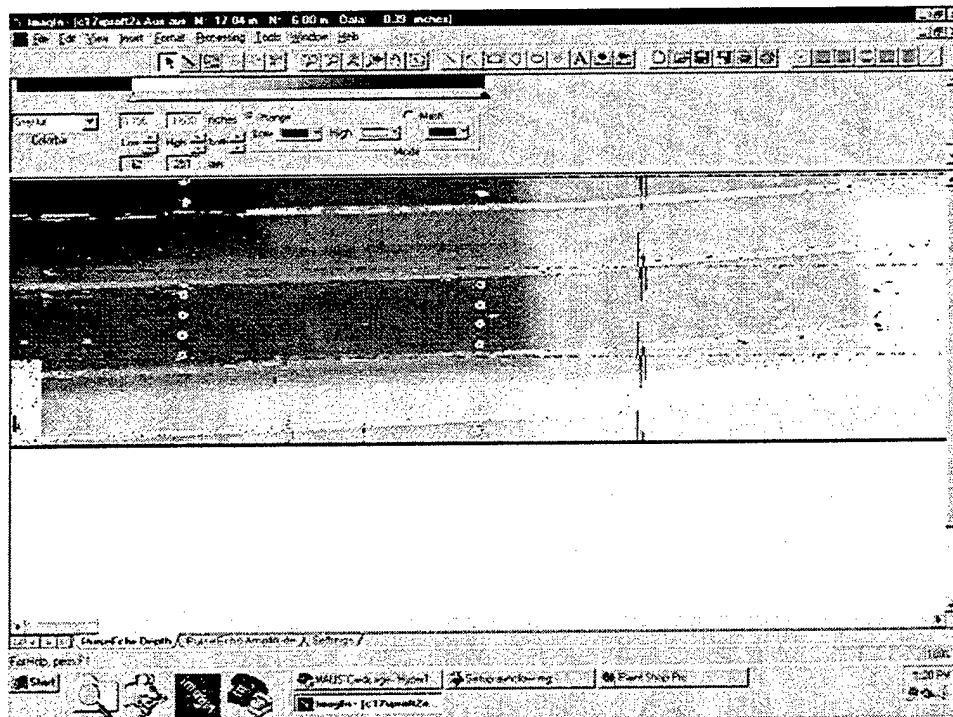
C-scan data display creates an area map of the inspection surface. It is an effective method to present an array of inspection data, improve data interpretation, allow data storage, and to communicate the inspection results to those unfamiliar with nondestructive testing. Since data interpretation is easier using a C-scan image, the inspection reliability and repeatability are enhanced despite differences in operator skill levels. The operator interprets the C-scan parameters during data collection and stores this information for evaluation after the inspection is complete. The stored data is available for additional evaluation and is often archived for future reference. File transfers through modem or network connections enable evaluation of data by personnel at remote locations.

The C-scan is a graphic display format that correlates the signal data to the position on the inspection surface. It is easy to identify discontinuities in the C-scan image. Each pixel in the image represents a location on the part surface. The size of the area that is represented by a pixel is variable, ranging from 0.01 inches to 0.5 inches. Select a small pixel size to find small flaws, select a larger pixel size to ignore small flaws and find larger more significant flaws.

The C-scan display program is called ImagIn. It shows C-scan data during an inspection or after the data has been saved to the hard disk. In the MAUS IV, the program is started using the Start C-scan button on the Control page in the Setup window. The program can also be started offline using the ImagIn icon located in the toolbar at the bottom of the display screen. The program can also be installed on any PC with a Windows 95/NT operating system so that C-scan data interpretation is available for any interested user. This feature is quite useful for communicating inspection results to structural engineers for use in deciding the disposition of an inspected part.

Adherence to Microsoft programming standards was emphasized in the ImagIn program. Most functions can be selected through the menus at the top of the window, through toolbar shortcuts, with standard hot keys, or with context sensitive, quick access menus. An extensive Help menu is included to explain program features to an untrained operator.

Multiple data parameters are collected and stored in the C-scan file. Individual parameter views are selected with the tabs located at the bottom of the screen. The highlighted tab shows the parameter that is currently shown in the window, as shown in Figure 4.4.12-1. Additional data windows can be opened in the program so that multiple parameters can be displayed at one time. Figure 4.4.12-2 illustrates a C-scan where two windows are open.



GP94031116.cvs

**Figure 4.4.12-1. MAUS IV C-Scan Window (Single Scan)**

Each C-scan parameter shows different aspects of the signal response. For example, an ultrasonic pulse-echo signal includes the amplitude of the sound reflection, and the length of time before the reflected signal is detected. Knowing the velocity of sound through the material, the reflection time is translated into a thickness, or depth. Changes in the parameters are shown as color changes in the images. Typical depth and amplitude C-scan images are shown below. In the depth C-scan, the darker shades correspond to reflections near the top surface of the part. The lighter shades correspond to reflections deeper in the part. In the amplitude C-scan, the darker shades correspond to smaller amplitude for the signal reflections.

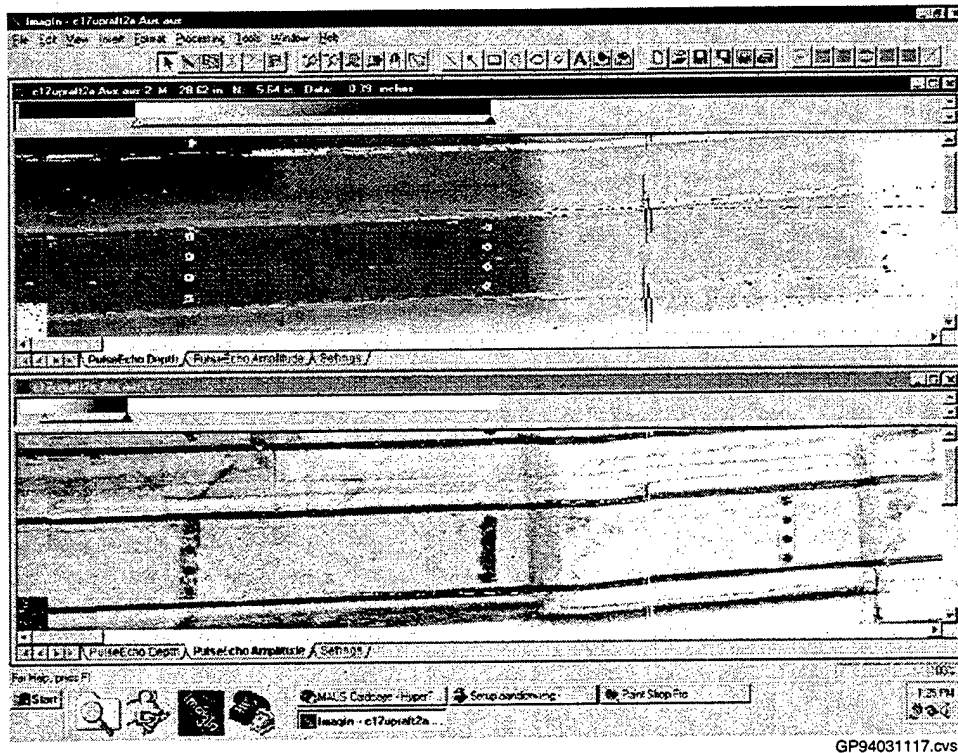
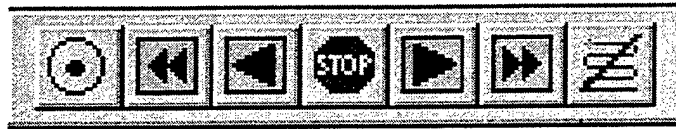


**Figure 4.4.12-2. MAUS IV C-Scan Window (Double Scan)**

Menus are included at the top of the ImagIn window. All program functions are accessed through these menus. In addition, toolbars are shown directly below the menus. These toolbars provide quick access to many of the program functions. General categories of these program functions include scanner control, viewing the image, annotation, image editing, and file handling.

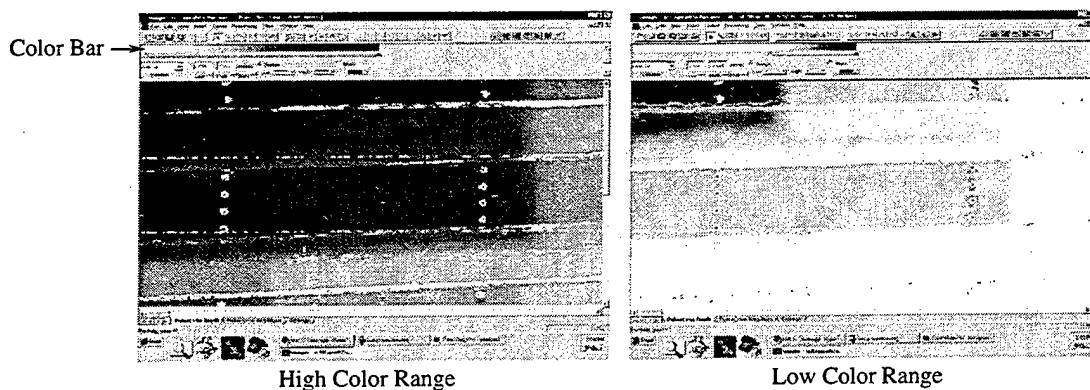
The scanner control toolbar, shown in Figure 4.4.12-3, duplicates most of the functions included in the Control page of the Setup program. These functions are included in the toolbar so that the operator does not have to switch between the ImagIn and Setup programs to access the scanner controls. The tools include forward, reverse, fast forward, fast reverse, and stop functions for the scanner. In addition, a Null tool is included that duplicates the Null All functions in the Setup window. Finally, a Stop C-scan tool is included to end an active C-scan session and return the program to the Setup Control Page. The scanner toolbar is only highlighted when an active C-scan session is in progress. The tools appear as gray shadows when the data collection is inactive.



GP94031118.cvs

**Figure 4.4.12-3. MAUS IV Scanner Control Toolbar**

A colorbar window is shown at the top of each data image. This window contains all of the variables that define the C-scan appearance. Several preset colorbars are included in the colorbar selection variable. The low and high edges of the colorbar relative to the data values are also adjusted in this window. This feature is used to concentrate the color changes within the portion of the data range that contains significant information. A mask feature is also available to overlay on the colorbar assignments. This mask feature presets a small range of data to a mask color creating a highlight effect for a small portion of the data range. Figure 4.4.12-4 shows the effect of changing the high/low color ranges. Figure 4.4.12-5 shows the effect of the mask feature.



GP94031119.cvs

**Figure 4.4.12-4. Effects of Changing High/Low Color Ranges**

When an inspection image is large, all of the data cannot be displayed on the screen at one time. Scroll bars are included on the edge of the C-scan window to move the window view within the large data image. A Far Move function, shown in Figure 4.4.12-6, displays a representation of the entire file showing the current display window location within the file. The display location can be repositioned in the Far Move window to change the data that appears in the C-scan window. Several Zoom functions are also available in the View menu and toolbar. Preset zoom scales range from 25% to 400%, or a custom zoom scale may be set. A data magnifier is also available to highlight a small portion of the C-scan data when the zoom scale is relatively small.

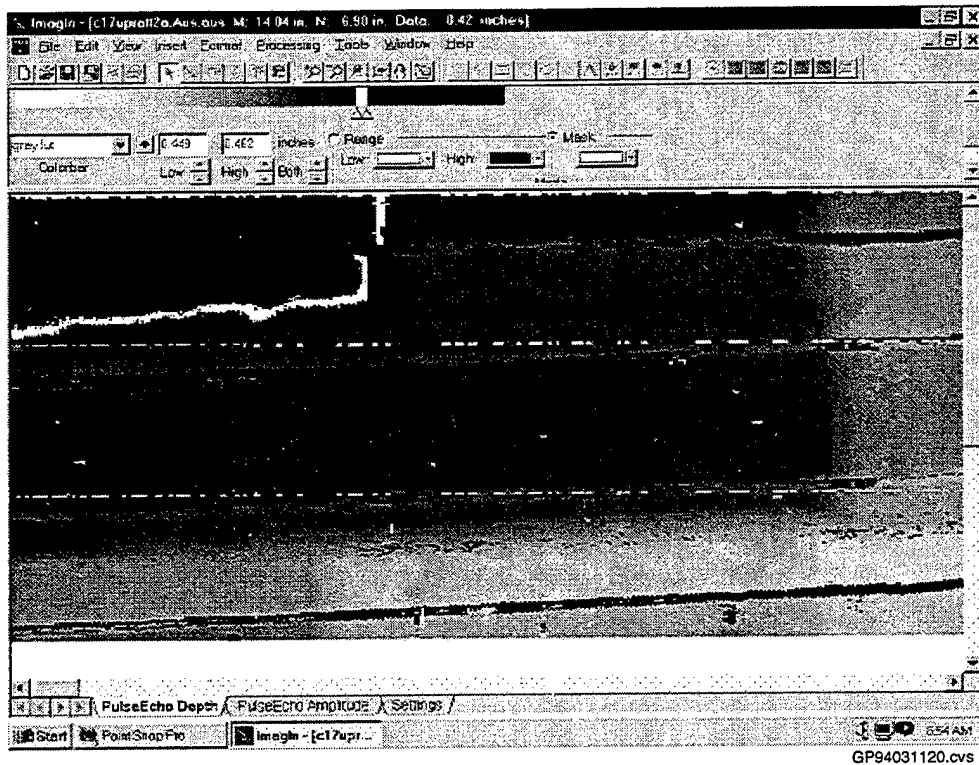


Figure 4.4.12-5. Effects of Masking Feature

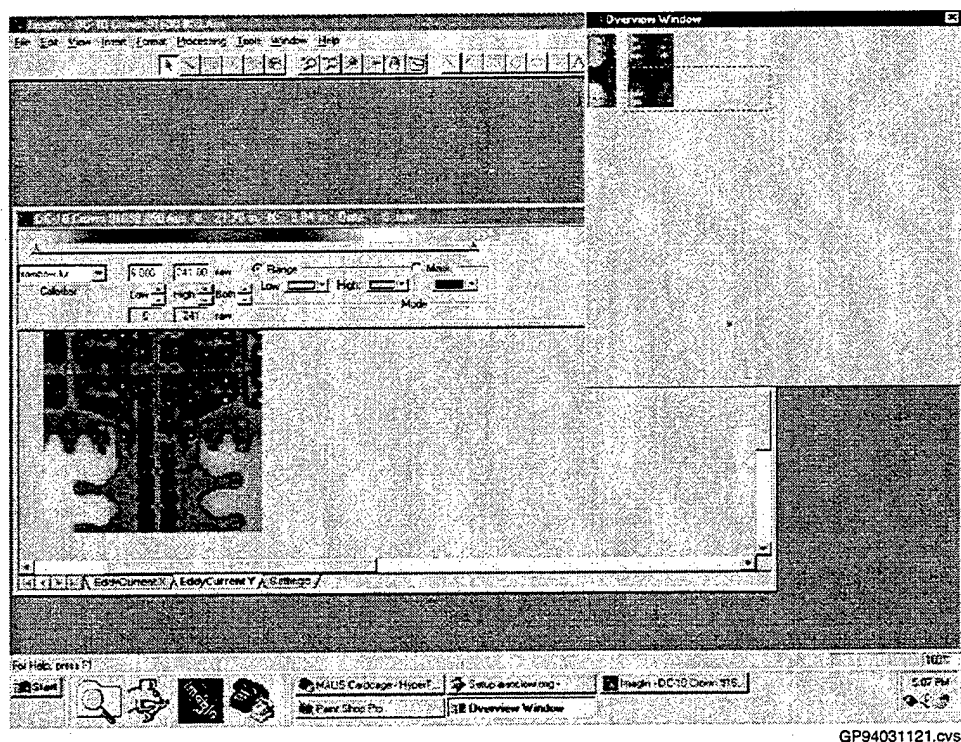


Figure 4.4.12-6. Window Showing Far Move Function

Data measurements are made directly on the C-scan image. The value of the data at each pixel location is shown as a Point reading. The size of an indication is shown with either a Line reading or an Area reading. Annotations and/or operator comments can be placed on the C-scan image for future reference. Typical annotations include text comments, point, line, and area measurements. Histogram functions are included in the annotations options. These functions provide an analysis of data distributions over a portion of the image using standard statistical parameters such as mean, mode, average, and standard deviation. The amount of data that is within or outside of a defect range is also computed. Once annotations have been placed, they can be moved, deleted, or modified using standard Microsoft editing methods.

Advanced analysis tools include a Data Combine function and a Data Merge function. The combine function mixes the signal responses from data parameters to create a composite data image. These images are very effective display tools for dual frequency eddy current applications. Figure 4.4.12-7 illustrates the Data Combine function. The Merge function joins separate C-scan images together to create a larger, seamless C-scan image. Data strips can be copied, moved, aligned, and stored as one large C-scan image of an entire inspection surface. This function is very useful for the inspection of large areas. Figure 4.4.12-8 illustrates the Data Merge function.

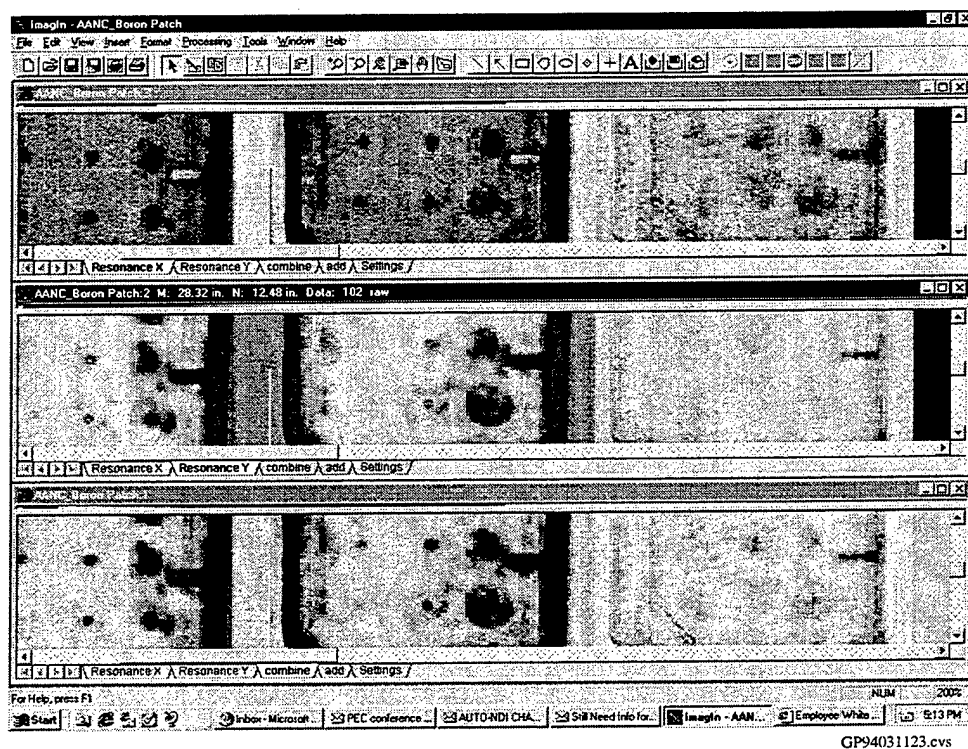


Figure 4.4.12-7. Window Illustrating the Data Combine Function

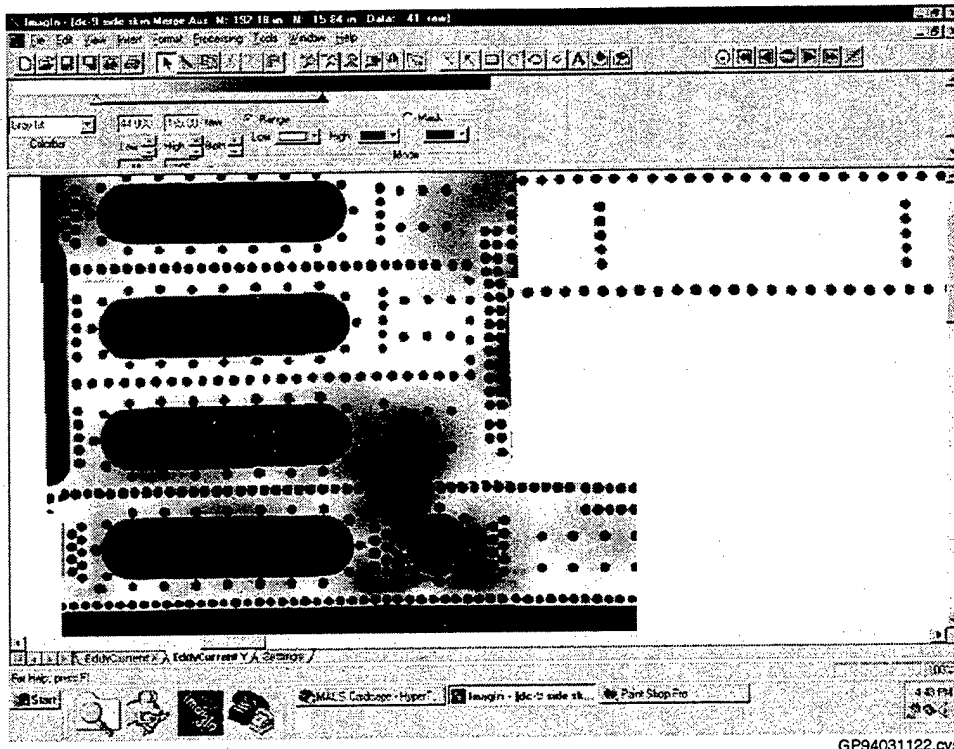
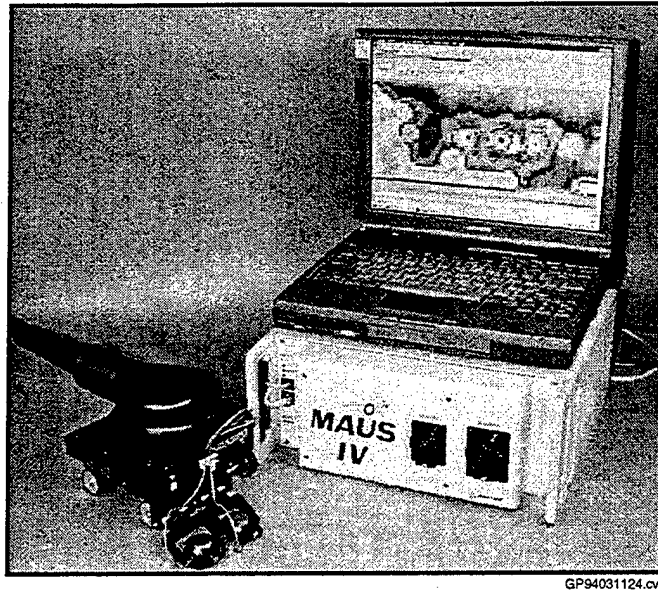


Figure 4.4.12-8. Window Illustrating Data Merge Function

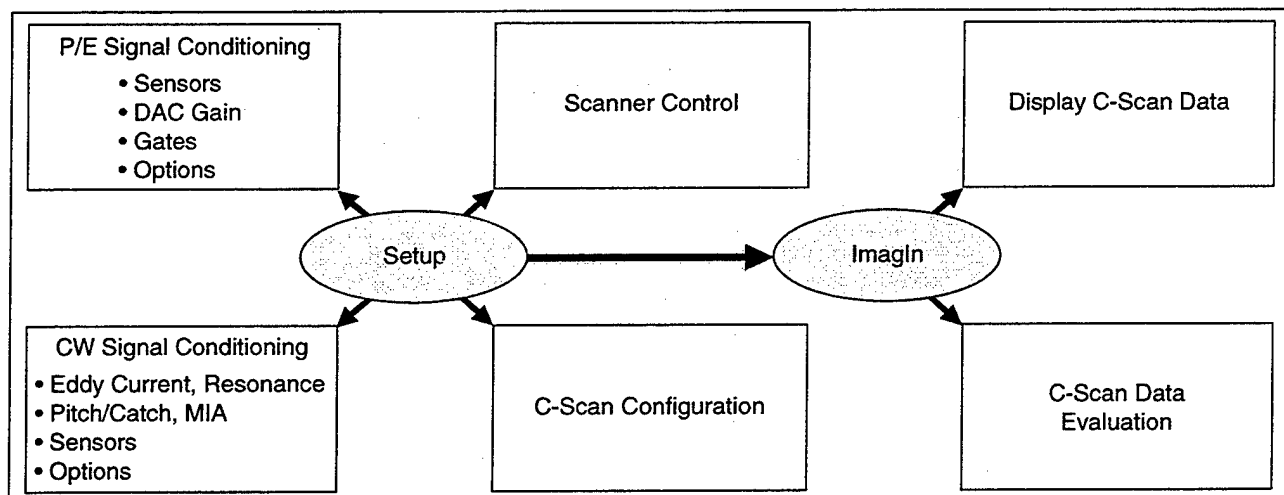
## 4.5 Production Readiness Review

The final system design was set in August, 1997. Figure 4.5-1 illustrates the final configuration. A typical scanner, also shown in Figure 4.5-1, positions sensors on the inspection surface at preset speeds and data acquisition intervals. The laptop computer functions, described in Figure 4.5-2, provide the overall system coordination to display the sensor and inspection information. The signal conditioning layout, as shown in Figure 4.5-3, consists of the Power PC-based CPU card, a 100MHz timing/digitizer card, three MAUS III pulse-echo signal conditioning cards, three new MAUS IV continuous wave signal conditioning cards, and MAUS III motion control and high voltage power cards. The signal conditioning chassis includes the new MAUS IV front panel interface for automatic sensor signal switching[5].



GP94031124.cvs

**Figure 4.5-1. Prototype MAUS IV System**



GP94031125.cvs

**Figure 4.5-2. Summary of MAUS IV Software Functions**



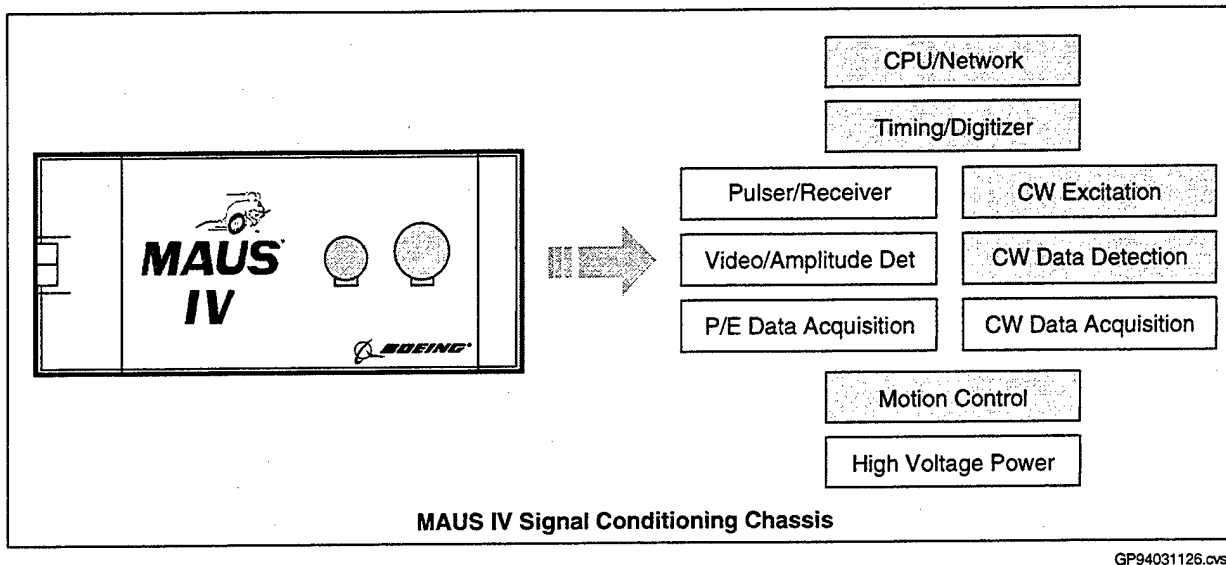


**Figure 4.5-3. Summary of MAUS IV Signal Conditioning Functions**

The MAUS III ACCESS database was updated to include the new MAUS IV components. This database provides full part procurement listings based upon system configuration definition, parts inventory, vendor and manufacturer information. An outline of this database is included in Figure 4.5-4.

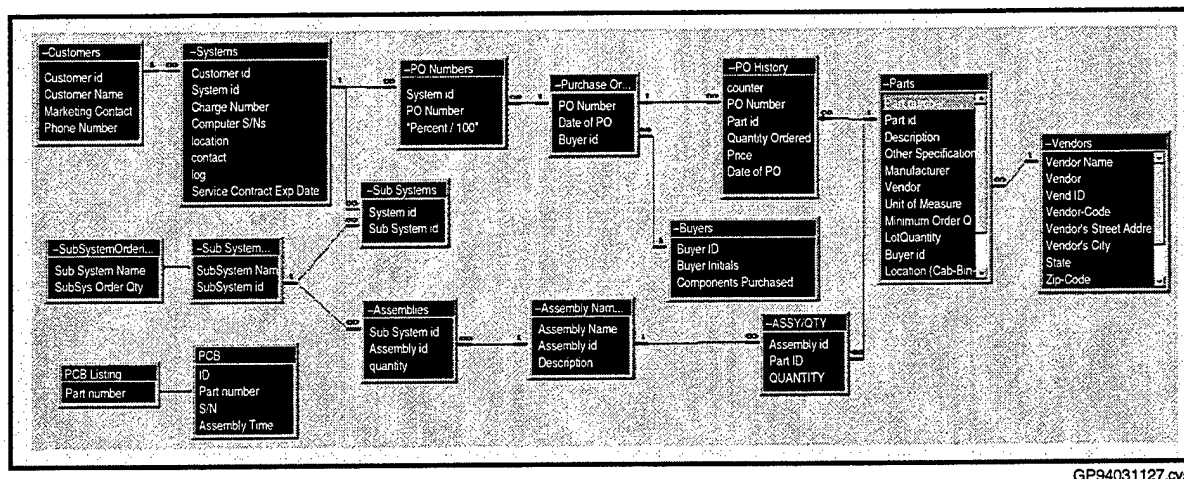


**Figure 4.5-4. Outline of ACCESS Database**

Several efforts in this program addressed system affordability issues. Sixty percent of the MAUS III system cost was touch labor performed within the Boeing Company. Fabrication included mechanical parts for the scanners and chassis, electronics boards, and cabling. Subcontractors were investigated and estimates were sought to perform many of these tasks. All MAUS IV mechanical parts are now fabricated through private machine shops. Two of the

electronics boards, the CPU and timing/digitizer, boards are currently procured through a private circuit card fabricator. Additional electronics boards will be added to the external fabrication list within the next year. Currently, no vendors have been identified for cable fabrication. An additional 20% of the system cost was associated with the workstation computer and associated equipment. The computer represented half of this cost with workstation support equipment such as printers, monitors, and optical disk drives representing the remaining costs. Changing the software from a UNIX-based user interface to a Windows 95/NT user interface reduced the material costs for the computer substantially. In addition, the support equipment is no longer offered with the package since this equipment is typically already in place in standard office environments. These affordability initiatives have resulted in a 32% reduction in the fabrication costs for a MAUS IV. These savings have been incorporated in the commercial catalog pricing resulting in average cost reductions of 35%.

#### **4.6 System Performance Evaluation**

The completed system was delivered to Tinker AFB, OC-ALC personnel in late March, 1998. A two month evaluation period was set to identify problems, improvements, and changes in the system software and hardware. Inspection applications that were investigated during this evaluation period included Milstar Radome, E-3 Rotodome, E-4B Radome, and KC-135 lap seam inspections. An evaluation log was maintained to record comments throughout this period. During this initial two month period, forty-four items were recorded in the log. These items could be separated into two categories: software and hardware. Many of the problems encountered were ultimately traced to an intermittent failure in the Fieldworks computer laptop network capability. The network function completely failed at the end of May. The full system was returned to Boeing for resolution of the laptop problem and the items listed in the evaluation log. The system was delivered again to OC-ALC personnel in early September for an additional two month evaluation period. Twenty-two items were added to the log in this period. The Fieldworks computer laptop failed a second time during this evaluation period. It was replaced by a Hitachi laptop for the remainder of the evaluation period. A summary of the full evaluation sequence is illustrated in Figure 4.6-1.

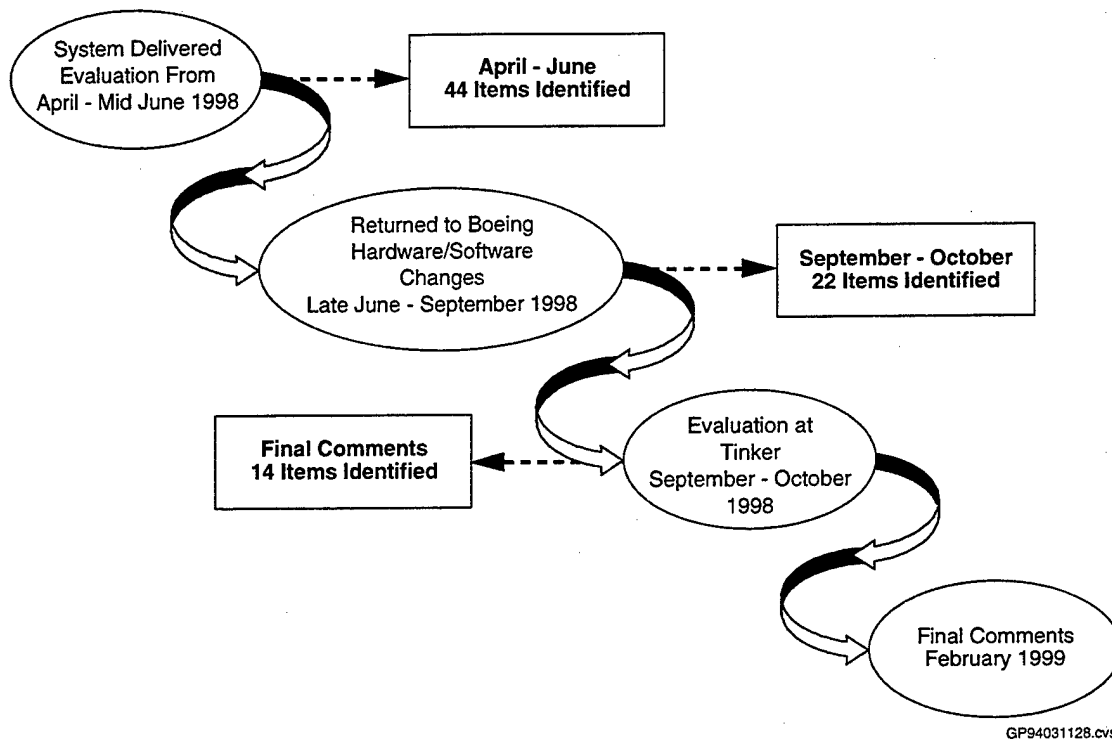


**Figure 4.6-1. Summary of MAUS IV Evaluation Process at OC-ALC**

The OC-ALC personnel contributed invaluable assistance during the evaluation period. They recorded all system inconsistencies in an evaluation log and identified opportunities for improvements in the scanner and program operations. The log items were separated into two major categories: Software and Hardware issues. These issues were sub-divided into related topics within these two major categories. A summary of the log items is illustrated in Figure 4.6-2.

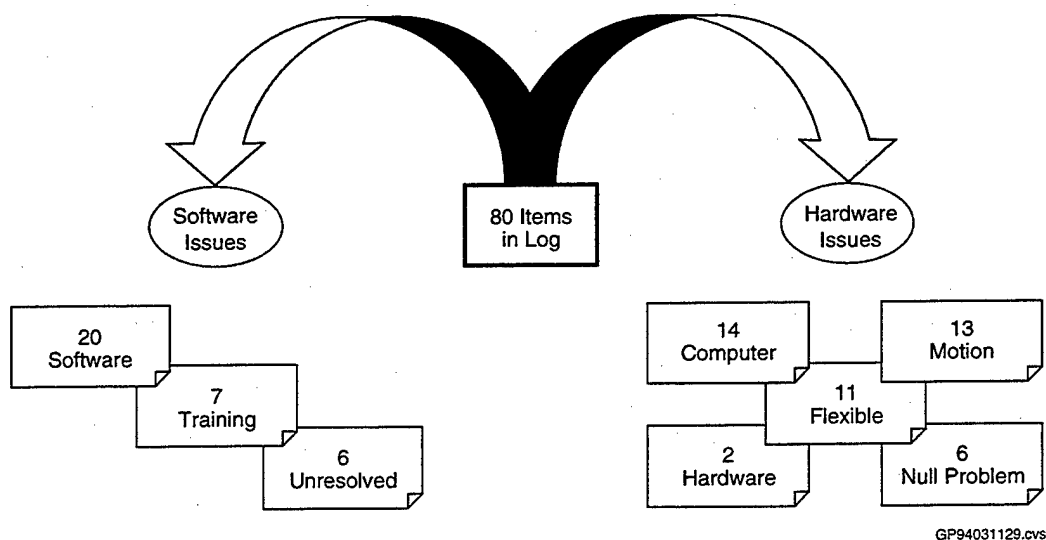


**Figure 4.6-2. Summary of MAUS IV Evaluation Log Items Documented at OC-ALC**

#### **4.6.1 Software Issues**

Thirty-three items were included in the log related to software problems. Twenty of these entries were investigated and programming changes were made to repair the problem. Seven of these entries were misunderstandings about the software operation and were resolved by explaining to the operator the specific function. Changes to the Help menus and Training guide were initiated to improve operator understanding of these items. Six of the items remain unresolved at this time.

#### **4.6.2 Hardware Issues**

Forty-six items were included in the log related to hardware problems. Fourteen of these entries are traced to the laptop computer problems. Eleven of the entries identified problems with the flexible track and bar scanner. Design modifications were incorporated into both drawings sets to address these problems. Nine of the entries were problems with scanner control. This was considered a hardware issue because the scanner control is an integral part of the mechanical scanners. However, these problems were resolved with a redesign of the scanner control software. Six of the entries were traced to Null problems on the Continuous Wave Data Acquisition circuit board. This board was replaced. Two additional circuit boards were replaced to address the remaining two log items.

#### **4.6.3 Suggested Improvements**

Several improvements suggested by the OC-ALC personnel have been incorporated into the MAUS IV system. These improvements included additional scanner controls, auto-set operations for offset and stroke, and relative data/position readings. These changes result in more efficient setup and system operation.

The scanner speed controls were originally placed in the Setup-Control page. After using the system, it became clear that it was time-consuming to return to the Control page from the Image window to change scanner settings. In particular, it was difficult to stop the scanner quickly if an emergency should arise. A scanner stop button was added to the Image window toolbar to allow the operator to quickly stop the scanner motion while remaining in the window. This worked quite well and additional functions were requested. The Scanner toolbar currently contains

scanner stop, forward/backward, fast forward/backward, null, and Stop scan functions. This toolbar significantly improves system operation.

The scanner offset and stroke are set often when the flexible track and variable stroke scanner are used. It is quite common to set these variables to define the area of inspection after the track has been placed on the inspection surface. OC-ALC personnel found it very cumbersome to select a numerical value for these settings and then to verify the actual position. They suggested that it would be more efficient to position the sensor at the desired position and have the software automatically read the position. Two SET buttons were added to the software to read the Offset and Stroke positions.

Large amounts of C-scan data were collected on the KC-135 aircraft during the evaluation period. The OC-ALC personnel requested a method of correlating this data with the physical locations on the aircraft. A position offset variable was added to the Image software. This variable corresponds to a position pointer on the C-scan data. The pointer can be positioned at any location in the image such as at the data point representing a splice or body station. All position readings within the C-scan are then displayed relative to the position pointer. The result of this effort is that an indication within a C-scan image can now be referenced directly to a body station location.

Continuous wave sensing methods, such as eddy current, measure sensor changes relative to a null position. The actual data value for the sensor null is variable. OC-ALC personnel requested a software change to incorporate a data reference variable. When this variable is set to the sensor null value, all data are displayed as absolute readings relative to the sensor null.

#### **4.6.4 Inspection Application Evaluations**

Inspection applications that were investigated during this evaluation period included KC-135 lap seam inspections, F-16 horizontal stabilizer and inlet duct, E-4B radome, Milstar radome, and E-3 rotodome test samples. The majority of the evaluation efforts were performed on the KC-135 lap seam inspections.

### ***KC-135 Lap Seam Inspections***

Previous experience with the MAUS III system indicated that the dual frequency eddy current inspection capability was well suited for corrosion detection in the KC-135 lap seams and doublers. This is an excellent application for the variable stroke scanner and the flexible track. In particular, the flexible track easily adapts to the complex curvatures encountered at various sites on the aircraft. A track section can bridge inconsistent surfaces such as when an access panel is removed or where tear straps are present on the outside of the fuselage. The variable stroke scanner allows for changes in scan area to accommodate small or large areas of lap seam or doublers. Figure 4.6.4-1 shows a data examples from a lap seam inspection.

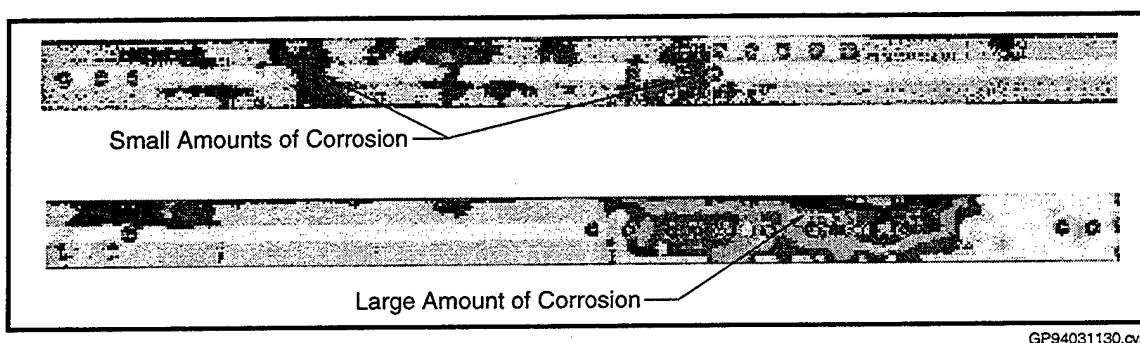


**Figure 4.6.4-1. MAUS IV Eddy Current C-Scan of Corroded KC-135 Lap Joint**

Substantial inspection time improvements are realized using the MAUS IV rather than the MAUS III. Inspection times have been reduced by up to 75%. These time savings result from efficiencies in data collection. No inspection downtime occurs since the track sections are moved while the system continues to run. The signal collection process is faster and all of the data is collected in a single pass. Currently, the OC-ALC personnel are preparing to include this MAUS IV inspection into the production maintenance program for all KC-135 aircraft.

### ***F-16 Applications***

The MAUS IV provided an automated alternative to an existing manual inspection designed to detect disbonds under the inlet duct coating. The pulse-echo amplitude method easily imaged the disbonds. In addition, some cracks were observed during routine maintenance on a trailing edge rib of an F-16 horizontal stabilizer. A low frequency eddy current inspection was developed for MAUS IV to detect cracking in this rib without requiring disassembly of the structure.

### ***Milstar Radome***

The Milstar radome consists of a relatively porous, non-metallic laminate. The MAUS IV bondtesting methods and pulse-echo methods were used to evaluate a test sample. Signal responses were quite similar to the E-4B test standard with the best results obtained using 0.5 inch diameter pulse-echo sensors. Process development will continue on this application with on-aircraft experience when an aircraft is available.

### ***E-3 Rotodome***

The bondtesting methods were evaluated for the E-3 rotodome application using a series of E-3 standards. Good results were obtained using the resonance sensors. However, these sensors require water to couple the sensor to the part surface. Moderate results were obtained with the pitch/catch and the MIA methods. However, the speed of inspection is quite slow when using these methods since vibrations in the sensor can translate to noise in the signal. Figure 4.6.4-2 illustrates a C-scan collected with a MIA sensor. Most of the flaws were clearly detected under plies 1-8. Some of the flaws in the 9<sup>th</sup> and 10<sup>th</sup> layer were not detected.

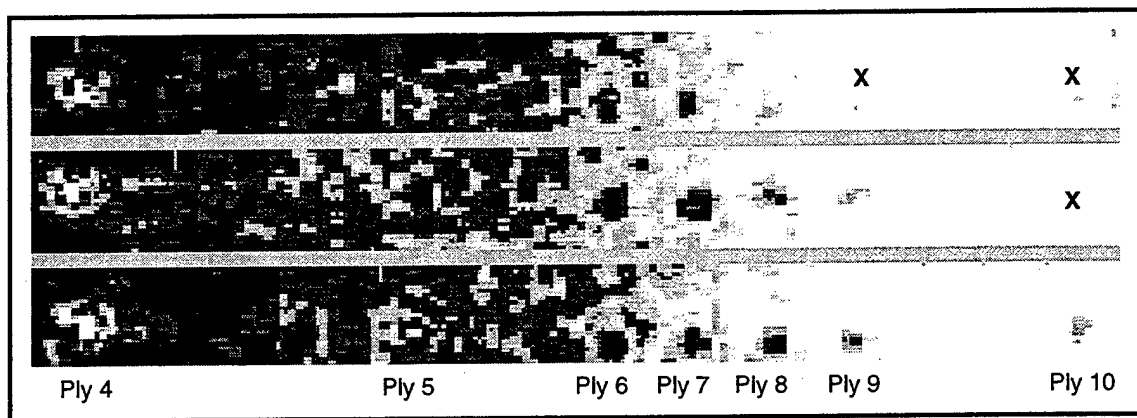


**Figure 4.6.4-2. MAUS IV MIA C-Scan of Unbonds in E-3 Rotodome Test Standard**

## **4.7 Implementation Plan**

The results of this program have been transitioned to a commercially available product, MAUS IV. Currently nine MAUS III systems have been upgraded to the MAUS IV configuration. Six new MAUS IV systems have also been fabricated. Introduction of this system into production inspection environments requires a general training package, and inspection specific techniques and procedures. Plans for system maintenance and spare parts provisioning are also required before final implementation of the inspection system is complete.

### **4.7.1 Training**

A training manual is provided with each system[6]. This manual includes chapters describing general system operation, equipment packing/unpacking, cabling, system start-up/shutdown, C-scan data collection, and data system setup. Sample applications are shown with step-by-step instructions for setup variable adjustments. The manual provides a self-guided tutorial for an new operator but does not include any application specific training information.

The Help menu, available from any point in the program, displays all of the information included in the Users manual in an on-line format. Full help menus, as well as context sensitive "What's This" text, provide detailed information about the system operation and software menu options.

An additional training guide for application specific training should be generated along with the inspection procedure, or technical order. Standard formats for this additional training guide are provided with the system. When multiple applications are developed for a system, a self-guided CD-ROM training package should be created to combine the general system training information with these application specific lessons.

### **4.7.2 Safety Issues**

Safety concerns when using the MAUS IV system generally relate to positioning the scanner. A manual safety package is included with the system to hold the track scanner in place if the vacuum supply is interrupted. This system must be placed with considerations for where the scanner will move if the vacuum supply fails. It must be placed so that an operator will not be hurt if the scanner swings away from the part when it releases.

The MAUS IV operates on standard line voltage power. When operating in a fueled environment, the system must be placed in a well-ventilated location, at least three feet above the hanger floor. The system should not be operated when significant fuel vapors are present.

### **4.7.3 Maintenance Plans**

Each MAUS IV system is delivered with a one year full service warranty. This warranty covers all aspects of the system with the exception items that become defective due to normal wear, or damage resulting from accident, misuse, abuse, or negligence. The Boeing Company reserves the right to charge on a time and material basis for repairs that may result from these



actions. Extended warranties are also offered in the standard catalog price list to retain this warranty support after the first year.

A maintenance manual is included with each MAUS IV system. This manual contains routine maintenance procedures such as cleaning, alignment, and calibration. Minor repair procedures that can be performed on-site are also described. Major repairs are performed at the Boeing facility. The Boeing Company will, at its option, repair or replace any item under warranty without charge at The Boeing Company repair center. Repair at customer facilities is quoted as requested. Instructions for returning a system to Boeing are included in the Maintenance manual.

#### **4.7.4 Software Support**

The efforts in this program have resulted in a completed MAUS IV software package with an initial 1.0 revision level. The Boeing Company provides software support and updates throughout the warranty period. Written records of software inconsistencies should be submitted to Boeing. These records must include a description of the problem, and supporting information to isolate the operational steps that were followed to encounter the problem. Software repairs/updates are released as x.y revision levels to the original software. Minor changes and repairs result in an increment of the y portion of the revision number. Major software changes result in an increment of the x portion of the revision number.

Software revisions are supplied to an operator as auto-install files sent through e-mail or on floppy disks. Readme.doc files are supplied with each software revision to describe the changes introduced in the new revision. MAUS IV operation has been tested and verified as Y2K compliant. Since the computer operating system is Windows-NT additional patches supplied by Microsoft Corporation to support Y2K compliance in the general Windows-NT environment may be added as they become available.

#### 4.7.5 Spare Part Provisioning

The maintenance manual[7] contains a listing of consumable items that should be provisioned with each system. These items, described in Figure 4.7.5-1, are typically replaced within a twelve month period. A spare parts provisioning system should include these items as well as the items described in Figure 4.7.5-2. The items in Figure 4.7.5-2 are not considered consumable parts, however, they can wear over time and require replacement. A full MAUS IV spare parts list is shown in Figure 4.7.5-3. It is not necessary to stock the items described in Figure 4.7.5-3, since typical system operation will not result in system damage. However, these items are available from Boeing if a part failure does occur.

Part Number	Description
MAUS3-Med-Sensor-Cables	Set of four sensor cables
MAUS4-JAZDISK	JAZ disk
MAUS4-WARRANTY	1 year extended warranty
MAUS4-WHEELS1	Medium scanner wheels
MAUS4-WHEELS2	3" scanner and large scanner wheels

Figure 4.7.5-1. Consumable Items

Part Number	Description
MAUS4-PC-HDISK	Spare removable hard disk drive for PC computer
MAUS4-PC-PS	Spare power supply for PC computer
MAUS4-PC	Spare PC laptop computer
MAUS4-NTCBL	Network cable assembly
MAUS4-DBCBL	Debug cable assembly
MAUS4-MOTOR1	Motor for hand scanners
MAUS4-MOTOR2	Motor for variable stroke scanner
MAUS4-MOTOR3	Motor for track carriage
MAUS4-RESOLVER	Position measurement for all scanners
MAUS4-ENCODERBELT	Rubber belt for hand scanners index resolver
MAUS4-DRIVEBELT1	Drive belt for variable stroke scanner
MAUS4-DRIVEBELT2	Drive belt for medium scanner
MAUS4-DRIVEBELT3	Drive belt for 3" scanner
MAUS4-DRIVEBELT4	Drive belt for large scanner

Figure 4.7.5-2. Recommended Spare Parts Inventory

Part Number	Description
MAUS4-WARRANTY	1 year extended warranty
MAUS4-PC-HDISK	Spare removable hard disk drive for PC computer
MAUS4-MOUSE	External computer mouse
MAUS4-NTCBL	Network cable assembly
MAUS4-DBCBL	Debug cable assembly
MAUS4-JAZ1	JAZ subsystem
MAUS4-JAZDISK	JAZ disk
MAUS4-CASE1	Soft case for MAUS IV electronics and computer
MAUS4-CASE2	Soft case for MAUS IV accessories
MAUS4-HCASE	Hard shipping case for MAUS IV
MAUS3-Med-Scanner	Medium MAUS IV scanner
MAUS3-Med-Cable	Main scanner cable
MAUS3-Med-Drive	Drive motor, gear, and belt for medium scanner
MAUS3-Med-Index	Index axis assembly medium scanner
MAUS3-Med-Scan	Scan axis assembly medium scanner
MAUS3-Med-Wheel	Set of four wheels medium scanner
MAUS3-Med-Front	Front bracket medium scanner
MAUS3-Med-2Bar	Dual sensor mount medium scanner
MAUS3-Med-1Bar	Single sensor mount medium scanner
MAUS3-Med-Sensor-Cables	Set of four sensor cables
MAUS3-Lrg-Scanner	Large MAUS IV scanner
MAUS3-Lrg-Cable	Main scanner cable
MAUS3-Lrg-Drive	Drive motor, gear, and belt for large scanner
MAUS3-Lrg-Index	Index axis assembly for large scanner
MAUS3-Lrg-Scan	Scan axis assembly for large scanner
MAUS3-Lrg-Wheel	Set of four wheels for large scanner
MAUS3-Lrg-Front	Front bracket for large scanner
MAUS3-Lrg-2Bar	Dual sensor mount for large scanner
MAUS3-Sml-Scanner	Small MAUS IV scanner
MAUS3-Sml-Cable	Main scanner cable
MAUS3-Sml-Drive	Drive motor for small scanner
MAUS3-Sml-Index	Index axis assembly for small scanner
MAUS3-Sml-Scan	Scan axis assembly for small scanner
MAUS3-Sml-Wheel	Set of two wheels for small scanner
MAUS3-Sml-Front	Front bracket for small scanner
MAUS3-Sml-2Bar	Dual sensor mount for small scanner
MAUS3-Sml-1Bar	Single sensor mount for small scanner
MAUS4-Var-Scanner	Variable Stroke scanner
MAUS4-Var-Cable	Main scanner cable
MAUS4-Var-Drive	Drive motor, gear, and belt
MAUS4-Var-Scan	Scan axis assembly
MAUS4-Var-Wheel	Support wheel
MAUS4-Var-Mount1	Sensor attachment plate with quick disconnects
MAUS4-Var-Mount2	Sensor attachment plate
MAUS4-Var-Holder	Sensor holder
MAUS4-Var-Sensor-Cables	Set of four sensor cables
MAUS4-Track-Carriage	Variable Stroke scanner

Figure 4.7.5-3. Complete Listing of Spare Parts for MAUS IV

Part Number	Description
MAUS4-Track-Cable	Main cable for carriage
MAUS4-Track-Drive	Drive motor, gear, and belt
MAUS4-Track-Index	Index axis assembly
MAUS3-SE-PEA225	2.25 MHz, ¼" delay line pulse-echo sensors, set of 4
MAUS3-SE-PEA50	5 MHz, ¼" delay line pulse-echo sensors, set of 4
MAUS3-SE-PEA10	10 MHz, ¼" delay line pulse-echo sensors, set of 4
MAUS3-SE-PEB225	2.25 MHz, ½" delay line pulse-echo sensors, set of 4
MAUS3-SE-PEB50	5 MHz, ½" delay line pulse-echo sensors, set of 4
MAUS3-SE-RS110	110 kHz resonance sensors, set of 2
MAUS3-SE-RS160	160 kHz resonance sensors, set of 2
MAUS3-SE-RS260	260 kHz resonance sensors, set of 2
MAUS3-SE-RS330	330 kHz resonance sensors, set of 2
MAUS3-SE-MIA1	6 kHz MIA sensors, set of 2
MAUS3-SE-MIA2	8 kHz MIA sensors, set of 2
MAUS3-SE-PC	Pitch/catch sensors, set of 2
MAUS3-SE-EC1K	1 kHz eddy current sensors, set of 2
MAUS3-SE-EC10K	10 kHz eddy current sensors, set of 2
MAUS3-SE-EC100k	100 kHz eddy current sensors, set of 2
MAUS3-SE-EC10M	1 MHz eddy current sensors, set of 2
MAUS3-SS-PE25	Sensor sleeves for all ¼" pulse echo sensors, set of 4
MAUS3-SS-PE50	Sensor sleeves for all ½" pulse echo sensors, set of 4
MAUS3-SS-PEDL	Delay lines for all ¼" pulse echo sensors, set of 4
MAUS3-SS-R110	Sensor sleeves for 110 kHz resonance sensors, set of 2
MAUS3-SS-R160	Sensor sleeves for 160 kHz resonance sensors, set of 2
MAUS3-SS-R260	Sensor sleeves for 260 kHz resonance sensors, set of 2
MAUS3-SS-R330	Sensor sleeves for 330 kHz resonance sensors, set of 2
MAUS3-SS-MIA1	Sensor sleeves for 6 kHz MIA sensors, set of 2
MAUS3-SS-MIA2	Sensor sleeves for 8 kHz MIA sensors, set of 2
MAUS3-SS-PC	Sensor sleeves for pitch/catch sensors, set of 2
MAUS3-SS-ECA	Adapters for ¼" sensors in EC sensor brush mount, set of 2
MAUS3-SS-ECB	EC sensor brush mounts, set of 2

**Figure 4.7.5-3. Complete Listing of Spare Parts for MAUS IV (Cont.)**

## 5.0 CONCLUSIONS

In conclusion, the "Large Area Composite Inspection System" program sponsored by the Materials Directorate was successful in that all program goals were accomplished, and in some cases, goals were exceeded. The full-scale development program produced a multi-modal inspection system that incorporated ultrasonic pulse-echo, ultrasonic resonance and eddy current inspection capabilities. The system was made portable in that all components of the system could be packed into a carrying case weighing no more than 25 pounds. The system also provided the ability to collect, view, manipulate and archive the image-based data collected. Feedback from end users was generally positive and most of the changes requested were incorporated.

The production prototype development program sponsored by the Manufacturing Technology Directorate added to the program success by incorporating additional sensor modes to improve the robustness of the system. In addition, user friendliness was improved through transition from UNIX-based to Windows NT software. One of the key technical successes of this portion of the program the development and validation of the segmented, flexible scanning track, which improved the ability to perform remote scanning in curved areas. This was a key in reducing the estimated cycle time for inspection of KC-135 lap seams from 400 hours (MAUS III) to 250 hours (MAUS IV). Through improved system production processes and selective subcontracting, the cost of the MAUS system was reduced by 32%.

## 6.0 RECOMMENDATIONS

Based on the results of the "Large Area Composite Inspection System" program, a program should be established to facilitate the transition and implementation of the MAUS IV in the KC-135 PDM line for detection of corrosion in lap seams. With the additional bond testing sensors incorporated into MAUS IV, more extensive evaluations of the system relative to inspection of E-3 and E-4 radomes should be considered.

The raster scanning motion feature of the MAUS IV proved to be adequate for inspection of composite laminates, bondlines and thinner metallic structure, such as that found in an aircraft fuselage. For thicker metallic structure, such as that found in a wing, the raster-scanning feature limits the ability to detect flaws. In order to overcome some of the depth of penetration problems and effects caused by ferromagnetic fasteners, the ability to center a probe over a fastener and rotate the probe would be beneficial. To improve the flexibility of the MAUS IV and push it's applications base beyond thinner structure, development of rotational motion capabilities should be considered.

As time passes, new sensor technologies are being developed to address many of the inspection concerns described in this report. Examples of these include magnetoresistive and remote field eddy current probes, electromagnetic acoustic transducers for non-coupling ultrasonic inspection and broadband resonance-based probes for ultrasonic spectroscopy. The MAUS has shown to be a useful tool relative to data collection and archiving and it may be beneficial from time to time to investigate merging new sensors with the MAUS in order to broaden the impact of these new technologies.

## **7.0 REFERENCES**

1. MDC Report #IR0507, Large Area Composite Inspection System Interim Report, 01 October 1991 - 31 March 1992.
2. MDC Report #IR0501-9, Large Area Composite Inspection System Interim Report, 01 April 1992 - 31 January 1994.
3. MDC Report #IR0501-10, Large Area Composite Inspection System Quarterly Report, 01 March 1994 - 30 June 1994.
4. MDC Report #IR0501-11, Large Area Composite Inspection System Quarterly Report, 01 July 1994 - 30 September 1994.
5. MAUS IV System Description (to be published in December 1998)
6. MAUS IV Users Manual (to be published in December 1998)
7. MAUS IV Maintenance Manual (to be published in December 1998)